AD-A058 888 GENERAL DYNAMICS SAN DIEGO CA CONVAIR DIV F/G 11/4
BORON/ALUMINUM LANDING GEAR FOR NAVY AIRCRAFT.(U)
SEP 78 N62269-74-C-0619
UNCLASSIFIED CASD-NADC-76-003 NL

1 OF 2
ADA
058888

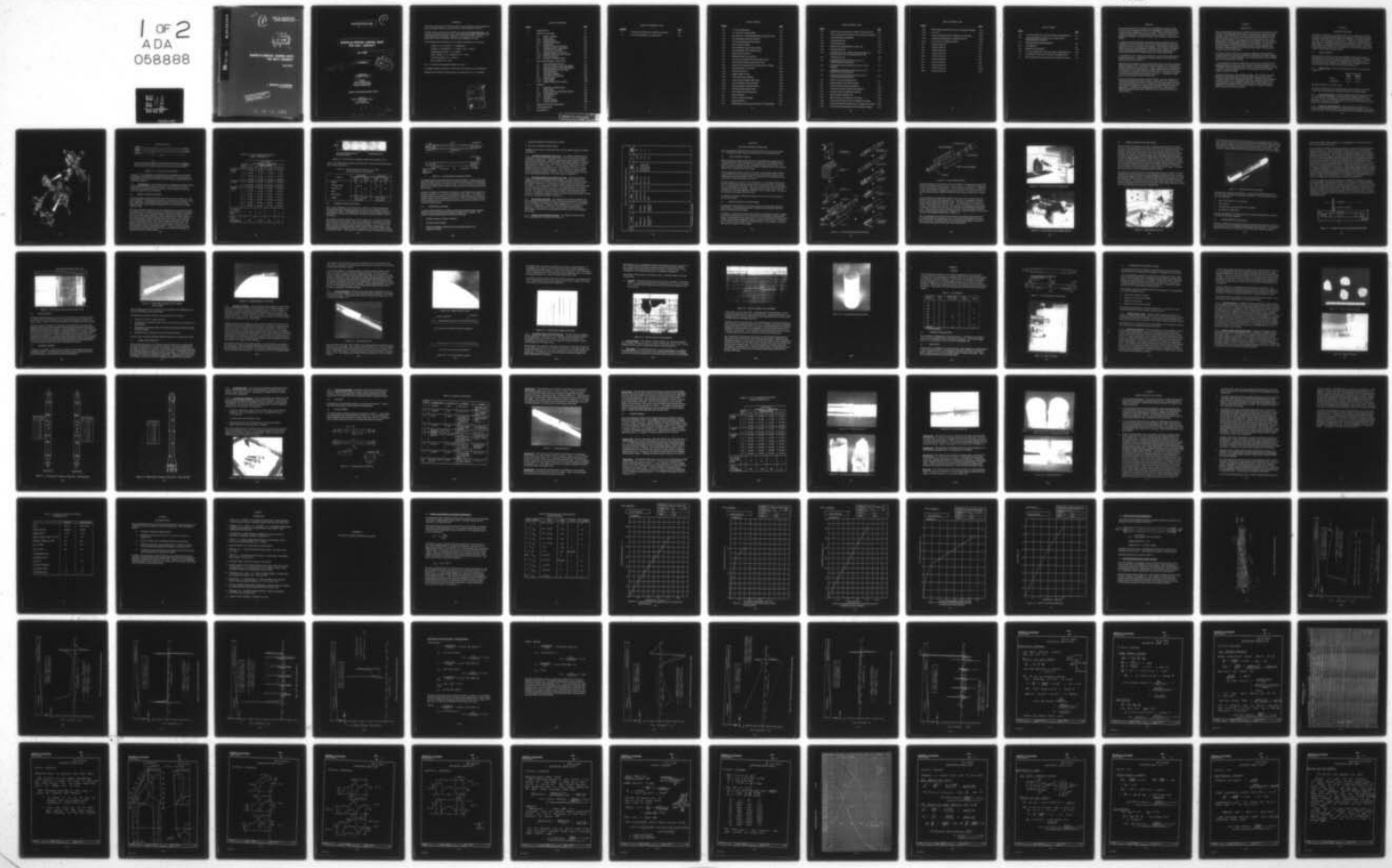

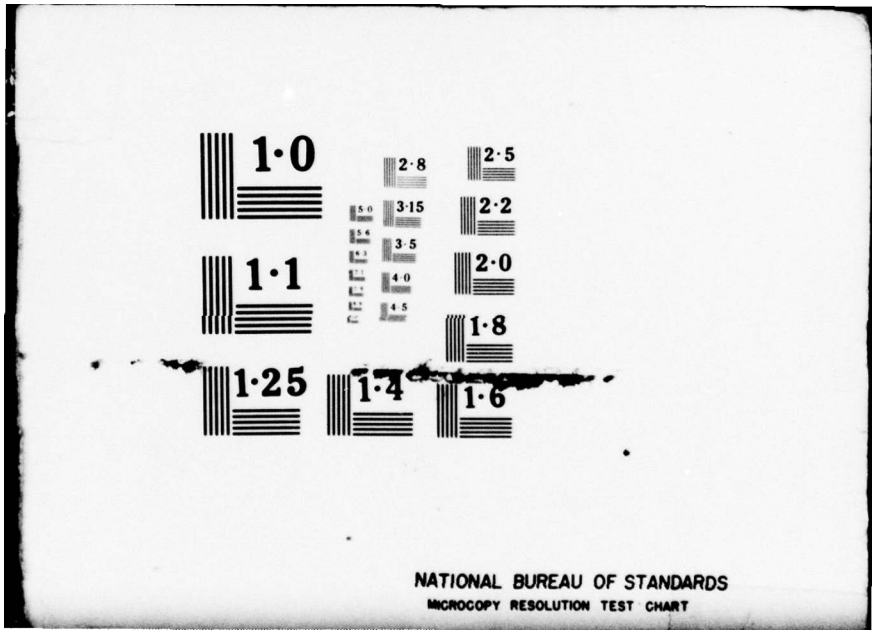
1·0
1·1
1·25
2·8
3·15
3·5
4·0
4·5
5·0
2·5
2·2
2·0
1·8
1·4
1·6
NATIONAL BUREAU OF STANDARDS
MICROCOPY RESOLUTION TEST CHART

REPORT NO. CASD-NADC-76-003
CONTRACT N62269-74-C-0619

BORON/ALUMINUM LANDING GEAR FOR NAVY AIRCRAFT

FINAL REPORT

GENERAL DYNAMICS
Convair Division

(14) REPORT NO. CASD-NADC-76-003

(1)

(6) BORON/ALUMINUM LANDING GEAR FOR NAVY AIRCRAFT.

(9) FINAL REPORT. Jun 74-Aug 77.

(11) September 1978

(12) 129p.

Prepared Under
Contract N62269-74-C-0619
(15)

Prepared for
Naval Air Development Center
Air Vehicle Technology Department
Warminster, Pennsylvania 18974

Approved for Public Release Distribution Unlimited

Prepared by
GENERAL DYNAMICS CONVAIR DIVISION
P.O. Box 80847
San Diego, California 92138

FOREWORD

This report was prepared by General Dynamics Convair Division, Advanced Composites group, San Diego, California, under the terms of Contract N62269-74-C-0619.

This final report covers the entire program from June 1974 through August 1977. The program was sponsored by the Aircraft & Crew Systems Technology Directorate, Naval Air Development Center (NADC), Warminster, Pennsylvania 18974. Messrs. A. Manno and H. Slavin, Code 60834, were the Project Engineers for NADC.

The following Convair personnel were the principal contributors to the program:

Design: F. H. Doyal and K. T. Younghusband

Analysis: H. McCutchen, R. A. Ankeny, and R. S. Wilson

Engineering Processes: C. R. Maikish

Impact Testing: M. D. Campbell and G. L. O'Barr

Corrosion Testing: D. G. Treadway

Static Testing: N. R. Adsit

Mr. F. H. Doyal was the program manager for Convair.

The fatigue testing was conducted at NADC under the direction of Mr. Harold Slavin.

Additions and corrections to the final report were made by Mr. M. D. Weisinger.

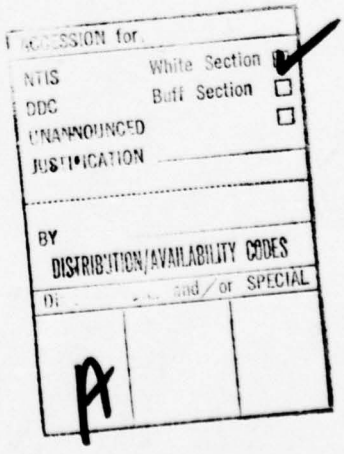

TABLE OF CONTENTS

TABLE OF CONTENTS, Contd

LIST OF FIGURES

LIST OF FIGURES, Contd

LIST OF FIGURES, Contd

LIST OF TABLES

SUMMARY

This report summarizes work conducted by General Dynamics Convair Division for the Naval Air Development Center (NADC) under Contract N62269-74-C-0619, "Boron/Aluminum Landing Gear for Navy Aircraft." The program objective was to evaluate the application of boron/aluminum composite material to a typical Navy landing gear component, with primary emphasis upon evaluation of component reliability.

A replacement composite drag link was designed using boron/aluminum tube construction to the required envelope, ultimate loads, fatigue spectrum, and carrier environment for the A-7 nose gear lower drag link. The resulting composite link design was a 28-ply boron/aluminum tube diffusion bonded to titanium end fittings. A test specimen was designed identical to the replacement composite drag link, except that simplified test end fittings replaced the complex flight fittings.

A comprehensive stress analysis was conducted for both the replacement drag link and the test specimen. A finite-element computer analysis of the critical tube/fitting scarf joint was performed.

Eight full-size test specimens were fabricated using Convair's proprietary autoclave diffusion bonding process. Each diffusion bonded tube/fitting joint was subjected to ultrasonic inspection to evaluate extent of bonding. Difficulties were encountered due to contamination of the boron/aluminum to titanium diffusion bonded joint interface. This problem was essentially resolved during the course of the program but resulted in early specimens failing in static tension at 92% of DUL. Consequently, fatigue loads were scaled down to 75-80% of design levels.

Boron/aluminum links that had been damaged by pebble impact then subjected to a corrosive environment and notched, showed no reduction in static strength over an as-fabricated specimen and survived two lifetimes at 80% design fatigue load levels. This compared favorably with a notched 300M steel production link which failed in fatigue after 1.1 lifetimes at 70% design fatigue load levels. Both the boron/aluminum links and the 300M steel production link were notched and tested in the same sequence.

SECTION 1

INTRODUCTION

Many boron/aluminum metal matrix composite structures have been built for aircraft and space vehicle applications under numerous government and company sponsored programs. Boron/aluminum as an advanced composite exhibits high specific stiffness and strength, which leads to lower weight and smaller physical size, and/or greater range and payload. The confidence in boron/aluminum structures and the development of a new fabrication technique led to the decision to use over 250 boron/aluminum tubes in the midfuselage section of the Space Shuttle. The fabrication process developed for these boron/aluminum tubes is directly applicable to the fabrication of tubular landing gear struts and formed the basis for the fabrication procedure used during this program.

The objective of this program was to evaluate the application of boron/aluminum composite material to a typical Navy landing gear component with primary emphasis upon evaluation of component reliability. The component selected for this evaluation was the A-7 nose gear lower drag link.

A boron/aluminum drag link was designed that could be directly substituted for the existing 300M steel A-7 nose gear lower drag link. The design consisted of a 5.6-mil-diameter boron/6061 aluminum tube with titanium end collars attached to the tube by means of a diffusion bonded scarf joint. The end collars are electron beam welded to titanium end fittings.

Eight full size drag links, with simplified end fittings, were designed, fabricated and tested to determine the effect of impact damage, notches and a corrosive environment on their static strength and fatigue life. Difficulties were encountered during the program due to contamination in the boron/aluminum itself and at the boron/aluminum to titanium diffusion bonded interface. These problems were essentially resolved during the course of the program but resulted in premature failure of some of the earlier specimens.

SECTION 2

DESIGN AND ANALYSIS

The objective of this effort was to design a full-size Navy landing gear component using Convair's existing boron/aluminum tube technology. The component selected for design, fabrication, and test was the heavily loaded lower drag link assembly from the A-7 nose landing gear (see Figure 2-1). This link, in conjunction with the upper drag link, locks the nose gear in the extended position, absorbs drag loads during landing, and transmits catapult load to the airframe structure. The existing baseline link, shown in Figure 2-2, is machined from a 4340 steel forging and heat treated to 200 ksi ultimate tensile strength.

2.1 DESIGN CRITERIA

This program was intended to evaluate the feasibility of using boron/aluminum composite material in a heavily loaded Navy landing gear component. The design criteria used for the boron/aluminum component were based on those for the A-7 nose landing gear lower drag link. The composite link was designed to meet the structural and functional requirements of the steel baseline link.

2.1.1 DESIGN LOADS. Critical loads supplied by the Navy for the pin-ended drag link are:

	Design Loads (pounds)	
	Limit	Ultimate
Tension	157,300	236,000
Compression	94,000	141,000

The ultimate/limit factor of safety is 1.50.

The maximum tension load occurs during catapult of the aircraft from an aircraft carrier deck, and the maximum compression loading occurs during landing.

2.1.2 FATIGUE SPECTRUM. The design fatigue spectrum is presented in Table 2-1. This spectrum represents one lifetime of fatigue loading and is based on a simulation of the A-7 nose landing gear drag link spectrum multiplied by a scatter factor of 2.0. This spectrum is considered very severe due to the inclusion of a limit tension load (catapult) for every flight.

2.1.3 ENVELOPE REQUIREMENTS. Space constraints were placed on the composite drag link design to ensure its compatibility with the existing A-7 nose landing gear interfaces and to preclude interference with other components during retraction

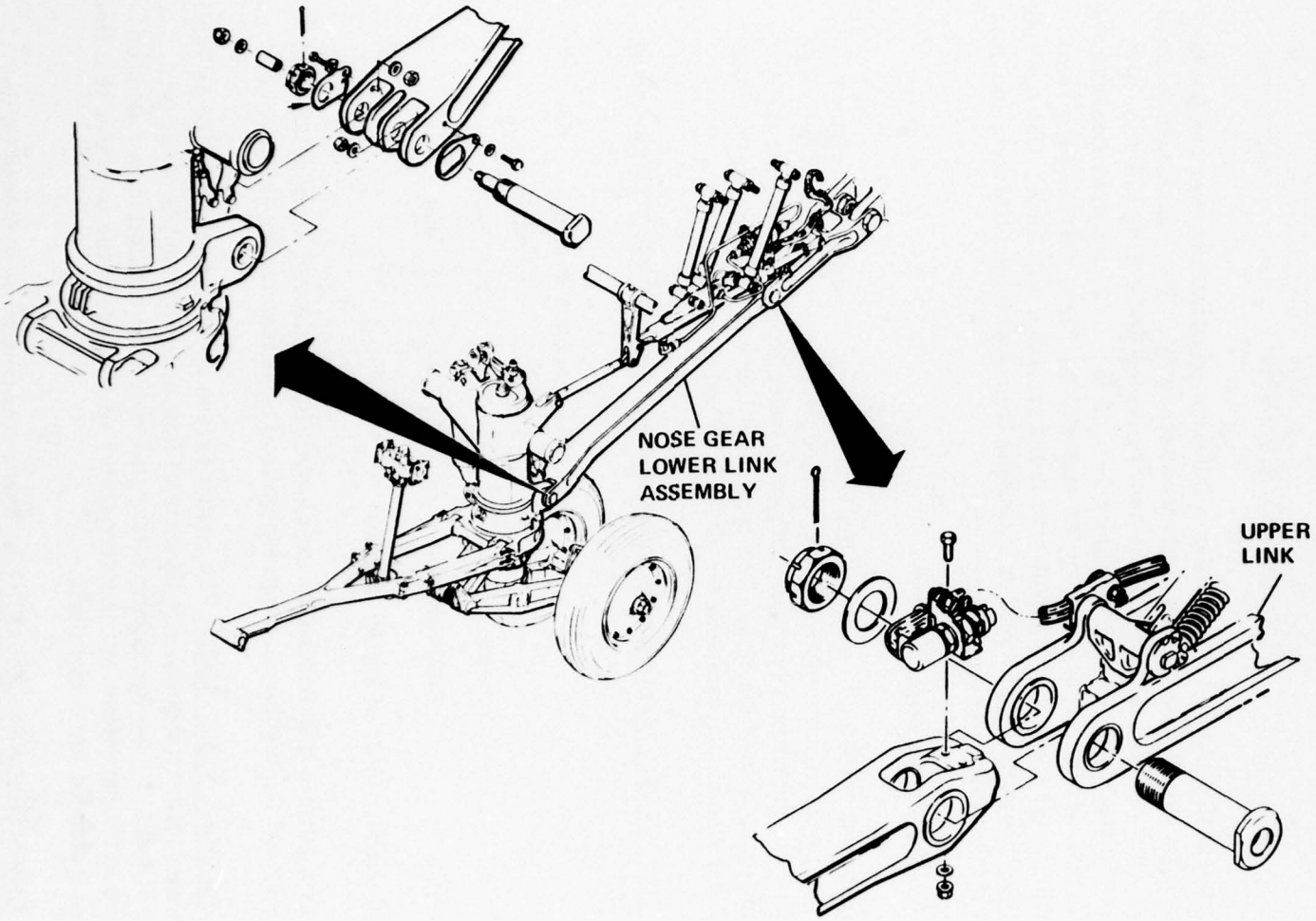

Figure 2-1. A-7 Nose Landing Gear

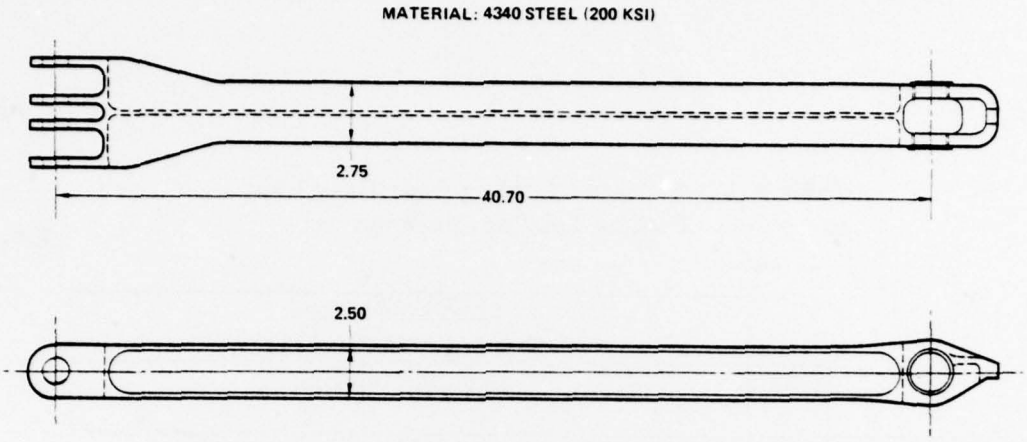

Figure 2-2. A-7 NLG Lower Link Assembly

of the gear. The end fittings of the composite link were designed to mate with the existing lugs on the shock strut cylinder and upper drag link. The boron/aluminum tube diameter was limited to 3-1/8 inches to provide clearance during extension and retraction of the gear.

2.1.4 ENVIRONMENT. The composite drag link was designed to withstand typical carrier-based aircraft environmental conditions. In addition to the natural salt atmosphere, the operating environment contains corrosive chemicals produced by carrier stack gases and aircraft exhausts.

2.2 BORON/ALUMINUM MATERIAL

The boron/aluminum composite material selected for use on this program is 5.6-mil boron filaments in a 6061 aluminum alloy matrix. The material is purchased in 7-mil-thick, single-layer, diffusion bonded sheets containing 45-50% boron, by volume. Figure 2-3 shows a cross section microstructure for 5.6-mil boron/6061 aluminum monolayer sheet.

This material system resulted from previous development work that included screening candidate matrix and filament materials, characterizing the systems, determining material allowables, and environmental testing. Materials characterized used both 4-mil and 5.6-mil-diameter filaments, with and without silicon-carbide coatings, in a 6061 aluminum matrix applied by diffusion bonding, plasma spray, and green tape. The 5.6-mil-diameter filaments were found to produce a higher specific strength laminate, less property scatter, and a lower cost than the 4-mil filaments. The diffusion-bonded material was also shown to provide superior transverse strain characteristics and reduced fabrication problems. For these reasons, the present tube construction material system uses uncoated, 5.6-mil-diameter filaments in a diffusion-bonded 6061 aluminum matrix.

Table 2-1. A-7 Nose Landing Gear Drag Link
Fatigue Loading Spectrum

	Load No.	Load (pounds) (+) Tension, (-) Compression Landing Condition 1	2	3	4
Buffing Cycle	1	-25,300	-25,300	-25,300	-25,300
	2	-71,600	-71,600	-71,600	-71,600
	3	-25,300	-25,300	-25,300	-25,300
	4	-71,600	-71,600	-71,600	-71,600
Catapult	5	-25,300	-25,300	-25,300	-25,300
	6	+157,000	+157,000	+157,000	+157,000
Landing Cycle	7	-47,000	-94,000	-13,500	-14,800
	8	-29,000	-49,900	-70,200	-87,700
	9	-47,000	-94,000	-13,500	-14,800
	10	-29,000	-49,900	-70,200	-87,700
	11	-47,000	-94,000	-13,500	-14,800
	12	-20,300	-34,200	-48,600	-62,300
	13	-25,300	-25,300	-25,300	-25,300
No. Cycles in 50-Cycle Block		14	28	7	1
Total Cycles in One Lifetime		560	1,120	280	40

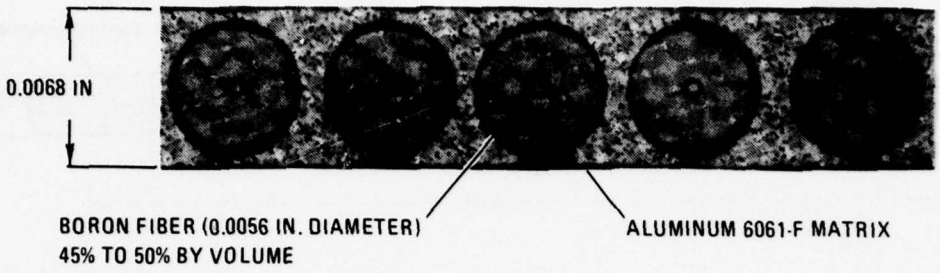

Figure 2-3. Microstructure of Diffusion-Bonded B/Al Monolayer Tape

Typical room temperature mechanical properties for 50 volume percent boron/aluminum are given in Table 2-2.

Table 2-2. Typical Mechanical Properties of 50 Volume Percent Unidirectional B/Al Material

Property	Longitudinal		Transverse	
	Strength (ksi)	Modulus (msi)	Strength (ksi)	Modulus (msi)
Tensile	216	31	20	20
Poisson's Ratio	0.23		0.13	
Compression	250	32	30	20
Shear	23	6		
Bearing (4D)	120			
Fatigue	150 ksi at runout (10^7 cycles)		6 ksi at runout (10^7 cycles)	

2.3 COMPOSITE DRAG LINK DESIGN

The A-7 nose landing gear lower drag link was resized as a seamless unidirectional boron/aluminum tube with integral titanium collars to which conventional titanium end fittings are welded. This configuration was chosen to take advantage of previously developed boron/aluminum tube fabrication processes, production facilities, and low-cost tooling.

The composite drag link configuration is shown in Figure 2-4. The tube is fabricated from single-layer sheet material, which is consolidated into a 28-ply tube at the same time it is joined to the titanium collars by diffusion bonding. A 35-to-1 tapered scarf joint at each end of the tube assembly transfers loads into the composite tube. Each boron/aluminum ply is stepped off with a step length of 1/4 inch and is diffusion bonded to the titanium collar. Peak stresses at the ends of the joint are minimized by providing

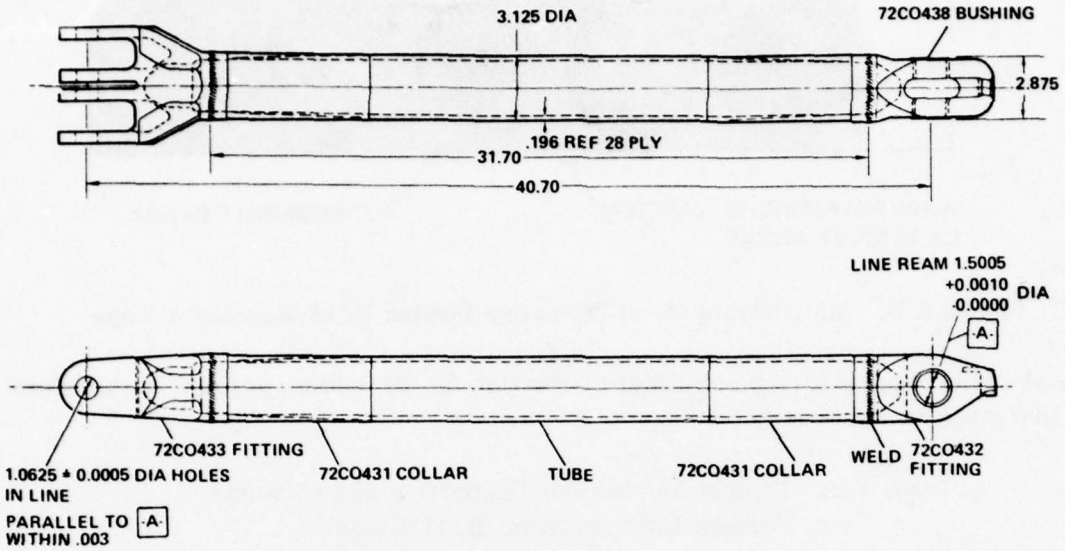

Figure 2-4. Boron/Aluminum Drag Link Assembly

the minimum gage of each part at the point of load introduction. Peak stresses at ply steps in the center portion of the joint are minimized by providing strain compatibility between the composite tube and titanium collars. Each collar extends 3/4 inch beyond the end of the composite tube to isolate the composite material from the high temperature weld zone.

Titanium end fittings were designed to mate with A-7 nose landing gear interfaces and smoothly transition to a cross section matching that of the collars. The fittings are attached to the tube assembly by an electron-beam welding technique that involves the addition of filler wire into a diffused electron beam. This special technique is necessary to minimize stress concentrations in the weld zone as the weld cannot be stress relieved by ordinary means.

2.4 STRUCTURAL ANALYSIS

To insure structural adequacy in addition to obtaining a minimum weight composite landing gear link, extensive analytical design procedures were employed. The purpose of this analytical task was to provide the following:

a. Margins of safety for ultimate conditions.

b. Predicted modes of failure.

c. Analysis of transition region from the boron/aluminum tube to the titanium end fittings.

d. Analytical substantiation of fatigue life of the link.

e. Flaw sizes for damage tolerance testing.

Highlights of the analyses are discussed below, and the complete analysis is included in Appendix A.

2.4.1 ANALYSIS PARAMETERS AND LOADS. The composite landing gear link is designed to replace the steel drag link of the A-7 aircraft in regard to structural and functional requirements. Composite components are usually critical in static ultimate load conditions since their performance under fatigue conditions is relatively high compared to metallic parts. Static loads are given in Paragraph 2.1.1 and the fatigue spectrum is shown in Table 2-1. Critical stresses in the B/Al tube occur along the interface with the titanium sleeve. See paragraph 2.4.2 below. Overall stability of the link is checked in Appendix A and is not critical. Fatigue analysis was not performed due to lack of S-N data; however, flaw growth analysis was made for several assumed initial flaws. This work is shown in Appendix A.

2.4.2 DIFFUSION BONDED SCARF JOINT ANALYSIS. Joining is the greatest challenge in any efficient composite member design. The major emphasis of the analytical work done on this program was on the diffusion-bonded scarf joint analysis. The SOLID SAP (Reference 1) finite element computer program was used to aid this analysis. A fine mesh model consisting of 1,586 grid points with 1,360 axisymmetric solid quadrilateral elements was set up. This model adequately shows peak stresses at ply drop-off points. Mechanical and thermal stress unit load conditions were run. The problem of residual stresses remaining after the diffusion bonding process is not adequately understood to permit a rigorous analysis at this time. Further discussion of this effect is included in Appendix A.

2.4.3 END FITTING ANALYSIS. Two configurations of titanium end fittings were used for both the forward and the aft ends of drag links produced under this program. One set of fittings was designed as the "flight configuration" and one set was designed as the "test configuration." Analyses for all four fitting types are included in Appendix A. Fatigue analyses are shown as well as static strength lug and net section checks. Analysis of the weld joining the titanium sleeve to the end fitting is also included.

2.4.4 SUMMARY OF MARGINS OF SAFETY. The minimum Margins of Safety for the composite link are summarized in Table 2-3.

Table 2-3. Minimum Margins of Safety Summary *

PAGE	PART NAME	PART NO.	MATERIAL	H.T. KSI	CRITICAL CONDITION	TYPE OF LOADING	M.S.	FACTOR INCLUDED
								%
	Tube		Boron/Alum.	--	Ult. Comp.	Comp.	+.061	15
	Fitting-Fwd	72C0432	Ti-6AL-4V	130	Ult. Ten.	Shear out & Bearing	+.02	15
	Fitting-Aft	72C0433	Ti-6AL-4V	130	Ult. Ten.	Shear out & Bearing	+.02	15
	Weld-Fitting to Sleeve	72C0432 & 72C0433	Weld	130	Ult. Ten.	Tension	+.36	11

*Test fittings are not included.

SECTION 3

DRAG LINK SPECIMEN FABRICATION

The boron/aluminum drag link specimen fabrication process is illustrated in Figure 3-1. A detailed description of each operation is given in the following sections.

3.1 TUBE ASSEMBLY TOOLING

Special tooling was required to fabricate the boron/aluminum tube assembly for the composite specimen. This tooling consists of a rigid, split outer mandrel that forms the outer surface of the tube and a thin vacuum-tight envelope around the tube and inner mandrel that transmits the necessary diffusion bonding pressure to the composite. Figure 3-2 is an exploded view of the tooling.

The mild steel outer mandrel is made in two halves, split along the length of the tube, and is machined inside to the desired composite tube outside diameter with the ends counterbored to accept the titanium collars. The outer surface is machined to provide a clearance fit with the thin-walled outer sleeve.

The inner mandrel, outer sleeve, and two end spacers are assembled around the outer mandrel/composite tube assembly and then welded at each end to effect a vacuum-tight seal. A small stainless steel tube is welded over a drilled hole in one of the end spacers to permit evacuation of the assembly. The inner mandrel and outer sleeve are made from thin-wall, mild steel tubing that is annealed and cut to proper length. End spacers are machined from stainless steel plate stock.

The split outer mandrel and end spacers constitute more than 90% of the tooling cost and are fully reusable.

3.2 BORON/ALUMINUM TAPE PROCESSING

Boron/aluminum tape material was received in single-layer sheets approximately 30 inches square. The incoming material had to undergo several inspection operations before processing and tube assembly.

Each sheet was inspected for visible surface defects and the thickness checked. Samples were taken from each material lot for volume percent determination and filament bend testing. Volume percent values ranged from 45.5 to 48.3, well within the specified range. Average filament tensile strength was found to be greater than 500,000 psi, corresponding to a laminate tensile strength greater than 225,000 psi. All material was found to be free from major defects and was accepted.

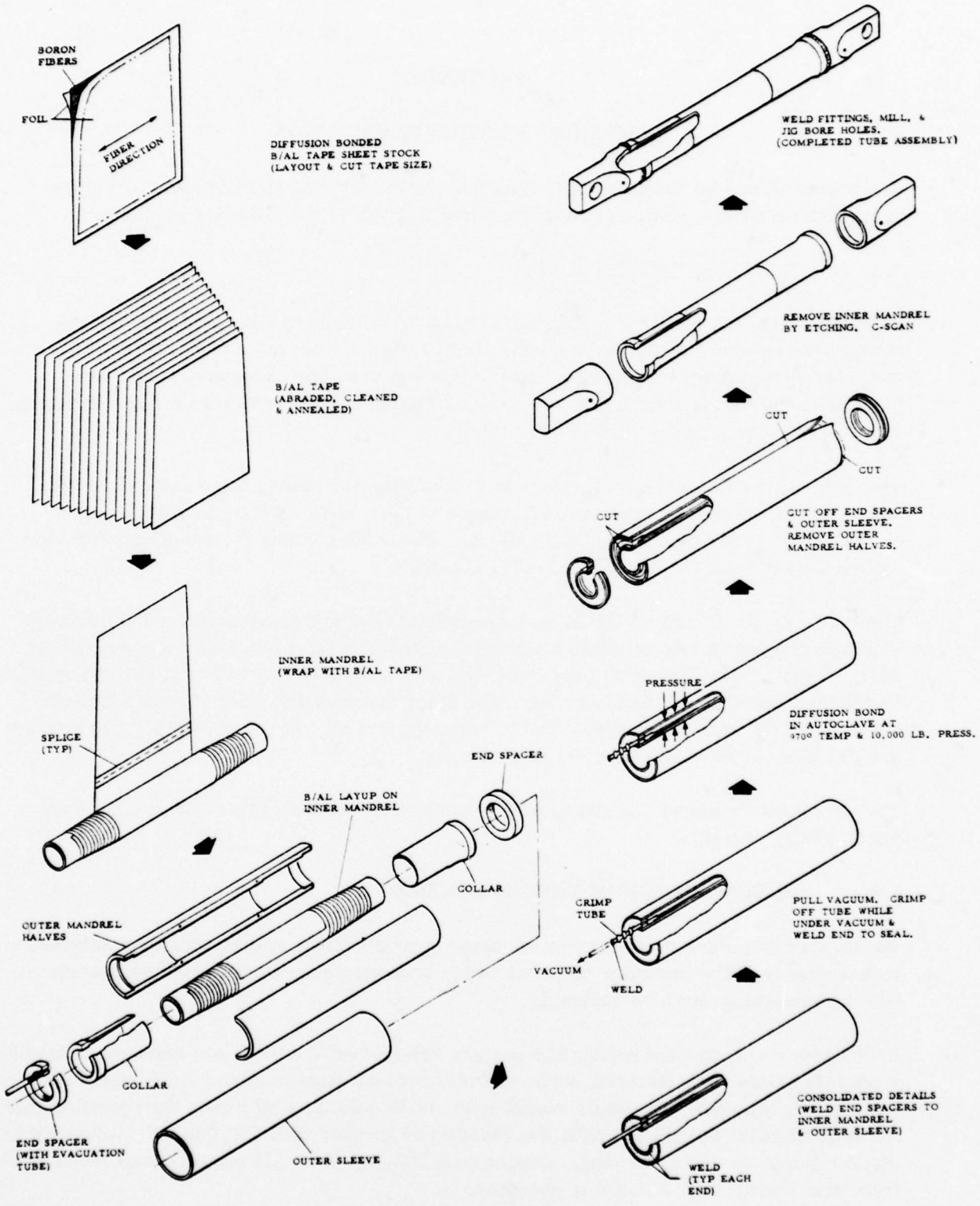

Figure 3-1. B/Al Drag Link Specimen Fabrication

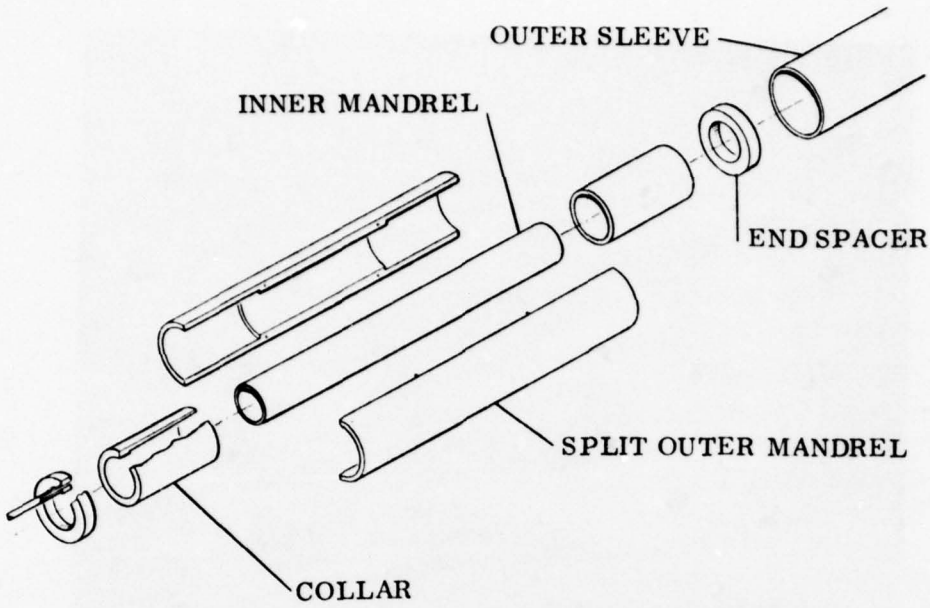

Figure 3-2. Tube Assembly Tooling

Following inspection, each sheet was processed through an abrading machine where both surfaces were simultaneously abraded by a series of rotary wire brushes to roughen the surfaces and remove any foreign matter. After brushing, the sheets were oven annealed to reduce the possibility of splitting in subsequent operations. The sheets were then cut into flat patterns of proper length and width on the tape cutting machine shown in Figure 3-3.

The flat patterns were trapezoidal in shape so that, when rolled, a helical taper was produced on the outside of the composite wrap. This taper was designed to match the internal taper machined in the titanium collars. The flat patterns were cleaned with acetone and then rolled onto an inner mandrel. As each flat pattern was rolled onto the mandrel, it was spliced to the next one. The splicing was accomplished by spotwelding a 2-mil thick, 1/2-inch wide, 6061 aluminum foil strip to both of the butted composite sheets. Splicing and tube rolling was accomplished in a combined operation in the Convair production tube winding machine shown in Figure 3-4.

After all flat patterns were rolled onto the mandrel, the assembly was removed from the winding machine and adjustments made to center the tape and equalize the helical steps on each end. The tightly wrapped tape was then unwound slightly to enlarge the outer diameter and provide a better fit with the outer mandrel.

Figure 3-3. Boron/Aluminum Tape Cutting Machine

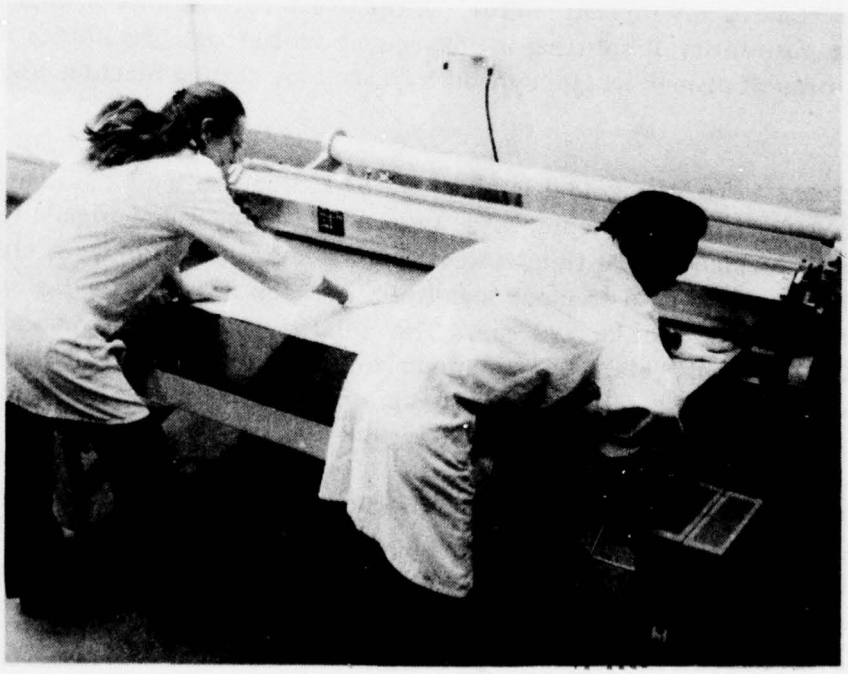

Figure 3-4. Boron/Aluminum Tube Winding Machine

3.3 BORON/ALUMINUM TUBE PROCESSING

Tube end collars were machined according to drawing 72C0435 from 6Al-4V titanium bar stock. The tapered inner surface of each collar was wire brushed and cleaned with acetone, the collars positioned over the ends of the previously wound tape/mandrel assembly, and this entire assembly was placed into one-half of the split outer mandrel. The split outer mandrel was previously coated with a high-temperature parting agent to prevent it from sticking to the B/Al during bonding. The other half of the split outer mandrel was fitted into place and tack welded to the first half. Sliding the outer sleeve over the outer mandrel and installing the two end spacers completed the pack assembly. The pack assembly was then made vacuum tight by tungsten-inert-gas welding the outer sleeve and inner mandrel to the end spacers. The welded assembly was checked for leaks, evacuated, and the evacuation tube crimped off while under vacuum. The end of the evacuation tube was then permanently sealed by welding.

The sealed pack assembly was placed in the high pressure autoclave (Figure 3-5) where consolidation of the boron/aluminum tape and bonding to the titanium collars was accomplished through diffusion bonding. The diffusion bonding autoclave cycle involves heating the assembly to 950F while under 10,000 psi isostatic pressure and holding for approximately 30 minutes. The high autoclave pressure deforms the ductile, thin-walled inner mandrel transferring pressure to the boron/aluminum, which coupled with the near-molten state of the aluminum matrix produces a diffusion bond.

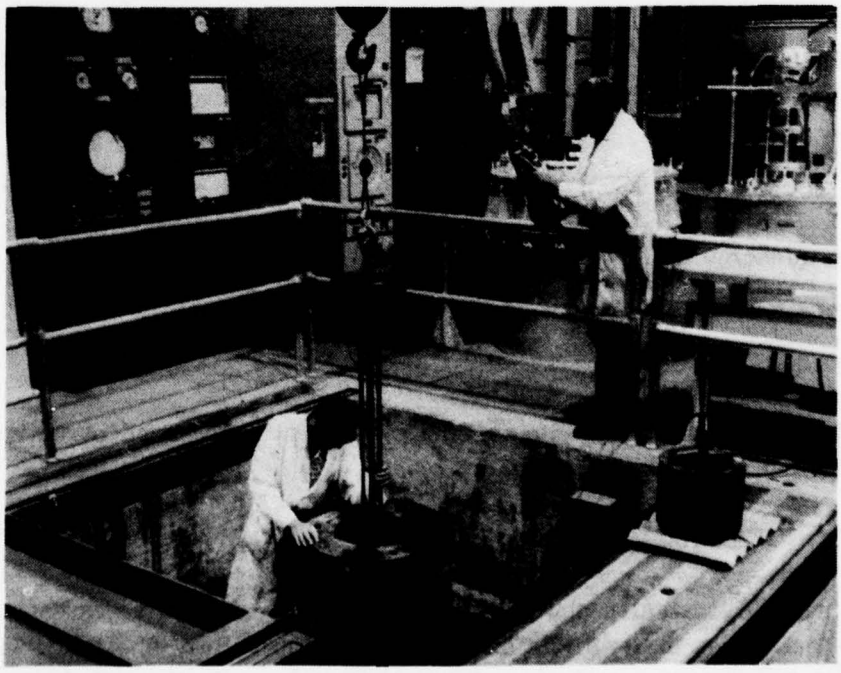

Figure 3-5. High-Pressure Autoclave

On removal from the autoclave, the outer sleeve was cut and peeled off like a banana skin. The inner mandrel was also cut at each end and the welded end spacers removed. The split outer mandrel was then removed and the outer tube surface masked off. The inner mandrel was chemically etched away in a bath of nitric acid and water. Figure 3-6 shows a typical diffusion-bonded tube assembly after removal of the inner mandrel.

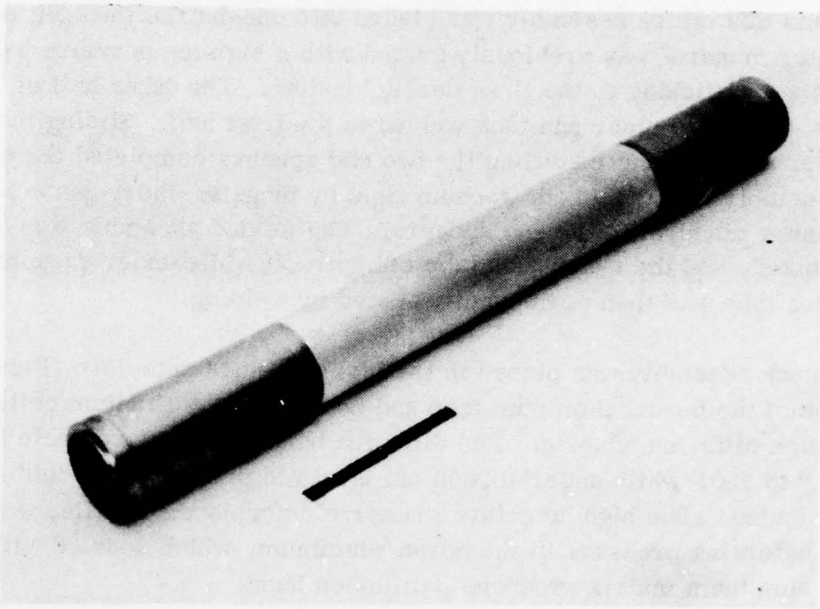

Figure 3-6. Diffusion-Bonded Tube Assembly

The bonded tube assembly was subjected to a special heat treatment that produces a 6061-T62 matrix with improved mechanical properties. This heat treatment consists of the following steps:

a. Heat to 975F and hold for one-half hour.

b. Water quench.

c. Cryogenic soak in liquid nitrogen for five minutes.

d. Age at 350F for eight hours.

Following heat treatment, the tube assembly was sent to the nondestructive evaluation laboratory for ultrasonic inspection.

3.4 NONDESTRUCTIVE EVALUATION

Each tube assembly was ultrasonically inspected to determine the extent and distribution of any non-bond areas in the diffusion-bonded titanium collar/tube joint. The ultrasonic inspection performed uses an immersion, pulse-reflection, through-transmission

technique employing a single transducer for transmitting and receiving the ultrasonic pulses, and a cylindrical reflector.

The test setup to accomplish the ultrasonic inspection for the tube and tube/collar joint is shown in Figure 3-7. The tube assembly is centered about a 1.50-inch-diameter reflector bar and immersed in a water bath. An ultrasonic transducer scans along the longitudinal axis of the tube. The transducer is spherically focused to provide a well-defined ultrasonic beam aligned to intercept the centerline axis of the tube and reflector bar, which reflects incident energy back through the water to the originating transducer. If the bond is not complete, the voids cause reflection of the incident energy at that point and hence do not return any significant energy back to the transducer. The C-scan display of the ultrasonic instrument is gated to monitor the presence or absence of the echo signals returned from the reflector bar. These reflector signal outputs are coupled to a recorder that produces a 1:1 ratio line modulated off/on depending upon the condition of reflection/no-reflection as processed by the ultrasonic instrument. A C-scan recording is produced by rotary indexing the tube until total coverage of the inspection area is obtained. Figure 3-8 shows a typical C-scan recording of a drag link tube/collar joint. C-scan recordings for all drag link tubes are presented in Appendix B.

C-scan recordings made under this program were intended for qualitative evaluation only and therefore a representative standard was not developed for instrument calibration. The procedure used here was to adjust the signal gain to a level that would produce a C-scan recording with the typical bond-disbond pattern expected. This gain level was then used to inspect both ends of the tube. The scans can be used to compare areas within the same tube, but comparison with other tubes should not be made. In a production situation, a standard would be used to calibrate the ultrasonic instruments prior to inspecting each tube.

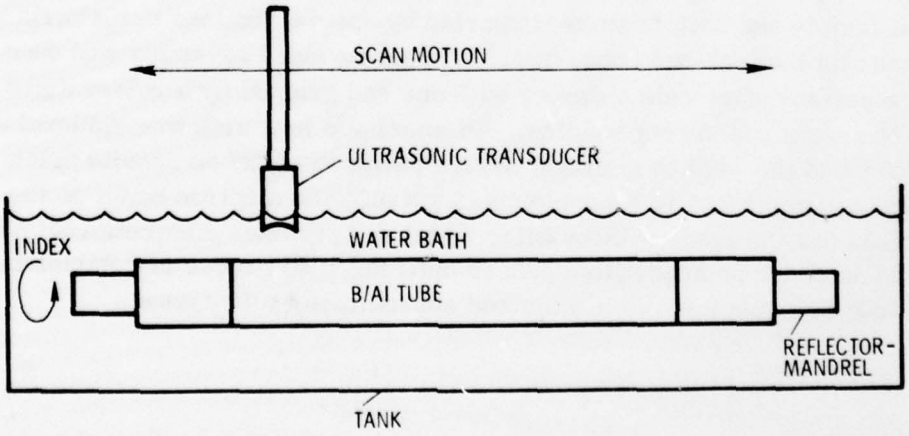

Figure 3-7. Ultrasonic Test Setup for Boron/Aluminum Tubes

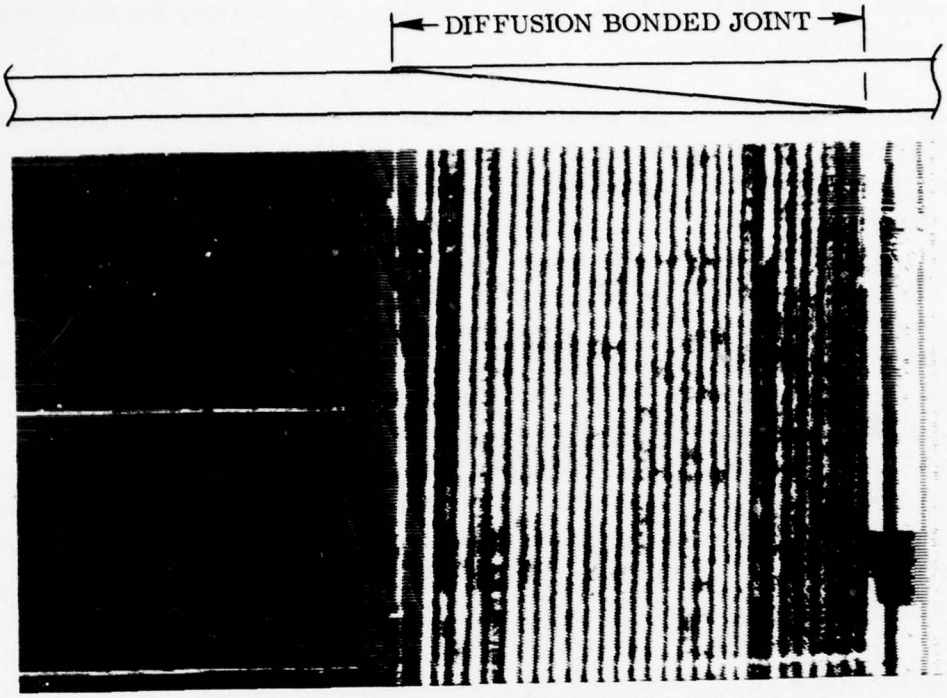

Figure 3-8. Typical Drag Link Tube/Collar Joint C-Scan

3.5 WELD ASSEMBLY

Following ultrasonic inspection, the weld zone on each collar was chemically cleaned in a solution of nitric and hydrofluoric acids and then tack welded to a titanium end fitting. Figure 3-9 shows a typical tube assembly and end fittings just prior to welding.

The tube assembly and fittings were supported by special fixtures to maintain proper alignment during the tack-weld operation. The tack-welded assembly was then fixtured inside the electron-beam weld chamber with one end gripped by a rotary drive mechanism that turns the assembly during welding. An aluminum heat sink was clamped around the collar adjacent to the weld to maintain the temperature of the composite below 350F. Welding was accomplished in a vacuum, using a diffused electron beam as the heat source. The first weld pass is made without filler metal and provides complete root penetration. Filler metal is added on subsequent passes until the weld groove is completely filled. A typical drag link specimen weld required approximately 25 passes.

3.6 SPECIMEN FINISHING

Following weld assembly, each specimen was returned to the machine shop for final machining operations. End fitting lugs were milled to proper thickness and parallel with tube centerline, and pin holes were bored to final diameter.

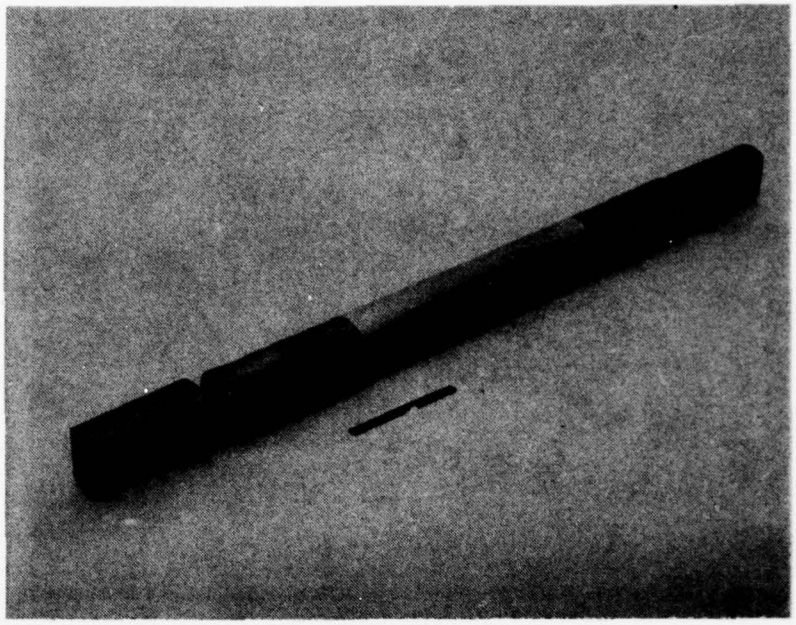

Figure 3-9. Typical Tube Assembly and End Fittings Before Welding

Final machining operations were required due to nonuniform weld shrinkage that can cause the end fittings to shift during welding.

Following final machining, specimens were protected from corrosion by:

a. Chemical conversion coating all surfaces.

b. Applying bead of polysulfide sealant at collar end to overlap collar and tube 0.10-inch minimum.

c. Applying one coat of epoxy prime to all interior and exterior surfaces except lug faces and pin holes.

d. Appling two coats polyurethane topcoat to all primed surfaces.

To reduce costs, only those specimens subjected to impact or corrosion were coated.

3.7 FABRICATION PROBLEMS

During the fabrication phase of the program several problems were encountered that were believed responsible for premature test failures. The problems encountered caused five of the tubes to be scrapped. Inner mandrel ruptures occurring during autoclave diffusion bonding were experienced on three occasions. Contamination of the titanium collars that degraded bonding was present to some degree on all tubes and forced scrappage of two otherwise acceptable tube assemblies. Slippage of the collar past the outer mandrel counterbore caused fiber breakage and premature statis test failure.

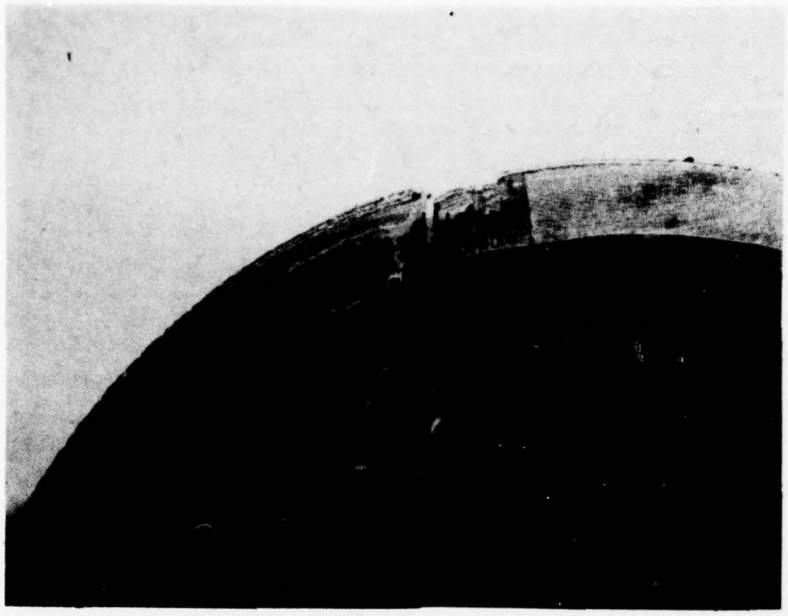

Figure 3.10. Mandrel Rupture on First Tube

3.7.1 MANDREL RUPTURE. The first composite tube assembly to be processed was lost due to rupture of the inner mandrel during autoclave diffusion bonding. The tube was not completely consolidated and diffusion bonded due to loss of pressure. The tightly wrapped composite material split through all layers at one location, as shown in Figure 3-10. The inner mandrel was forced to elongate excessively at this location until rupture occurred. Upon mandrel failure, vacuum was lost and no further pressure was transmitted to the composite tube.

Although previous mandrel ruptures on another program (Reference 2) were believed caused by problems with incoming mandrel material, the ruptures encountered on this program are related to mandrel sizes and elongation requirements. In sizing inner and outer mandrels, the annulus between the mandrels should be equal to or slightly larger than the thickness of the wrapped composite tape. If the annulus is too small the wrapped tape will not fit into the outer mandrel. If the annulus is too large, there will be a gap between the wrapped tape and the outer mandrel that must be closed during autoclave bonding. In order to close this gap successfully, both the composite wrap and the inner mandrel must elongate without rupturing.

In sizing the mandrels for the drag link specimen, excessive allowance was made for the wrapped tape. This inaccurate thickness allowance resulted from lack of data on the new winding machine's capabilities. Previous hand wrapping techniques produced 0.024-inch-diameter increase per ply. The diameter increase for the winding machine

was assumed to be 0.022 inch per ply but was found later to be on the order of 0.018 inch per ply; resulting in a 0.05-inch annular gap between the as-wrapped 28-ply composite tape and the split outer mandrel.

To solve this problem in a production situation, the outer mandrel diameter would be tailored to fit the as-wrapped tape with a minimal clearance. For this program, however, another solution was tried that would permit usage of all previously machined tooling and detail parts. Prior to inserting the wrapped tape into the split outer mandrel, the tape was manually unwound to the outer mandrel diameter thus eliminating the gap and reducing the elongation required of the composite tape. The inner mandrel was then permitted to elongate uniformly without rupturing. This unwinding technique was successful on 10 of the 13 tubes processed, and it is believed that mandrel ruptures could be eliminated completely be resizing the tooling.

3.7.2 COLLAR SLIPPAGE. Premature static test failure of specimen 001 appears to have been caused by slippage of one collar past the mandrel counterbore, which resulted in broken filaments. The composite tube fractured adjacent to the edge of one collar as illustrated in Figure 3-11.

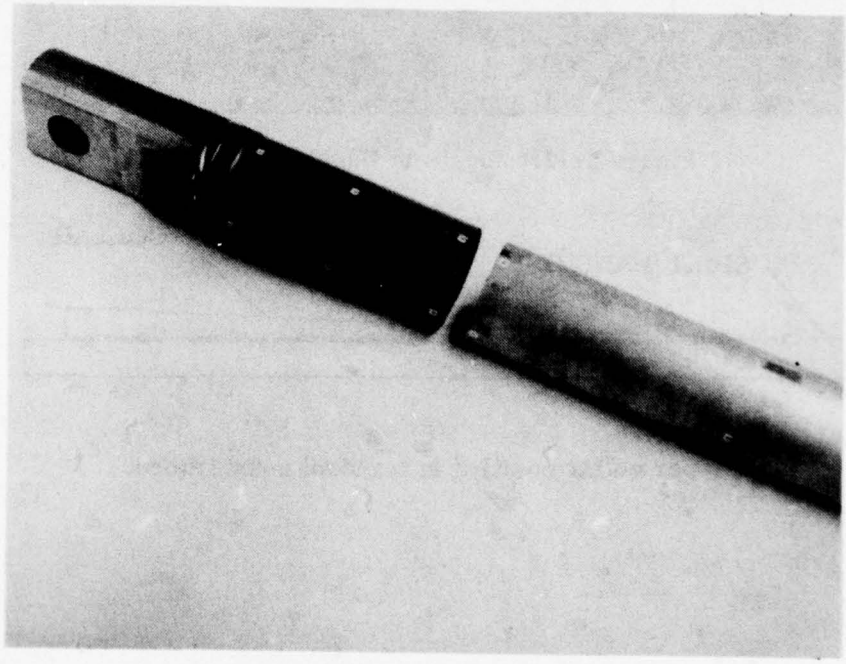

Figure 3-11. Failed Specimen 001

Visual inspection of the failed tube revealed collar damage adjacent to the failure surface in the form of an edge joggle. This condition, shown in Figure 3-12, was due to improper collar positioning in the split outer mandrel when autoclave pressure was applied. The collar, if positioned properly, is held in position by the mandrel counterbore as shown in Figure 3-13(a). This damaged collar slipped beyond the counterbore as shown in Figure 3-13(b).

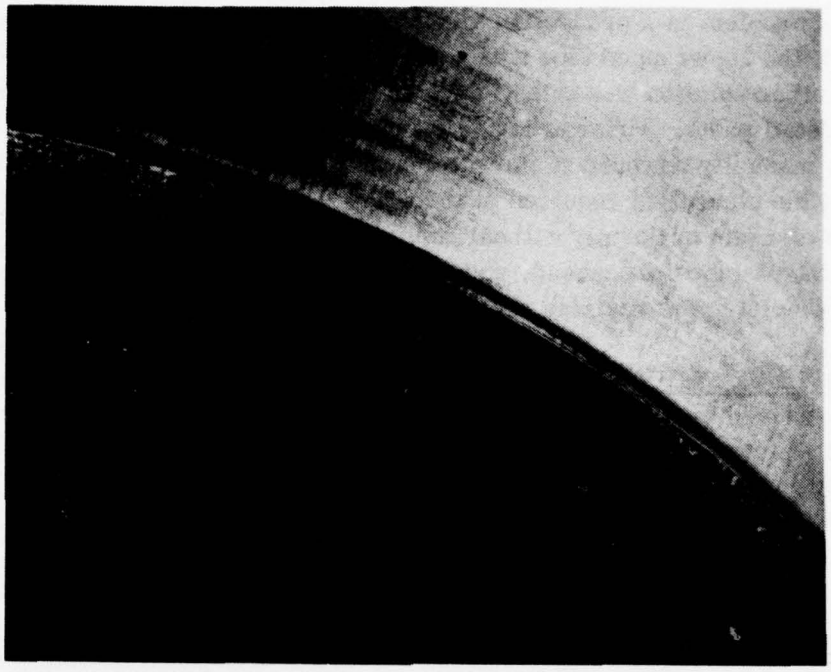

Figure 3-12. Joggle in Edge of Collar

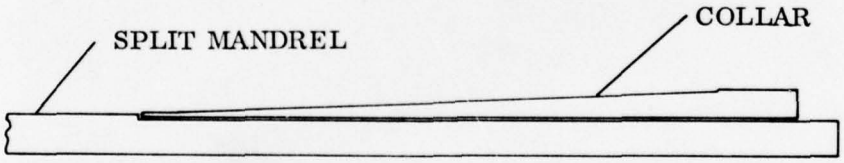

(a) Proper collar position in mandrel counterbore.

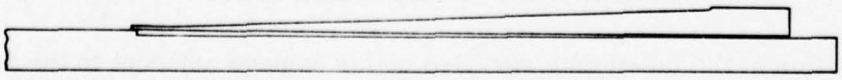

(b) Collar slippage beyond counterbore.

Figure 3-13. Collar positioning in Mandrel

The joggled collar was sectioned to determine the extent of composite damage. It would appear from Figure 3-14 that the two exterior plies of boron/aluminum were crushed during autoclave bonding. In addition to not carrying load, these broken plies created a notch-like stress concentration in an already high stress area. It is believed that premature failure was due solely to these broken surface plies.

To prevent recurrance of this problem, the mandrel counterbore was enlarged and the collar outside diameter temporarily increased. After autoclave bonding, the outside of each collar was machined to final configuration.

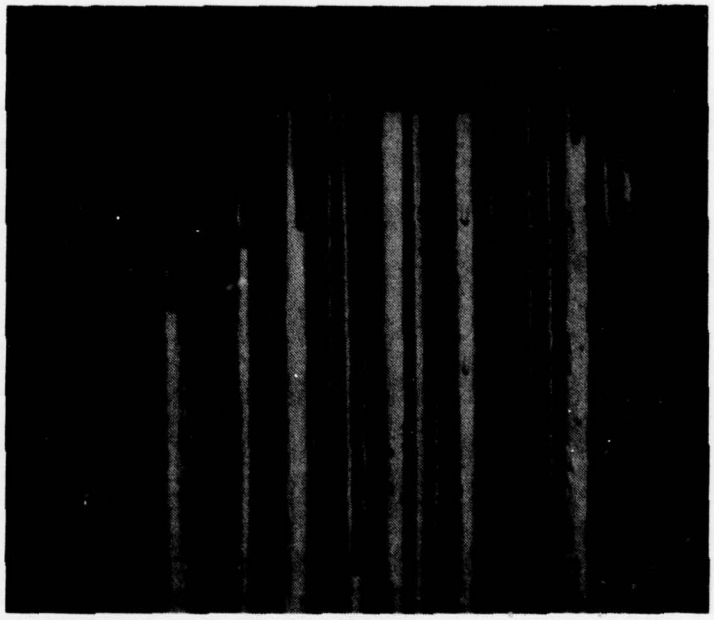

Figure 3-14. Cross Section of Joggled Collar Edge

3.7.3 DIFFUSION BONDED JOINT PROBLEMS. The most serious and difficult problem experienced on this program was obtaining consistent diffusion bonding of the composite tubes to the titanium collars. Unsatisfactory bond integrity was responsible for scrappage of two tube assemblies and premature failure of several others during static and fatigue testing.

With the helical wrap composite joint design, bonding of 100% of the joint overlap area is not possible since voids occur at the end of each ply step. In the desired tube joint, each ply is well bonded to the collar over a distance of 0.2-inch or 80% of the total overlap area. As a minimum, 50% of the total overlap area must be bonded with uniform distribution for acceptance.

Bond inspection was accomplished by the ultrasonic technique described in Section 3.4. The C-scans produced were used in qualitative evaluation of the tubular diffusion bonded joints to determine the general size and location of disbonded areas. C-scan recordings for all drag link tubes inspected are presented in Appendix B.

Several type of bond anomalies were found to exist. A brief description of each type is given below.

a. Disbonds — This bond discrepancy appears on C-scan recordings as an unbonded (white) area extending through several or through many plies, as shown in Figure 3-15. This type of bond irregularity is believed caused by contamination of the bond interface.

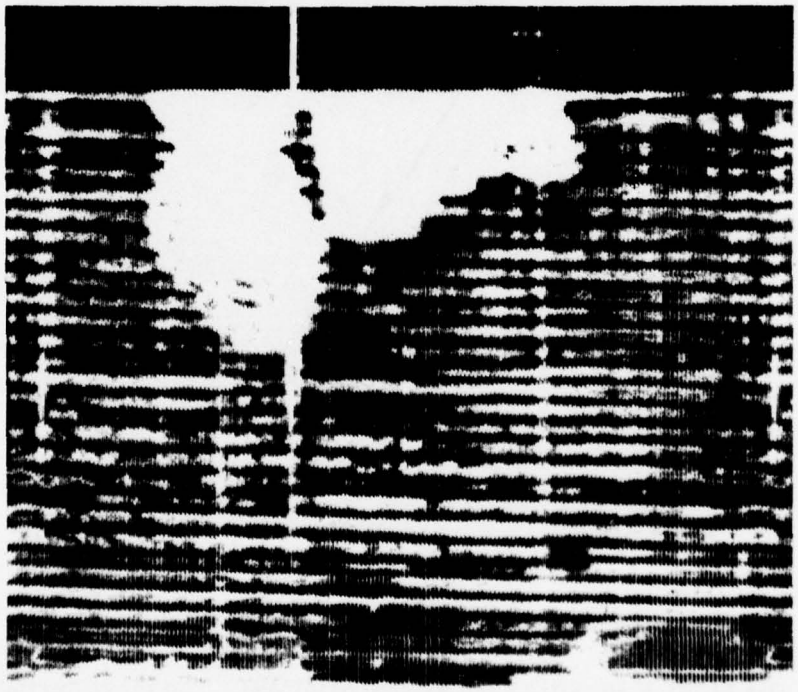

Figure 3-15. Typical Examples of Joint Disbonds

b. Ply-Tip Bonding — This condition, shown in Figure 3-16, appears as extremely narrow bonding at the ends of each ply, usually occurring in the outer 10 plies. Ply-tip bonding is believed caused by insufficient pressure at the joint interface.

c. Soft Bonding.— In a soft-bonded interface, the B/Al and titanium are in intimate contact but only about 10% of the contact area is metallurgically bonded. The bonding that occurs is uniformly distributed over the entire contact area in the form of thousands

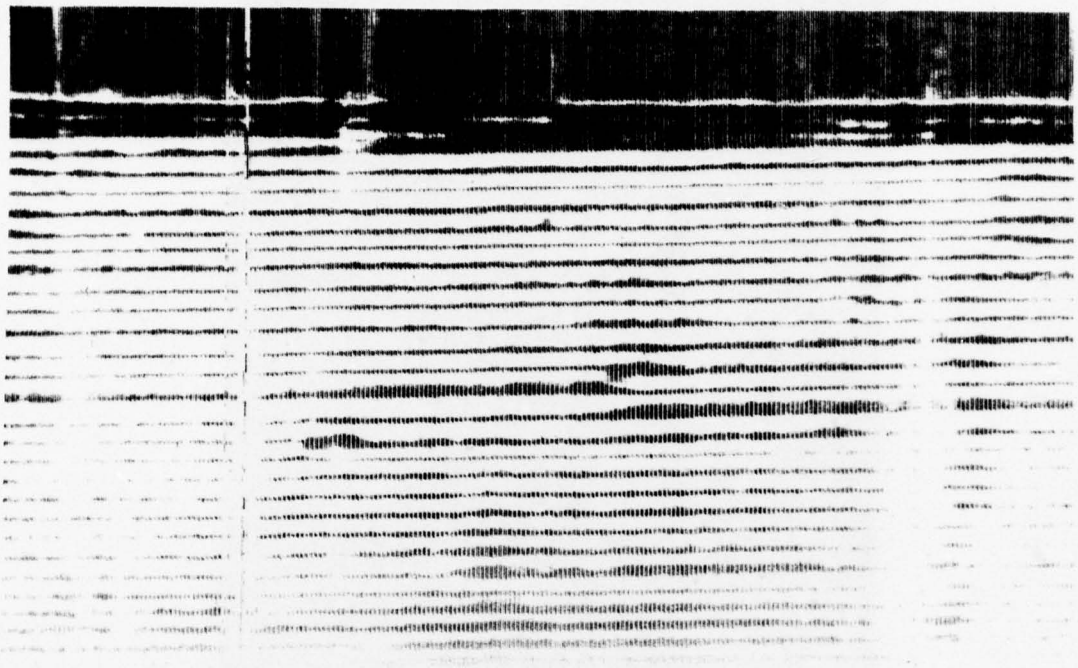

Figure 3-16. Typical Example of Ply-Tip Bonding

of tiny bonded areas per square inch. Soft bonding can be detected during a C-scan by properly adjusting the ultrasonic instruments using a representative standard. Soft bonding is believed caused by contamination of the joint interface but may be the result of insufficient time at bonding temperature.

During the course of tube fabrication, several modifications to the tube processing were tried in hopes of improving the tube/collar bonds. Aluminum metalizing of the titanium collars (see Figure 3-17) was found to be a source of contamination and was eliminated. Bonding of the last nine tubes was accomplished in a new 10,000 psi autoclave in lieu of the older 3,500 psi unit. A new autoclave cycle that incorporated a longer soak time at bonding temperature was used for tubes 012 and 013 with some success.

Since completion of drag link tube fabrication, several promising developments have been made on other programs that improve diffusion bond quality. Revised material specifications require a cleaner material with very little residual carbon contamination. Elimination of the B/Al air annealing operation reduces oxides on the tape surfaces and results in better diffusion bonds. An elevated temperature evacuation reduces the contaminants remaining in the pack assembly during bonding. It is believed that incorporation of these new material and process improvements would greatly improve the tube/collar bonds.

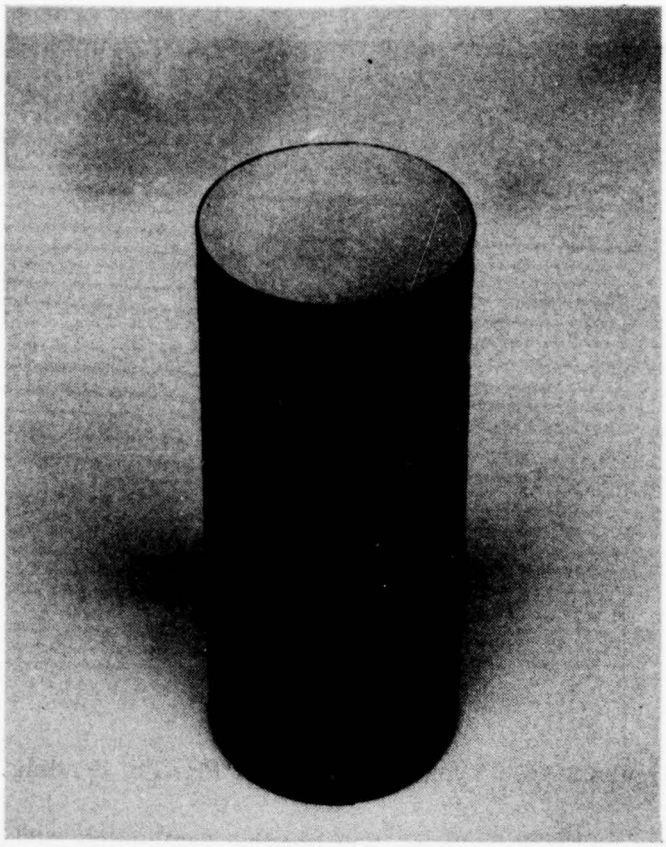

Figure 3-17. Aluminum Metal-Sprayed Collar

SECTION 4

TESTING

The overall program objective was to evaluate the application of boron/aluminum composite material to landing gear components of Navy aircraft with primary emphasis on evaluation of component reliability. The objective of the test phase of the program was to determine the effect of impact damage, notches, and corrosion on the static strength and fatigue life of the drag link specimens described in previous sections of this report. Eight full-size drag link specimens were subjected to the tests summarized in Table 4-1. This section of the report describes the tests conducted and the results obtained.

Table 4-1. Test Summary

Specimen Serial No.	Proof Test	Pebble Impact & Corrosion	Static Tension	Fatigue
001	X		X	
002	X		X	
003*	X			X
006	X			X
007*	X	X	X	
009*	X	X		X
012	X		X	
013	X			X
STEEL*	X	X		X

*Notched specimen

4.1 SPECIMEN CONFIGURATION

The test specimen configuration is shown in Figure 4-1. The tubular center portion of the specimen is identical to that of the flight configuration. The titanium fittings, however, were simplified to reduce material and machining costs.

4.2 PROOF TEST

All specimens were subjected to a static proof test, which consisted of loading in tension to 120% of design limit load. Proof testing was conducted in the static test machine shown in Figure 4-2 prior to environmental testing or notching of specimens. There were no specimen failures due to proof test loads.

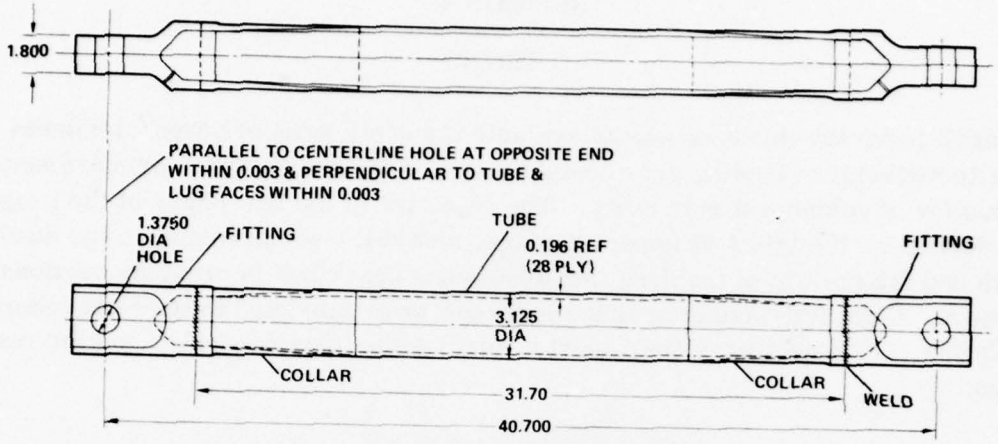

Figure 4-1. B/Al Landing Gear Test Specimen

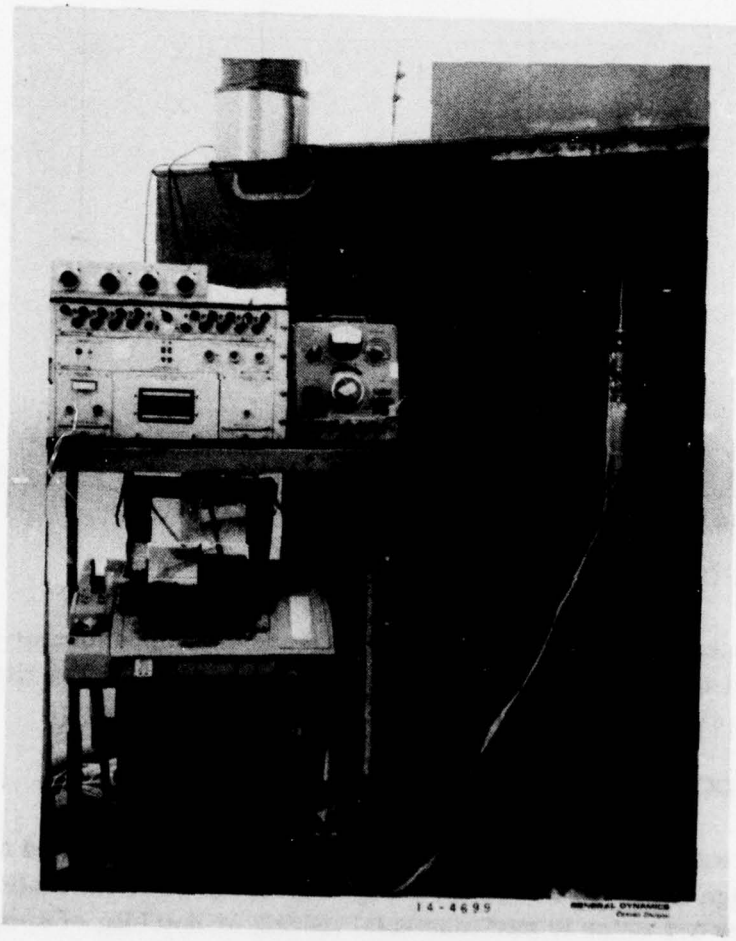

Figure 4-2. Static Test Setup

4.3 ENVIRONMENTAL EXPOSURE TESTING

Two drag link specimens were subjected to pebble impact and corrosion testing to simulate the types of damage that Navy landing gear components can see in service.

The boron/aluminum specimens were coated prior to testing with a typical landing gear corrosion protection system consisting of chemical conversion coating, epoxy primer, and polyurethane topcoat. In addition, circumferential bands of polysulfide sealant were applied where the composite tube enters the collars. This sealant, covering approximately 1/8 inch of both the tube and collar, is intended to prevent galvanic corrosion at the titanium/composite interface.

The specimens, along with a baseline steel link, were subjected to alternating impact and corrosion testing as follows:

a. Impact each specimen five times.

b. Subject to 14 days corrosion testing.

c. Impact five more times.

d. Subject to 14 days corrosion testing.

This procedure superimposes a corrosive environment on a damaged part to more accurately simulate the actual conditions expected in service.

4.3.1 PEBBLE IMPACT TEST. The pebble impact testing conducted here was designed to produce surface damage similar to that created by runway debris impacting the component during takeoff and landing. The composite drag link specimens were impacted with actual pea gravel while under load at typical takeoff and landing velocities.

Experimental work was conducted prior to actual testing to select equipment, materials, and a test method for conducting the pebble impact tests.

4.3.1.1 Impact Test Equipment. Early in the program, work was initiated to develop a gun system to propel pebbles of various sizes at the desired velocity of 200 feet/second. Initial firing tests using the method of propelling pebbles through a 50-caliber, smooth-bore barrel with specially loaded cartridge cases resulted in some undesirable effects. To maintain repeatability in the low-velocity ranges, the cases had to be tamped with filler material to provide proper confinement for initiation and completion of powder charge burning. The tamping material was blown out the barrel along with the pebble. This tamping material would not impact the test specimen, but it could possibly cause a false velocity measurement unless the gun were moved a significant distance from the velocity screens and thus from the test specimen. Furthermore, the velocity and powder charge relationships were not linear in the velocity ranges desired, and even with tamping the repeatability was marginal.

A method using a simple tube with an air regulator and an attached solenoid valve was tried. By regulating the air pressure behind the solenoid, the velocity of a pebble ejected from the tube was uniformly controlled when the solenoid valve was electrically activated. A foam wad of the same diameter as the tube was used as a piston to push the pebble. The maximum velocity was found to be a function of both air pressure and the length of the tube, and over 400 feet/second was attainable with the design used. This air gun was selected for all further tests based on its good repeatability and low recurring cost.

Projectile velocities were determined using a photoelectric chronograph. This instrument consists of two photoelectric screens set one foot apart and an electronic stopwatch controlled by the screens that measures the time required to travel the one-foot distance. This time reading can then be used to calculate projectile velocity.

Drag link specimens were installed in the static test machine shown in Figure 4-2 and placed under 80,000 pounds tension load during impact testing.

4.3.1.2 Projectile Selection. Preliminary testing was conducted to select a reasonable size pebble that would produce visible surface damage when impacting a B/Al drag link at 200 feet/second. The desired damage included chipped paint, exposed and broken filaments, and some local indentation. Some preliminary shots were made at a similar boron/aluminum tube configuration using several different pebble sizes. Nominal 1/4- and 3/8-inch-diameter pebbles at 200 feet/second did not produce significant visible damage and were thus eliminated from consideration. Pebbles weighing 1.4 to 1.6 grams and of approximately 1/2-inch diameter were selected for all subsequent tests based on their ability to consistently produce the desired magnitude of surface damage. Figure 4-3 shows several typical 1/2-inch projectiles used in the impact testing. All pebbles were selected from commercial granite gravel. Only those that were relatively smooth and round, between 7/16- and 9/16-inch diameter, and weighing between 1.4 and 1.6 grams were used for impact testing.

4.3.1.3 Impact Testing of Drag Link Specimens. Impacting of composite drag link specimens 007 and 009 was accomplished at Convair's Ballistic Test Range in the test setup shown in Figure 4-4. The specimens were installed in the static test machine and loaded in tension to 80,000 pounds. Each specimen was then impacted with 1/2-inch-diameter pebbles weighing from 1.4 to 1.6 grams at velocities between 170 and 210 feet/second. Impact locations and projectile velocities for the composite specimens are shown in Figure 4-5 and for the steel link in Figure 4-6. In almost all instances the projectiles shattered on impact, producing significant damage at the point of initial contact surrounded by less severe damage due to pebble fragments.

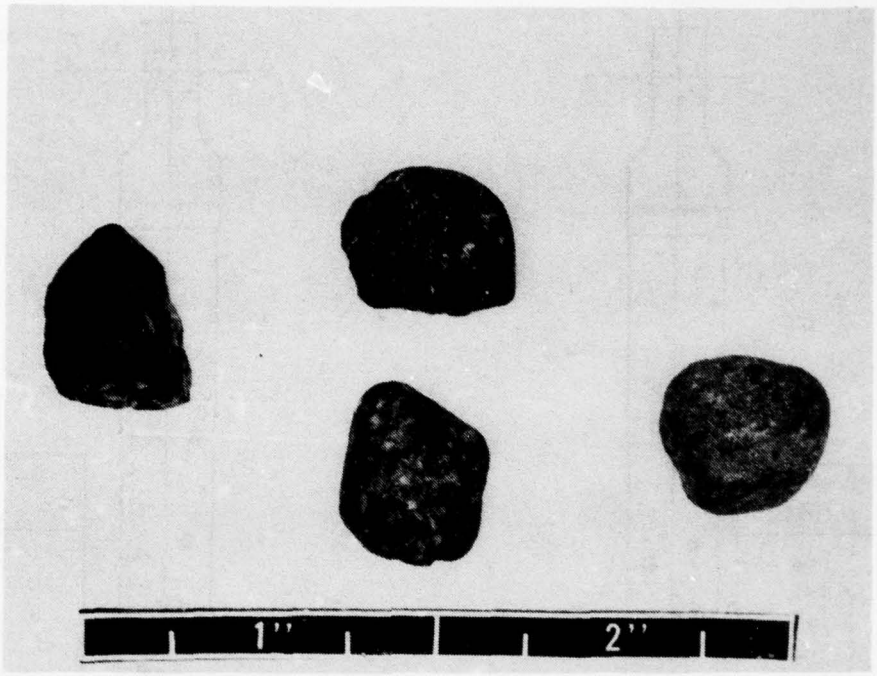

Figure 4-3. Typical 1/2-inch Projectiles

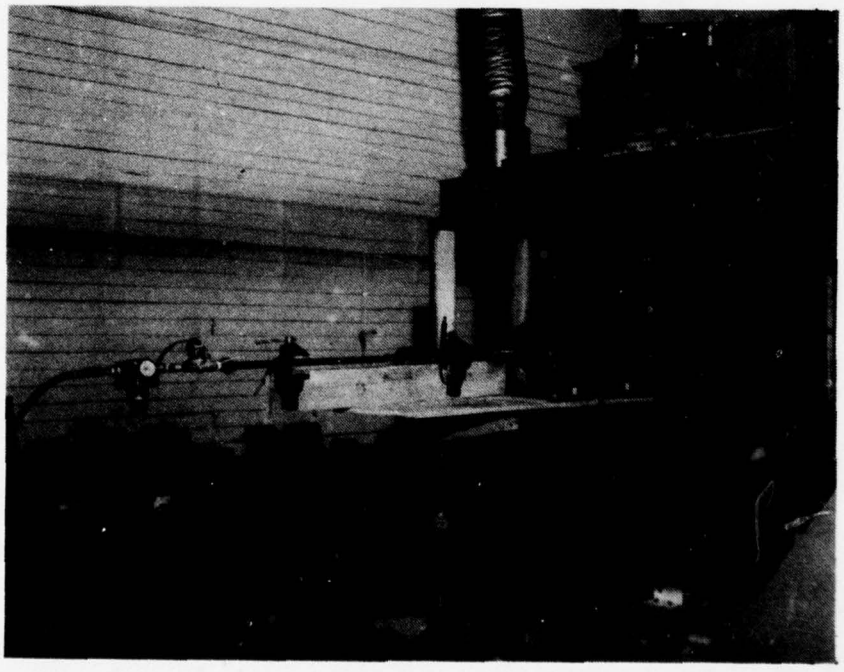

Figure 4-4. Impact Test Setup

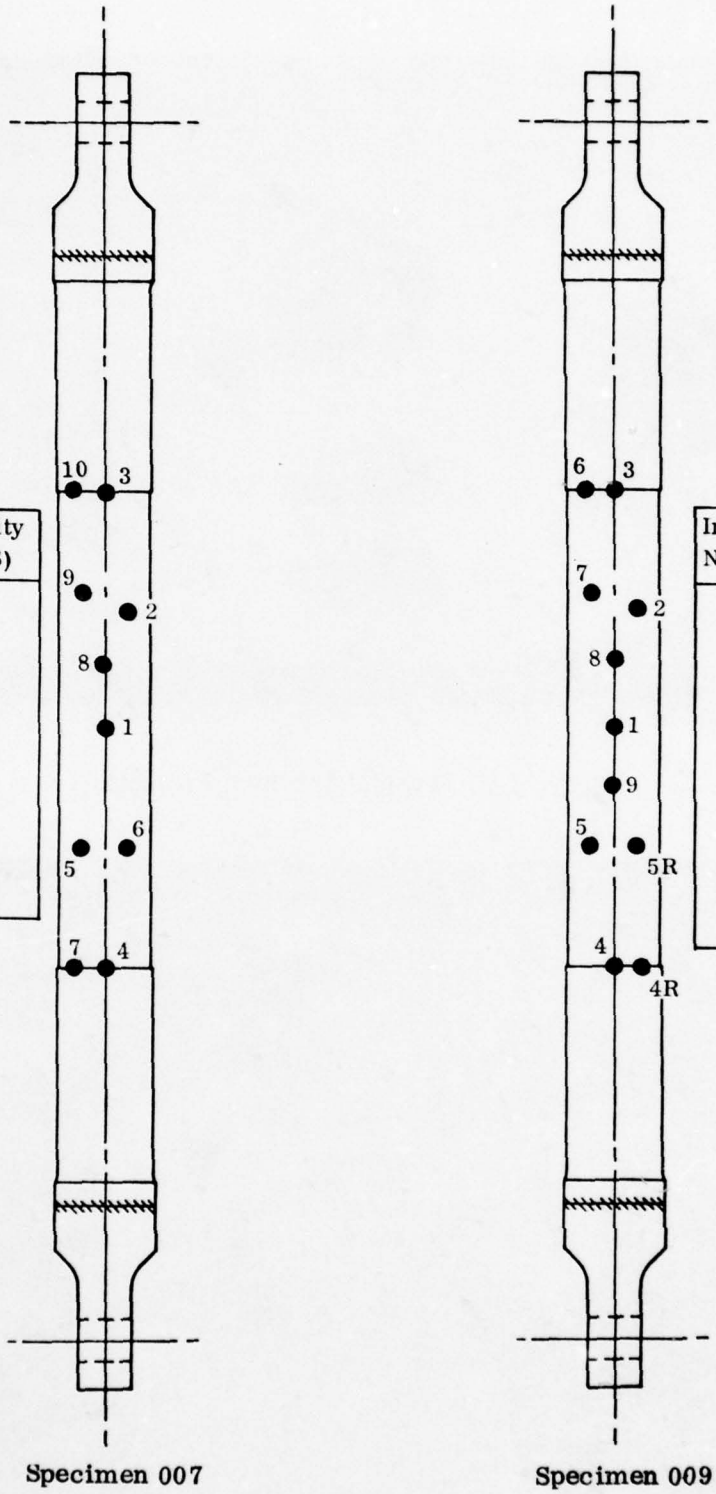

Impact No.	Velocity (FPS)
1	186
2	187
3	195
4	189
5	177
6	203
7	191
8	196
9	194
10	206

Specimen 007

Impact No.	Velocity (FPS)
1	201
2	184
3	198
4	187
4R	176
5	N/A
5R	204
6	170
7	173
8	191
9	209

Specimen 009

Figure 4-5. Pebble Impact Locations and Velocities — B/Al Specimens

Impact No.	Velocity (FPS)
1	209
2	199
3	201
4	193
5	206
6	207
7	191
8	179
9	197
10	179

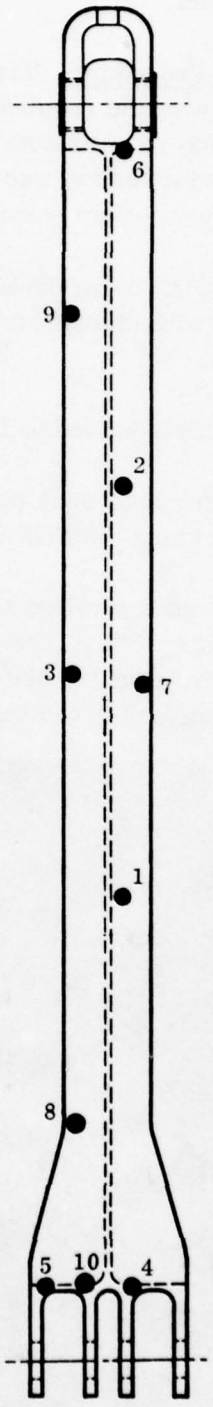

Figure 4-6. Pebble Impact Locations and Velocities — Steel Drag Link

4.3.2 CORROSION TEST. The corrosion environment the specimens were subjected to was an agressive one that vigorously attacks bare aluminum alloys and inferior organic coating systems. It was intended to simulate a severe corrosive aircraft carrier environment.

4.3.2.1 Corrosion Test Procedure. The corrosion testing was conducted in a salt spray chamber complying with the requirements of ASTM B117-64. The two drag link specimens (007 and 009) were exposed to six-hour cycles for a total of 28 days. As noted above, the corrosion testing was interrupted after 14 days for additional impact testing. Each six-hour cycle consisted of:

a. A forty-five minute spray using 5% sodium chloride solution which had been acidified to a pH of 3 with glacial acetic acid. The atomization rate was 1 - 2 ml per hour.

b. A two-hour purge with air heated to 120° F.

c. A three and one quarter hour soak period at 45 to 95 percent relative humidity achieved by using "wet bottom" conditions.

The cabinet temperature was controlled at 120 $\pm$ 5° F at all times and the saturator tower was maintained at 135 $\pm$ 5° F. The drag link specimens were positioned 30 degrees to horizontal and rotated 180 degrees daily. Figure 4-7 shows the two specimens plus a steel drag link in the cabinet.

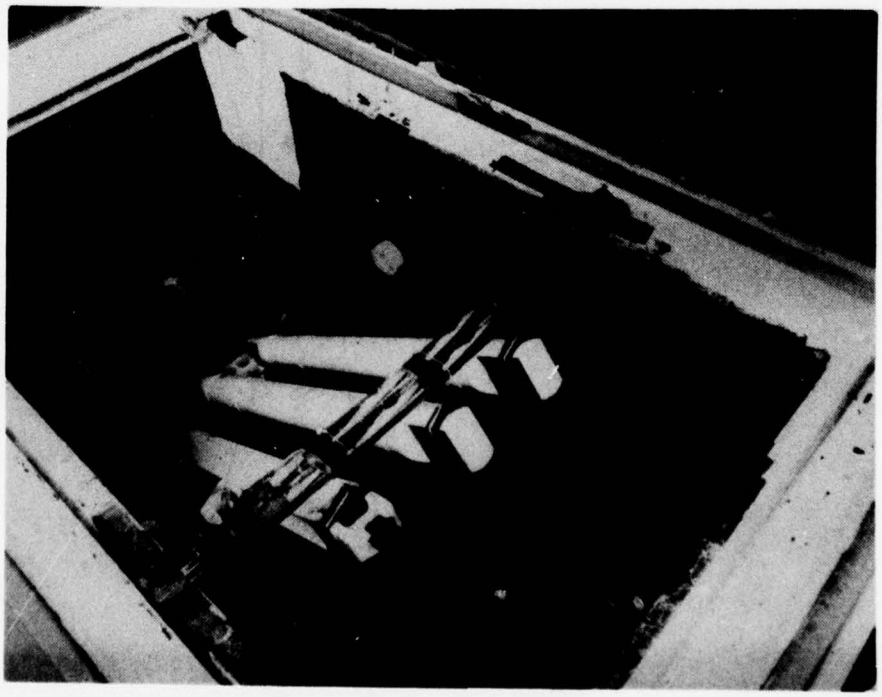

Figure 4-7. Steel Link and Boron/Aluminum Links in Salt Spray Chamber

4.3.2.2 Corrosion Test Results. Examination of both specimens following the 28 days of corrosion exposure revealed very little evidence of any corrosion having occurred. This was surprising since it had been expected substantial corrosion might occur in the regions where impact testing had resulted in significant damage.

4.4 NOTCHING

Specimens 003, 007 and 009 were notched in accordance with Figure 4-8. Notches were electrical discharge machined (EDM'd) in the specimens.

4.5 STATIC TESTING

The results of static and fatigue testing are summarized in Table 4-2. Static testing was accomplished in the test machine shown in Figure 4-2. The test machine has a 400,000-pound hydraulic ram that may be used to apply either tension or compression loads. Details of the static tests on the composite drag links are as follows:

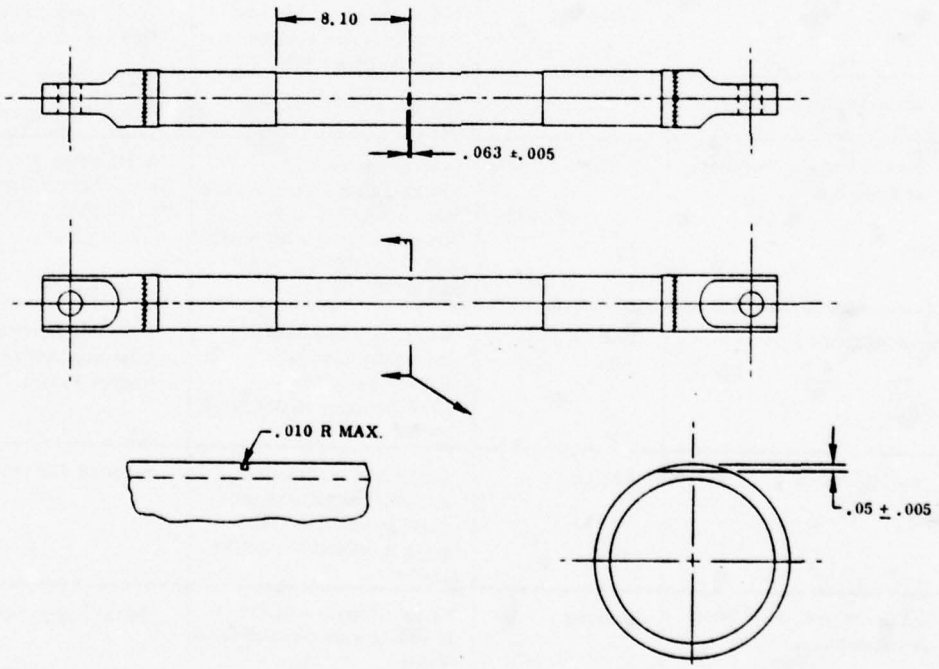

Figure 4-8. Notched Specimen Configuration

Table 4-2. Summary of Test Results

Specimen No.	Specimen Condition	Type of Test	Test Results	Comments
001	As fabricated	Static	Failed at 93% DUL	Broken fibers at edge of titanium collar prior to testing
002	As fabricated	Static	Failed at 91% DUL	"Ply tip" bonding noted at B/Al to titanium interface
003	Notched	Fatigue	Two lifetimes at 75% Design Fatigue Load levels then failed after 0.5 lifetime at 80% Design Fatigue Load levels	Large B/Al to titanium disbond noted prior to testing Notch depth = 0.05"
006	As fabricated	Fatigue	Failed after .2 lifetime at 90% Design Fatigue Load levels	"Soft" bonding noted at B/Al to titanium interface
007	Pebble impact, corrosion and notched	Static	Failed at notch at 90% DUL	Notch depth = 0.05"
009	Pebble impact, corrosion and notched	Fatigue & Static	Two lifetimes at 80% Design Fatigue Load levels, then .4 lifetime at 90% Design Fatigue Load levels then failed during calibration at 72% DFL	Initial notch depth = 0.05" Notch depth increased to 0.10" after .75 lifetime at 90% DFL
012	As fabricated	Static & Fatigue	Survived static test at 165% DLL then failed after 0.2 lifetime at 100% Design Fatigue Load levels	Specimen fabricated following several improvements
013	As fabricated	Fatigue	Survived 0.53 lifetime at 100% Design Fatigue Load levels then failed when inadvertently overloaded	Same as 012 above
Steel Link	Pebble impact, corrosion and notched	Fatigue	Failed after 1.1 lifetimes at 70% Design Fatigue Load levels	Notch depth = 0.05"

Specimen 001 - This specimen was first loaded in compression to 141,000 pounds (100% Design Ultimate Load) and then in tension to failure. Failure occurred at 220,000 pounds (93% Design Ultimate Load) when the composite tube fractured adjacent to the edge of one titanium collar, as shown in Figure 4-9. Visual inspection of the failure revealed collar damage adjacent to the failure surface in the form of an edge joggle. This condition, which is discussed in detail in paragraph 3.7.2, results in broken fibers and a notch-like stress concentration in an already high stress area. It is believed failure was primarily due to these broken surface plies.

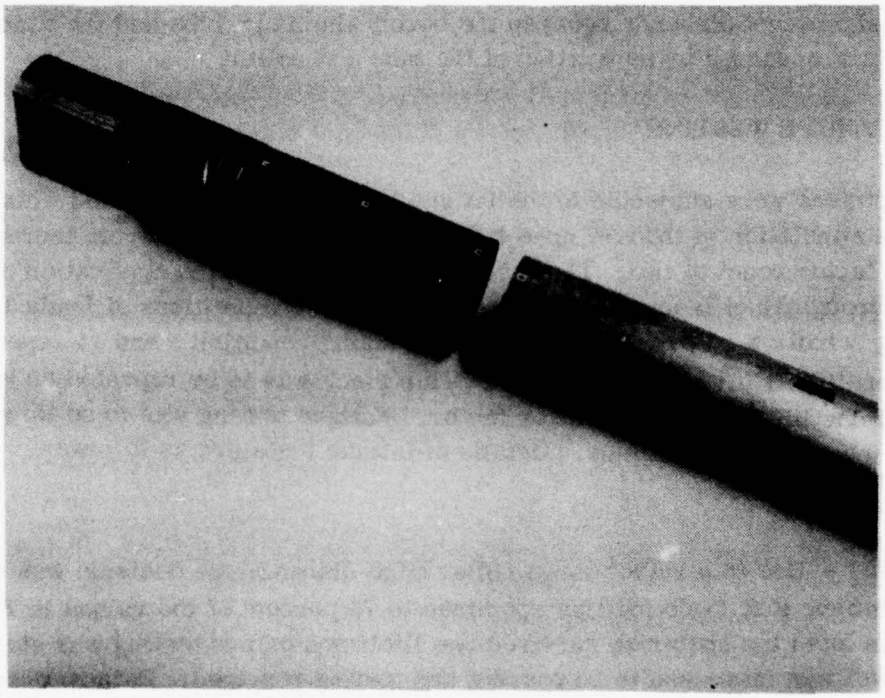

Figure 4-9. Failed Specimen 001

Specimen 002 - This specimen was first loaded in compression to 94,000 pounds (100% Design Limit Load) and then to failure in tension. Failure occurred at 215,000 pounds (91% Design Ultimate Load). Examination of the failure indicated failure of the outer three plies of the boron/aluminum tube inside the collar. The poor diffusion bonding condition that was observed is referred to as "ply-tip" bonding and is discussed in paragraph 3.7.3. This condition is believed to be caused by insufficient pressure at the joint interface during fabrication.

Specimen 007 - This specimen was first loaded in compression to 94,000 pounds (100% Design Limit Load) and then to failure in tension. Failure occurred through the notch at 207,850 pounds (133% Design Limit Load).

Specimen 012 - This specimen was fabricated using a procedure that incorporated various process improvements compared to that used to fabricate earlier specimens. These improvements included a new autoclave cycle that incorporated a longer soak time at bonding temperature. The specimen was first loaded in compression to 94,000 pounds (100% Design Limit Load) then tested statically in tension to 260,000 pounds (165% Design Limit Load). The test was terminated to prevent possible damage to the test set-up. The specimen was then fatigue tested at design spectrum loads (see Table 4-3) and failed after 0.2 lifetime. Pre-fatigue data indicated the presence of significant disbonds between the boron/aluminum tube and the titanium collar. Failure occurred by separation of the tube and collar.

4.6 FATIGUE TESTING

Several specimens were subjected to the fatigue loads shown in Table 4-3 which is based upon a simulation of the A-7 nose landing gear drag link spectrum increased by a scatter factor count of two. The test procedure involved the application of load numbers 1 through 13 of landing condition 4 followed by 7 repetitions of loads 1 through 13 of landing condition 3, then 28 repetitions of landing condition 2 and 14 repetitions of landing condition 1 for a 50 cycle-block. This block was to be repeated 80 times to reproduce one lifetime with a scatter factor. Fatigue testing was to be terminated after 160 blocks, i.e., 2 lifetimes. Details of fatigue tests are as follows:

Specimen 003 - Due to a rather large collar edge disbond, the decision was made to reduce all fatigue test loads for this specimen to 75 percent of the values in Table 4-3. At this level the specimen survived two lifetimes before testing was stopped. The load level was increased to 80 percent and testing resumed. Failure occurred in the joint area after 0.5 lifetime. The original collar edge disbond propagated longitudinally into the joint until the total net section area was unable to sustain the catapult tension load. Propagation of the disbond was indicated by strain readings taken long before failure. The failed specimen is shown in Figures 4-10 and 4-11.

Specimen 006 - This specimen failed after 19 percent of the required number of load cycles. The failure, shown in Figure 4-12, occurred at the boron/aluminum to titanium diffusion-bonded joint interface. Visual examination of the joint revealed large areas of "soft" bonding at the interface between the outer four plies of boron/aluminum and the titanium collar. Premature failure of the specimen can be attributed to this "soft" bonding condition which probably results from insufficient time at the diffusion bonding temperature. A more detailed explanation is given in paragraph 3.7.3

Table 4-3. A-7 Nose Landing Gear Drag Link
Fatigue Loading Spectrum

	Load No.	Load (pounds) (+) Tension, (-) Compression Landing Condition 1	2	3	4
Buffing Cycle	1	-25,300	-25,300	-25,300	-25,300
	2	-71,600	-71,600	-71,600	-71,600
	3	-25,300	-25,300	-25,300	-25,300
	4	-71,600	-71,600	-71,600	-71,600
Catapult	5	-25,300	-25,300	-25,300	-25,300
	6	+157,000	+157,000	+157,000	+157,000
Landing Cycle	7	-47,000	-94,000	-13,500	-14,800
	8	-29,000	-49,900	-70,200	-87,700
	9	-47,000	-94,000	-13,500	-14,800
	10	-29,000	-49,900	-70,200	-87,700
	11	-47,000	-94,000	-13,500	-14,800
	12	-20,300	-34,200	-48,600	-62,300
	13	-25,300	-25,300	-25,300	-25,300
No. Cycles in 50-Cycle Block		14	28	7	1
Total Cycles in One Lifetime		560	1,120	280	40

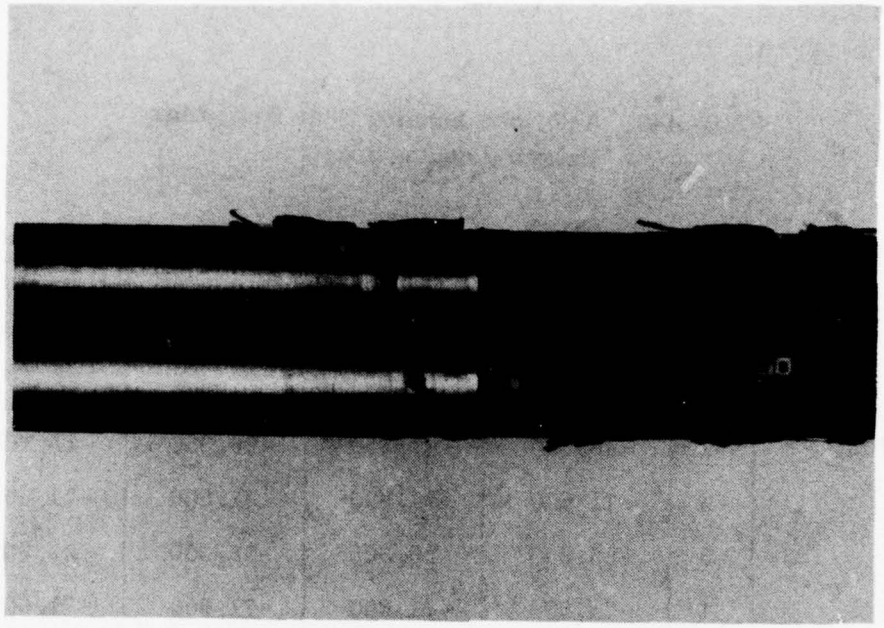

Figure 4-10. Failed Specimen 003

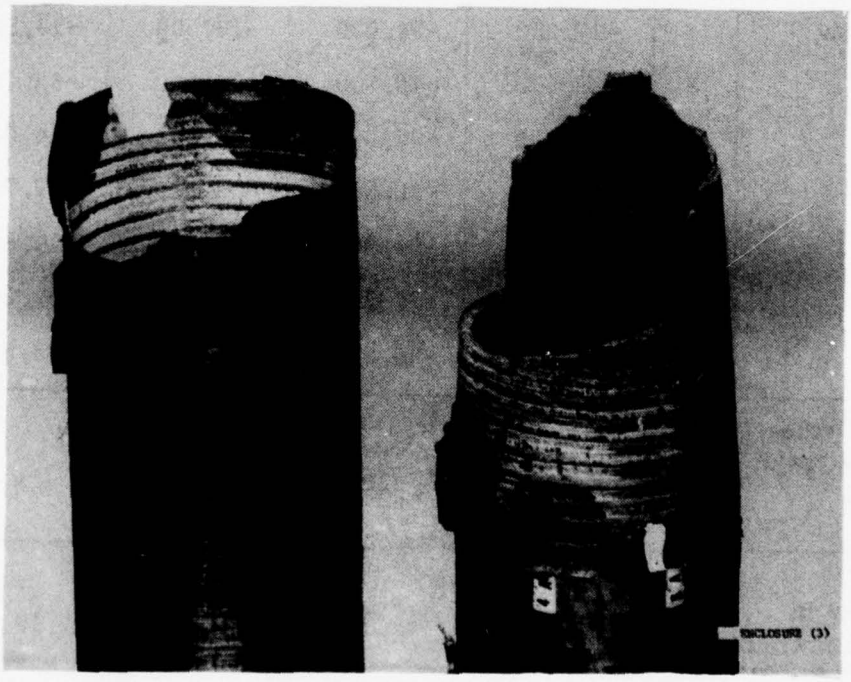

Figure 4-11. Specimen 003 Showing Failure of Joint Area

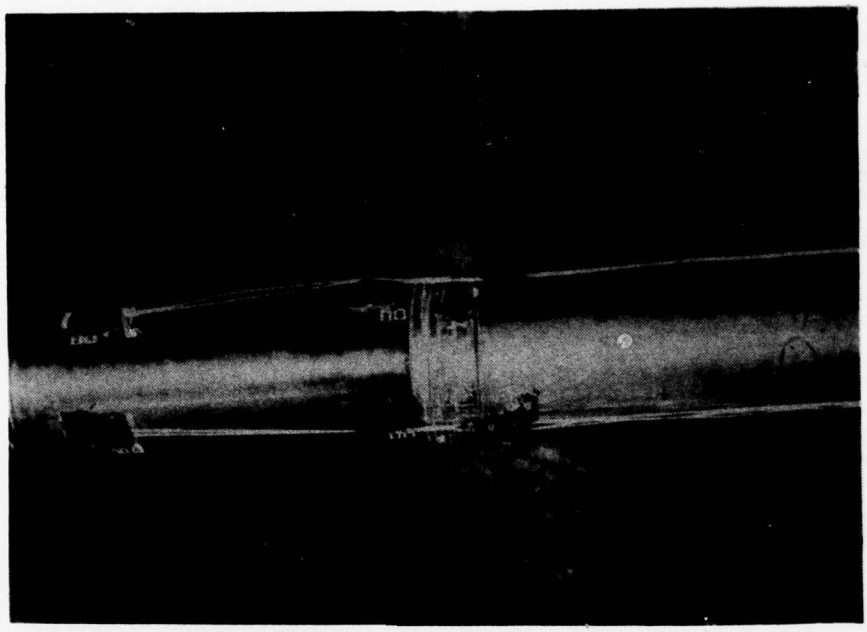

Figure 4-12. Failed Specimen 006

Specimen 009 - This specimen survived 2 lifetimes at 80% design spectrum fatigue load levels plus 0.4 lifetime at 90% design spectrum fatigue load levels. The 0.05-inch deep notch was increased to a depth of 0.100 inch to produce failure through the notch rather than in the joint area. The specimen was then failed in tension at 72% of Design Limit Load. Failure, as expected, occurred after notch, see Figure 4-13.

Specimen 012 - This specimen was originally scheduled for static testing only, but was both static and fatigue tested. See paragraph 4.5 for details.

Specimen 013 - This specimen was fabricated in the same manner as specimen 012 (see paragraph 4.5). It survived 0.53 lifetime at 100% design spectrum fatigue load levels. Prefatigue data indicated a disbond in the collar area. During a static tension calibration test after block 21, the specimen was inadvertently overloaded to failure. Failure occurred at approximately 190,000 pounds (121% Design Limit Load) when the collar and tube separated. Figure 4-14 shows the failure region.

Steel Link - An A-7 steel production drag link was notched (0.10" deep) and fatigue tested. It survived 1.1 lifetimes at 70 percent design spectrum fatigue load levels. Failure occurred through the notch during the catapult cycle.

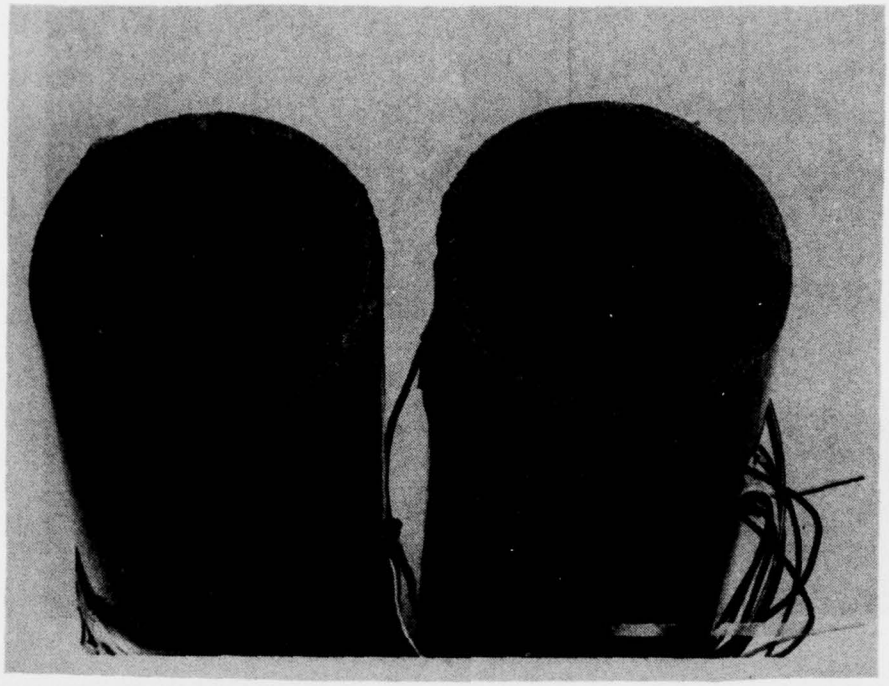

Figure 4-13. Failed Specimen 009 - Failure occurred through a 0.10 inch deep notch in the boron/aluminum tube wall.

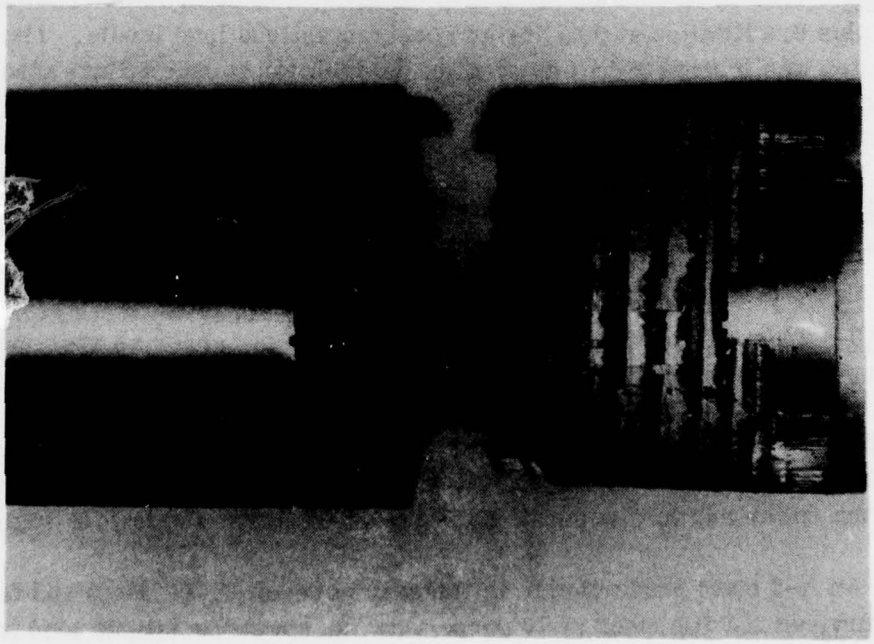

Figure 4-14. Failed Specimen 013

SECTION 5

OBSERVATIONS AND CONCLUSIONS

1. A Boron/aluminum-titanium A-7 nose gear lower link was designed and fabricated that could be substituted for the existing 300M steel link. A direct substitution, however, would require a redesign of the fitting and a method of nesting the strut without interference.

2. A Boron/aluminum link that had been damaged by pebble impact then subjected to a corrosive aircraft carrier type environment, notched, then statically tested in tension to failure demonstrated no reduction in strength over similar links tested in the as-fabricated condition. No degradation due to pebble impact or corrosion was apparent on the B/Al tubes since specimen 001 and 007 in Table 4-2 failed at almost the same value, and failure occurred at the notch.

3. A Boron/aluminum link that had been damaged by pebble impact then subjected to a corrosive aircraft carrier type environment, and notched, survived two lifetimes when fatigue tested at 80% of design fatigue loads. This compares favorably with an existing 300M steel lower link which, when notched and fatigue tested at 70% of design fatigue loads, failed after 1.1 lifetimes. The two links were tested in the same manner.

4. Diffusion bonding problems early in the program resulted in premature failure in static tension (92% DUL) and the decision to reduce fatigue test loads to 75 - 80% of Design Levels. The cause of the problem was eventually traced to the inconsistent quality of boron/aluminum tape shipped to Convair by the vendor. In the vendor's process, an organic fugitive binder is used to hold the boron filaments in place prior to the top and bottom aluminum foils being pressed around the filaments to make the tape. The adhesive is subsequently removed during processing by heating and vacuum pumping. A quantitative analysis on some of the tape samples at Convair revealed a large concentration of carbon which was traced back to residual deposits of fugitive binder in the tape. The high carbon content in the tape seriously interfered with the diffusion bonding process, contaminating the titanium collars and causing areas of disbond in the joint. Once the cause of the problem was pinpointed, several steps were immediately taken to prevent a recurrence of this problem. First, larger vacuum pumps were installed at the vendor and stricter pumping and vacuum testing requirements were stringently enforced to ensure that the fugitive binder was eliminated from the tape. Second, the vendor process specification and the Convair material specification were rewritten to reflect these changes. Finally, each lot of tape received at Convair now requires a carbon analysis test which rejects any tape that has higher than a 0.030% carbon content, which was found to be acceptable upper limit by test. Since the completion of the program, hundreds of Boron/aluminum components of similar design have been made for other programs (i.e., Space Shuttle Mid-fuselage). Diffusion bonding is now one of the least significant causes for rejection. Of

the last 500 tubes made in the Space Shuttle Mid-Fuselage Program since May 1975, only one tube was rejected and scrapped due to a questionable C-scan and diffusion bond.

5. It has been recently demonstrated on another program (Contact NAS1-13952 Low Cost High Performance Boron/Aluminum Titanium Diffusion Joints) that the scarf ratio can be reduced from 40t to 20t in an improved lightweight collar design. Three full size drag links for the Space Shuttle Main Landing Gear were proof tested and delivered with this new design. This represents a savings of 40% of the weight of the collars.

6. An evaluation of the current joint design indicates that the boron/aluminum stepped taper limits fatigue life because of the built-in stress risers. Clearly, by reversing the rolling of the tape so the helical taper is on the inside of the tube opposite the collar, an uninterrupted bond can be made between the B/Al and the collar. This change should increase fatigue life without changing the basic process or increasing costs. Analysis of past fatigue tests indicates that the first partial failure occurs at the outermost ply nearest the end fitting and progresses step by step toward the center until total failure takes place. This is a progressive failure mode and does not happen instantaneously. Eliminating the steps should transfer the load more efficiently. Since the bond area is almost doubled and the shear stress is halved, the joint is stronger both in static and fatigue. Reversing the taper causes a slight eccentricity between the collar and the tube. However, the overturning moment in tubular lap joint is easily resisted by the cirular collar configuration.

7. Advances in Boron fiber technology have made the 8-mil filament available as a replacement for 5.6-mil in B/Al tape. Though no tubes have been tested using the larger fiber, coupon tests indicate that no decrease in properties occurs. On the contrary, greater filament cross section and stiffness should better resist the stress concentration at the collar/tube junction and increase the static strength of the tubes. In addition, raw material and processing costs will decrease.

8. Improved analytical methods will be required to determine the stresses in the bond area. The complex stepped scarf joint coupled with the use of dissimilar metals and superimposed thermal residual stresses make an analysis difficult with current technology.

9. In a recent study made by Convair for NASA Langley Research Center on Boron Aluminum Landing Gears for Space Shuttle (NAS 1-13952, Report No. CASD-NAS-78-006) a less expensive material was proposed by Convair as an alternate to titanium. Substitution of a precipitation hardened stainless steel (17-4PH or PH13-8Mo) in place of titanium was intended to fulfill all the process requirements of a tube attachment as well as provide cost savings (since the raw material cost is considerably lower). Weight saving was originally not anticipated.

   A B/Al tube with attachments made from 17-4PH was fabricated and tested under

the NASA program. The design of this tube was based on drawings for a 1-inch diameter, 4-ply B/Al tube used in the mid-fuselage section of the NASA Space Shuttle. The inside collar taper was eliminated for reasons of simplicity, since the load transfer between plies in thin-walled tubes is not a problem. Instead, the collar was tapered on the outside edge after bonding to reduce the change in section at the joint interface. After 880 cycles of design limit stress at R = 1, the tube was pulled to failure in tension. The tube failed at a P/A joint stress of 186,000 psi which is nearly 40% greater than ever recorded on any test of any B/Al tubes with diffusion bonded attachments. Failure occurred by a clean tension break of the composite at the composite-collar junction, which is as expected.

The reason for this dramatic increase in joint properties is not yet fully understood but may be tied to the close match in modulus between stainless steel and unidirectional B/Al. Though the tube is smaller than the landing gear struts, it gives a strong indication that materials other than titanium may be advantageously used for attachments. In any case, it represents a breakthrough of major importance which will not only reduce cost but reduce the weight of joint critical tubes typical of landing gear struts. Three main advantages, therefore, would be higher joint strength, lower cost, and weld compatibility with existing steel fittings. A comparison of properties is shown in Table 5-1.

Table 5-1. Comparison of Properties of Titanium and Stainless Steel

	Titanium	Stainless Steel
Type	6AL-4V	Ph 13-8 MO
Heat Treat Cond.	Annealed	Rh-950
Density lb/in^3	0.160	0.29
Coeff. of Therm. Exp., $^oF\ (10)^{-6}$	5.3	9.3
Modulus, Tension, psi $(10)^6$	16.5	29.3
F_{tu}, 1000 psi	135	235
F_{ty}, 1000 psi	120	215
Machinability Rating	3	2
Weldability Rating	3	1
Cost $/lb	8	2.0
Corrosion Resistance	1	1
F_{tu}/Density Rating	1.0	1.0
E_t/Density Rating	1.0	1.0

SECTION 6

RECOMMENDATION

Recent developments have occurred which could greatly reduce weight and cost on B/Al landing gears since the completion of testing on this program. These developments include:

- Elimination of diffusion bonding problems
- Reduction of scarf ratio from 40t to 20t, resulting in cutting collar weight by 40%
- Increase in fatigue life by eliminating step taper at joint interface
- Potential 40% increase in joint efficiency and 75% reduction in material cost by changing collar material from titanium to pH stainless steel
- Availability of 8-mil Boron filament with reduced material and processing costs and potential for increasing joint strength

In addition to the above items, almost 800 tubes have been fabricated and delivered, primarily on the Space Shuttle Mid-Fuselage Program, which has vastly increased our experience and pushed the scrap rate to a low factor. Therefore, it is recommended that further testing of tubes be implemented, utilizing this new technology, which should result in additional cost and weight savings.

SECTION 7

REFERENCES

1. Cronk, M. J., "Solid Sap: User's Manual, Program P5679," General Dynamics Convair Division, San Diego, California, Report CASH-CIH-74-008, Sept. 1974.

2. Weisinger, M. D., Forest, J. D., and Miller, M. F., "Feasibility Demonstration Program for the Application of Boron/Aluminum to Space Shuttle," Report CASD-NAS-74-017, May 1974.

3. MIL-HDBK-5B, "Metallic Materials and Elements for Aerospace Vehicle Structures," Department of Defense, 1 September 1971.

4. Dittoe, F. A., "Sigma, Sample Standard Deviation, and Probability Levels," Structures Technical Memorandum No. 8, Convair.

5. General Dynamics Fort Worth Division Structures Manual.

6. Peterson, R. E., "Stress Concentration Design Factors," John Wiley & Sons, Inc., 1966.

7. Roark, R. J., "Formulas for Stress and Strain," Fourth Edition, McGraw-Hill Book Company, New York, 1965.

8. Structures Manual, Convair/Astronautics, 15 April 1960.

9. General Dynamics Convair Division Materials and Process, Memo M-172, dated 2 October 1974, To: J. E. Jensen, From: A. R. Robertson, Subject: Static and Fatigue Strength of Unstress-Relieved Titanium Welds.

10. Timoshenko, S. P., Gere, J. M., "Theory of Elastic Stability," Second Edition, McGraw-Hill Book Company, Inc., New York, 1961.

11. Dharmarajan, S. N. and McCutchen, H., "Shear Coefficients for Orthotropic Beams," Journal Composite Materials, Vol. 7, Oct. 1973, p. 530.

12. "Fracture Toughness Testing and its Applications," American Society for Testing and Materials Special Technical Publication (ASTM STP-381), 1964.

13. Waszczak, J. P., "Structural Analysis Methods for Advanced Composites," CASD-ERR-73-029, December 1973.

14. "Applied Fracture Mechanics," ASTM/STP 381, 1965.

APPENDIX A

ANALYTICAL STRESS AND DESIGN EVALUATION

A.1 DESIGN PARAMETERS AND MATERIAL PROPERTIES

The landing gear link is designed for ultimate loads, defined as 1.5 times limit loads, with a zero or slightly positive margin of safety. Material yielding will not be permitted at 1.15 times limit load.

The material properties used for the integral Ti-6Al-4V end fittings are annealed S basis values for bars from Reference 3. The mechanical properties used for the analysis of the boron/aluminum are shown in Table A-1. The calculated value for ν_{21} was obtained from:

$$\nu_{21} = \nu_{12} \frac{E_{22_T}}{E_{22_c}}$$

The value for ν_{12} and ν_{21} and the values for the modulii are initial values and are used in finite element analysis for internal load distribution. Since the tube is a single load path member, it was decided to use a reduced value for E_{11_c} during beam-column analysis. The minimum value observed for 32 test in Reference 2 was 28.9 x 10^6 psi. This was ratioed down to account for the fact that the test material had a higher volume percent of filaments than the B/Al specification minimum. Additionally, the modulus was measured at stress levels in excess of 100,000 psi. The value selected for use in beam-column analysis is:

$$E_{11_c} = 28.0 \times 10^6 \text{ psi}$$

"B" basis strength allowables were obtained from test data by choosing the low value where the number of samples was between 29 and 32 as described in Table 9.6.4.2 of Reference 3. "B" basis strength allowables were obtained by subtracting 3.0 sample standard deviations from the samples mean when there were six samples as described in Reference 4. The 250,000 psi compression ultimate allowable was estimated based on twelve Celanese compression specimens which were loaded to 10,000 pounds with no failures. The specimens averaged 0.140 inches thick by 0.257 inches wide for an average stress of 278,000 psi. Typical stress-strain curves are shown in Figures A-1 through A-5.

Table A-1. Room Temperature Unidirectional B/Al Laminate Properties

Cond.	Property	Value	Basis	Source	No. Samples
F	E_{11_T}	31.2×10^6 psi	Avg.	8	30
F	E_{11_c}	31.7×10^6 psi	Avg.	5	32
F	E_{22_T}	19.7×10^6 psi	Avg.	8	29
F	E_{22_c}	23.4×10^6 psi	Avg.	8	27
F	G_{12}	8.4×10^6 psi	Avg.	8	2
F	ν_{12}	0.23	Avg.	8	5
F	ν_{21}	0.15	Avg.	Calculated	
STA	$F_{11_{tu}}$	167,000 psi	B	8	6
F	$F_{11_{cu}}$	250,000 psi	Estimated	9	12
F	$F_{22_{tu}}$	13,100 psi	B	8	30
F	$F_{22_{cu}}$	36,100 psi	B	8	30
STA	F_{su}	19,000 psi	B	8	6

DATE 11/27/73

SYSTEM	5.6 mil Boron/6061 Alum.
LAMINA	V_f = 0.50 t = 0.0068
LAYUP	[0]
TEMP.	Room

Boron/Aluminum

CONDITION F

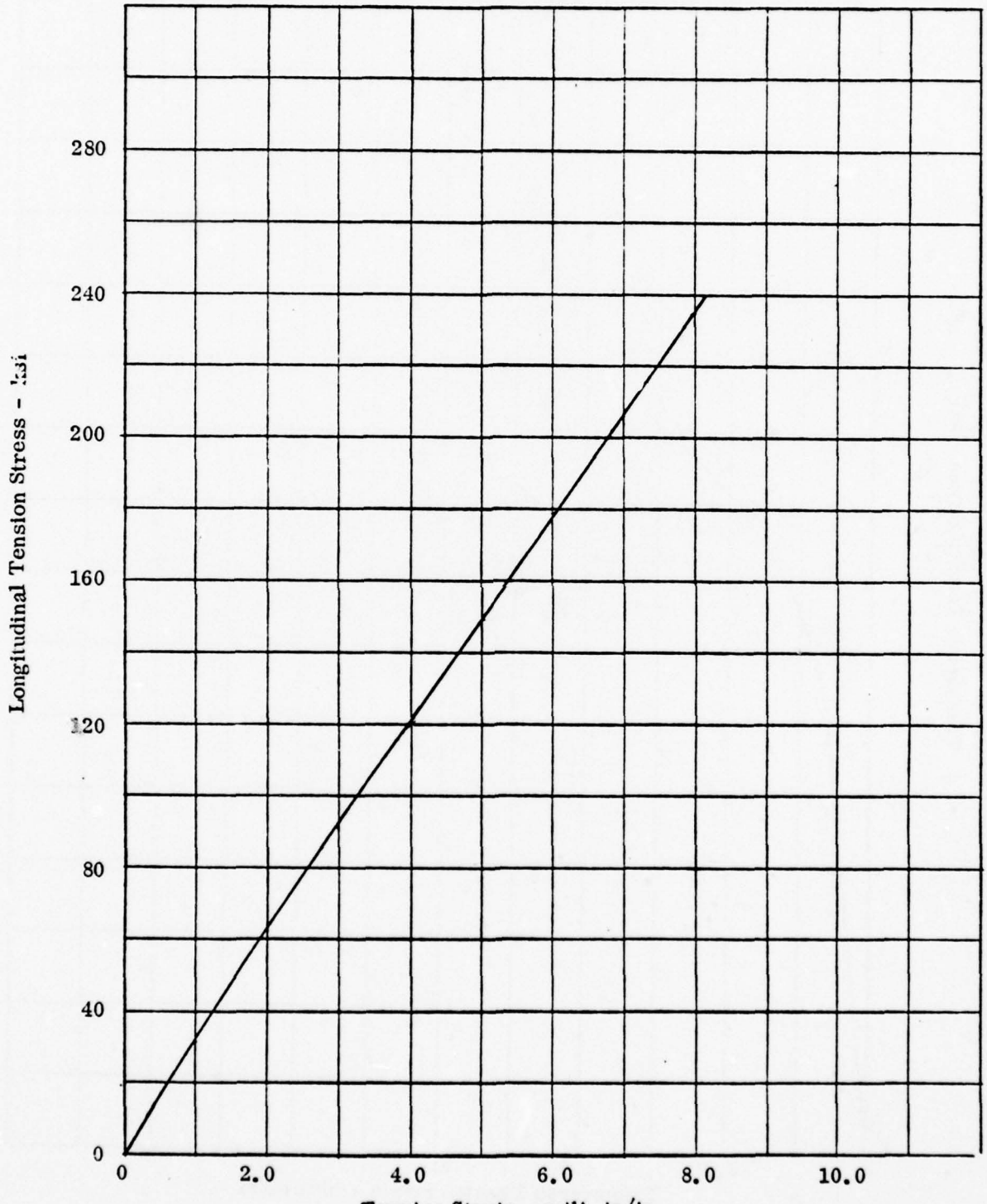

Figure A-1. Longitudinal Tension Stress-Strain Curve for Unidirectional Boron/Aluminum.

DATE 11/27/73

SYSTEM	5.6 mil Boron/6061 Alum.
LAMINA	V_f = 0.50 t = .0068
LAYUP	$[0]$
TEMP.	Room

Boron/Aluminum

CONDITION F

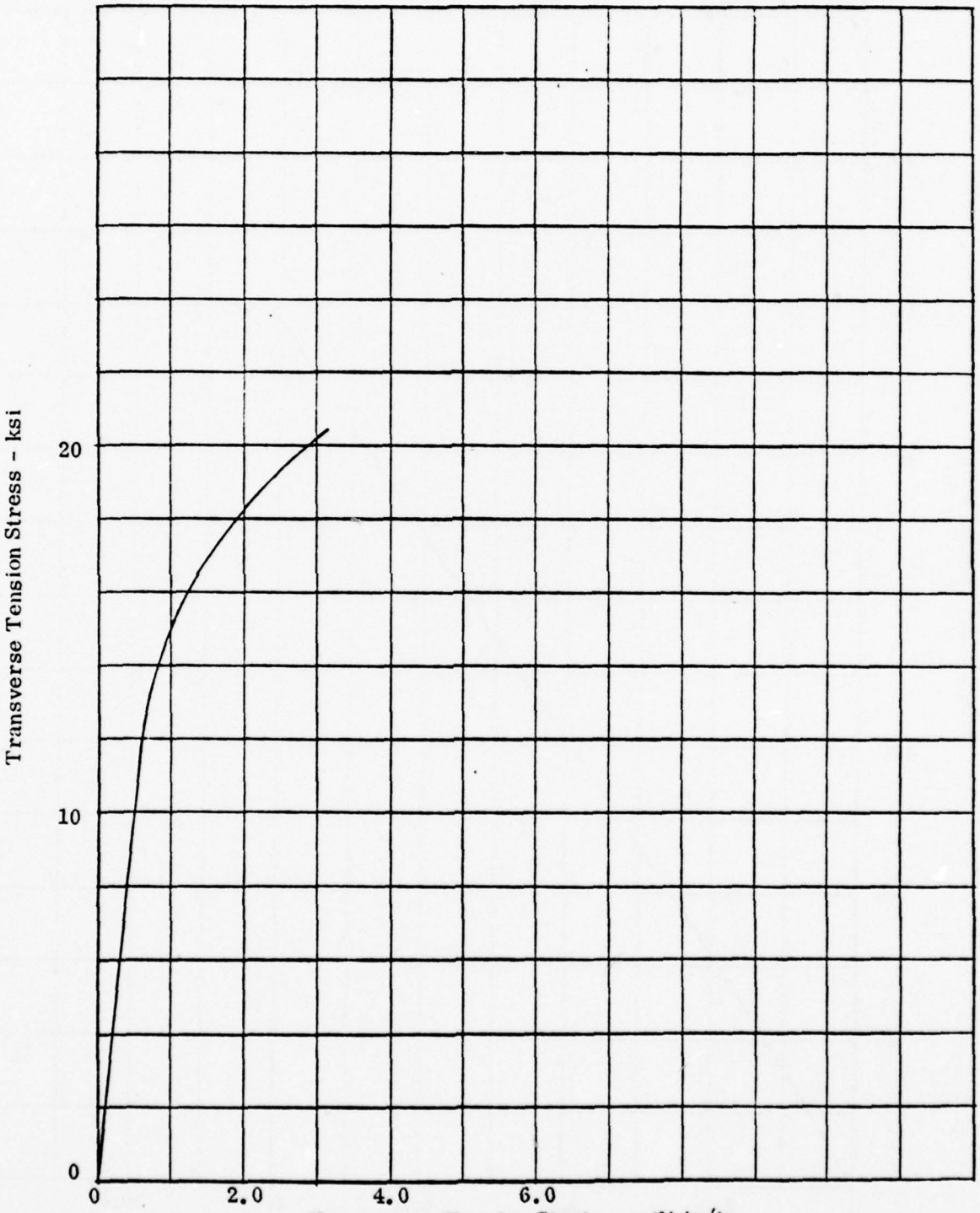

Figure A-2. Transverse Tension Stress-Strain Curve for Boron/Aluminum.

DATE 11/27/73

SYSTEM	5.6 mil Boron/6061 Alum.
LAMINA	V_f = 0.50 t = .0068
LAYUP	[0]
TEMP.	Room

Boron/Aluminum

CONDITION F

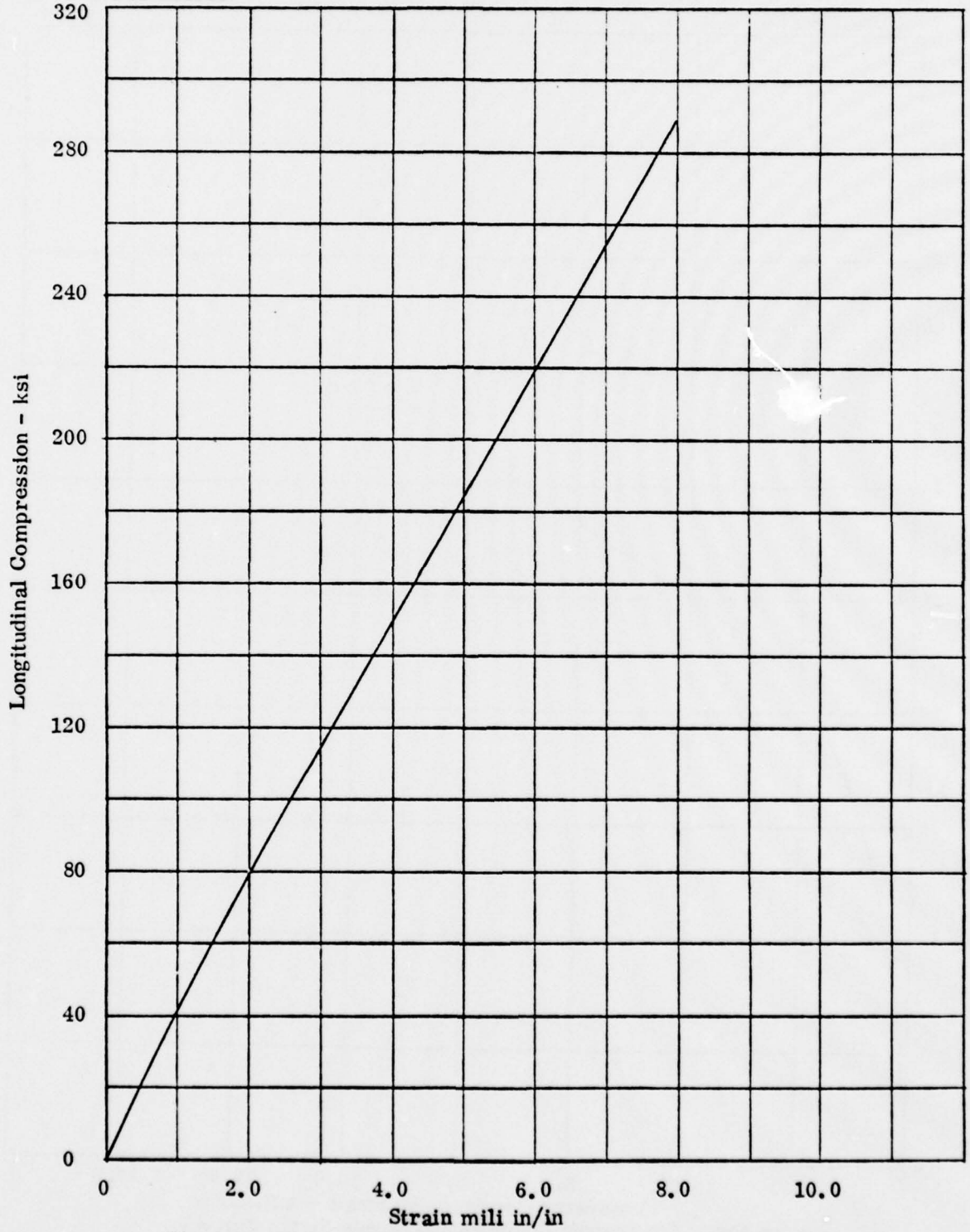

Figure A-3. Longitudinal Compression Stress-Strain Curve for Unidirectional Boron/Aluminum.

DATE 11/27/73

SYSTEM	5.6 mil Boron/6061 Alum.
LAMINA	V_f = 0.50 t = .0068
LAYUP	[0]
TEMP.	Room

Boron/Aluminum

CONDITION F

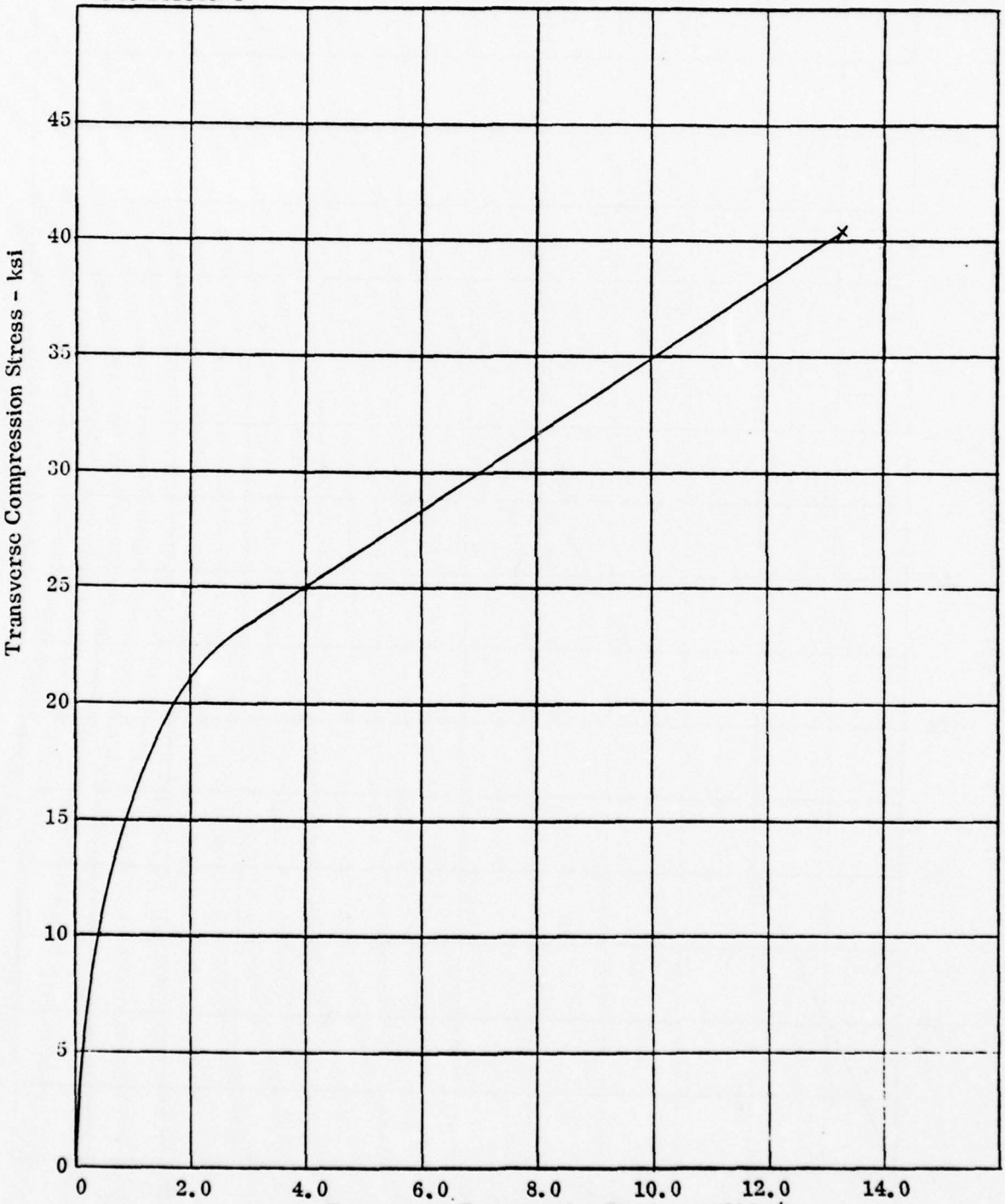

Figure A-4. Transverse Compression Stress-Strain Curve for Unidirectional Boron/Aluminum.

DATE 12/5/73

SYSTEM	5.6 mil Boron/HT 6061 Al
LAMINA	$V_f = 0.50$ t =
LAYUP	[0]
TEMP.	Room

Boron/Aluminum

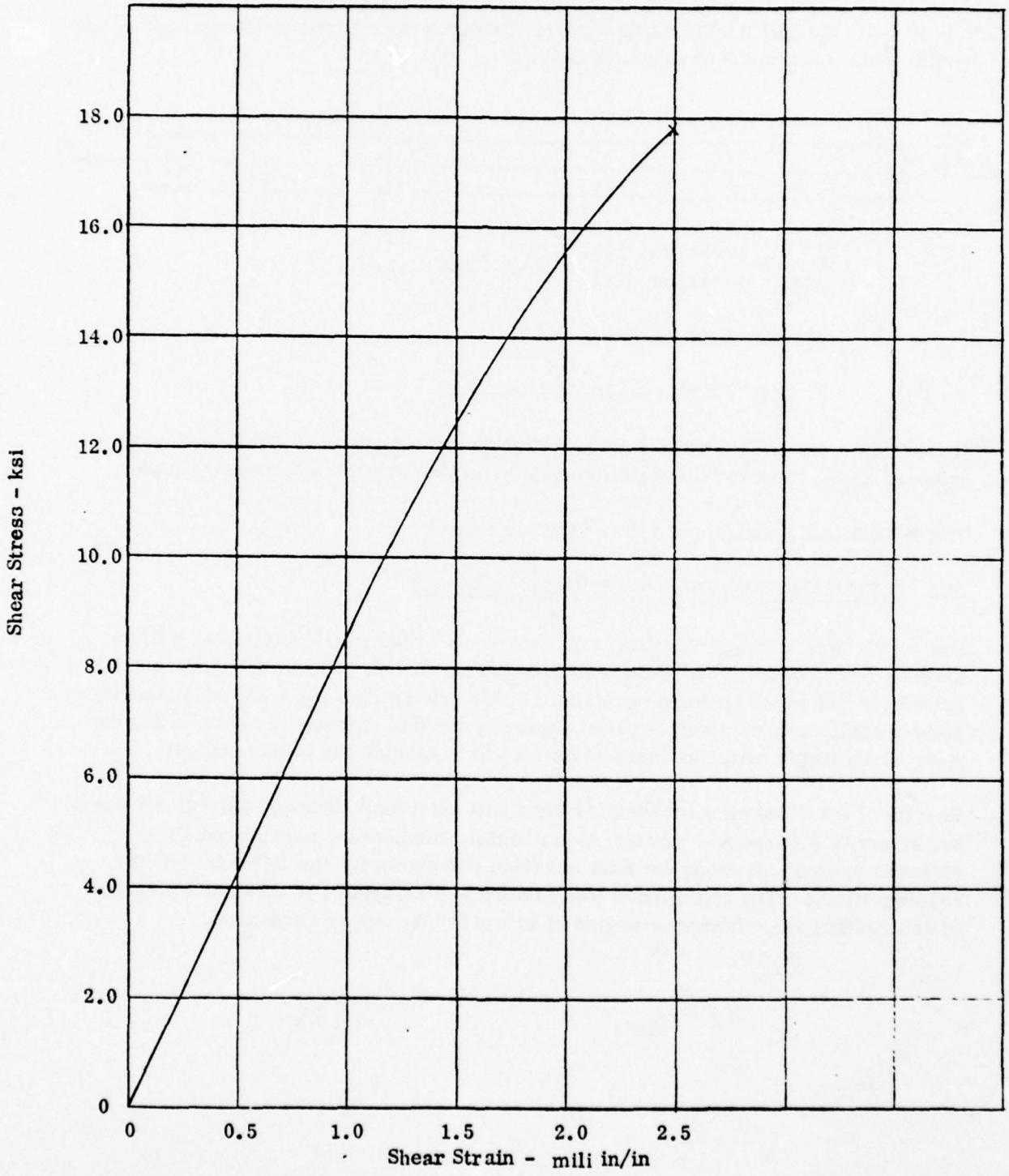

Figure A-5. Torsion of a Boron/Aluminum Tube.

A.2 DESIGN LOADS AND REQUIREMENTS

The ultimate loading conditions and analysis parameters utilized in the analysis of the landing gear link are summarized as follows:

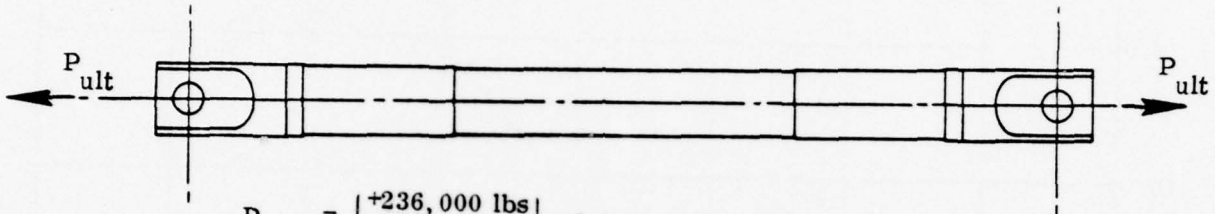

$P_{ult} = \begin{vmatrix} +236,000 \text{ lbs} \\ -141,000 \text{ lbs} \end{vmatrix}$ at room temperature

Ultimate Load Factor = 1.50

Fitting Factor = 1.15 static strength

In addition to the above loads, a manufacturing eccentricity of 0.030 inches was imposed on the strut for the st ›ility analysis at the ultimate compressive load.

The fatigue load spectrum is shown in Table 2-1.

A.3 DIFFUSION BONDED SCARF JOINT ANALYSIS

Due to the complexity of analyzing scarf joints with dissimilar materials, a finite element model of the local transition area was employed. The model utilizes an extremely fine mesh size and consists of 1,568 grid points with 1,360 axisymmetric solid quadrilateral elements. Model geometry for this analysis is shown in Figure A-6. Orthotropic material characteristics are accounted for in this analysis.

Results of the finite element analysis for a unit axial load condition (10,000 lbs comp) are shown in Figures A-7 through A-11. Axial, transverse, normal and shear stresses in elements along the joint interface are shown for the B/A tube and the titanium fitting. The appropriate load factors will be applied to these unit stresses in determining the minimum margins of safety for the design conditions.

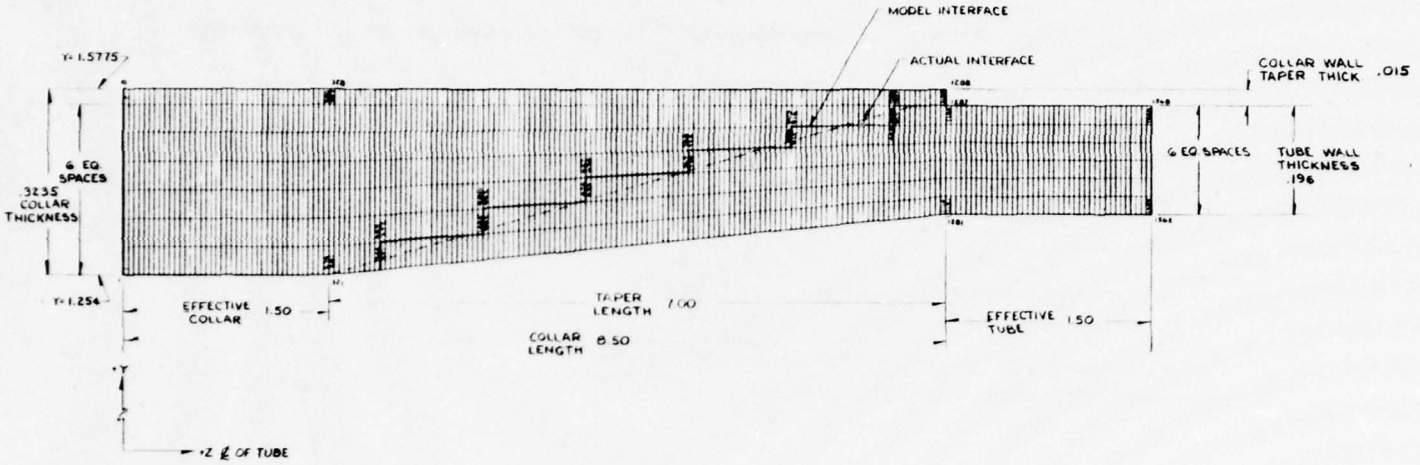

Figure A-6. Diffusion Bonded Joint Model Geometry.

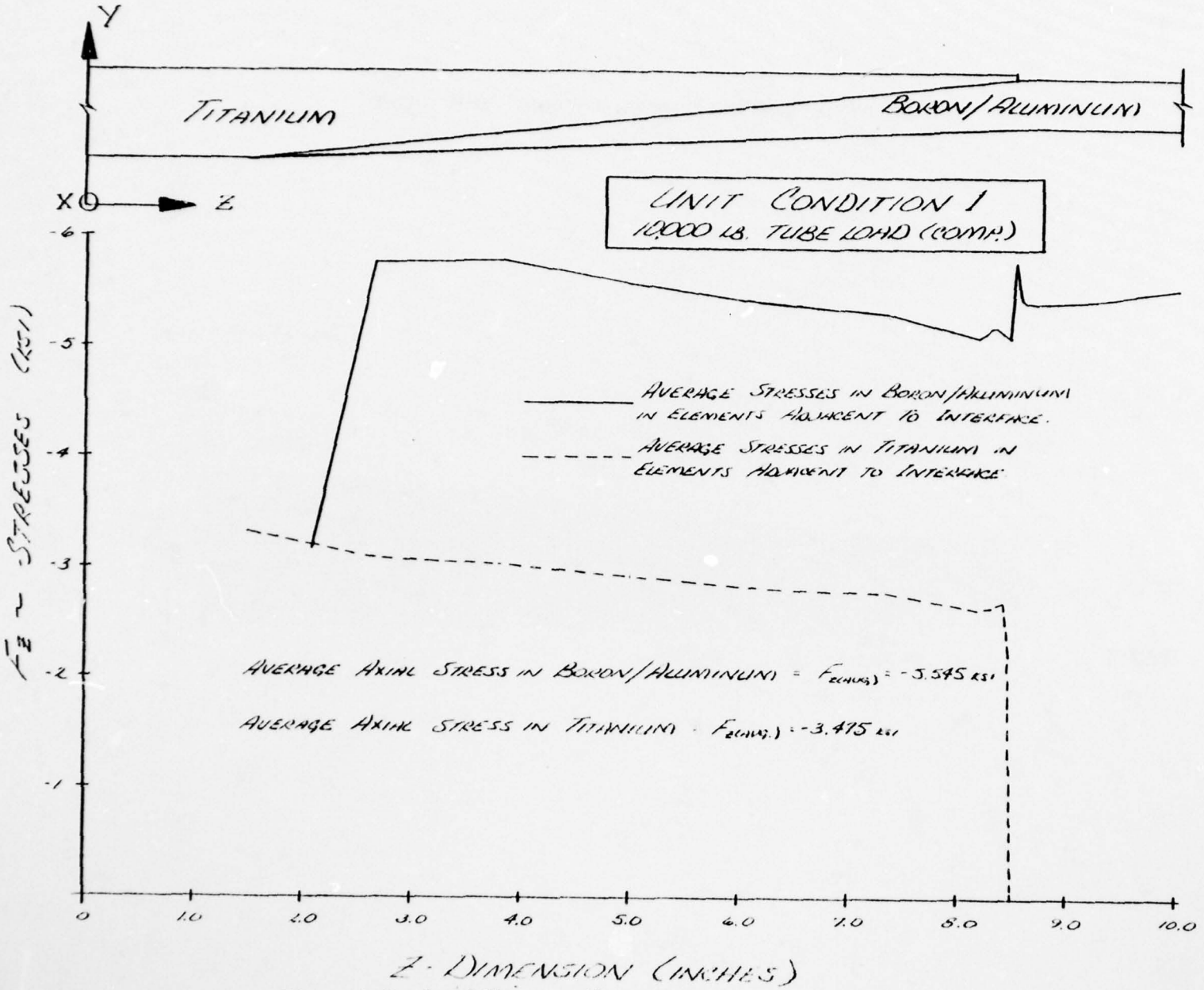

Figure A-7. Axial Stresses Along the Joint Interface

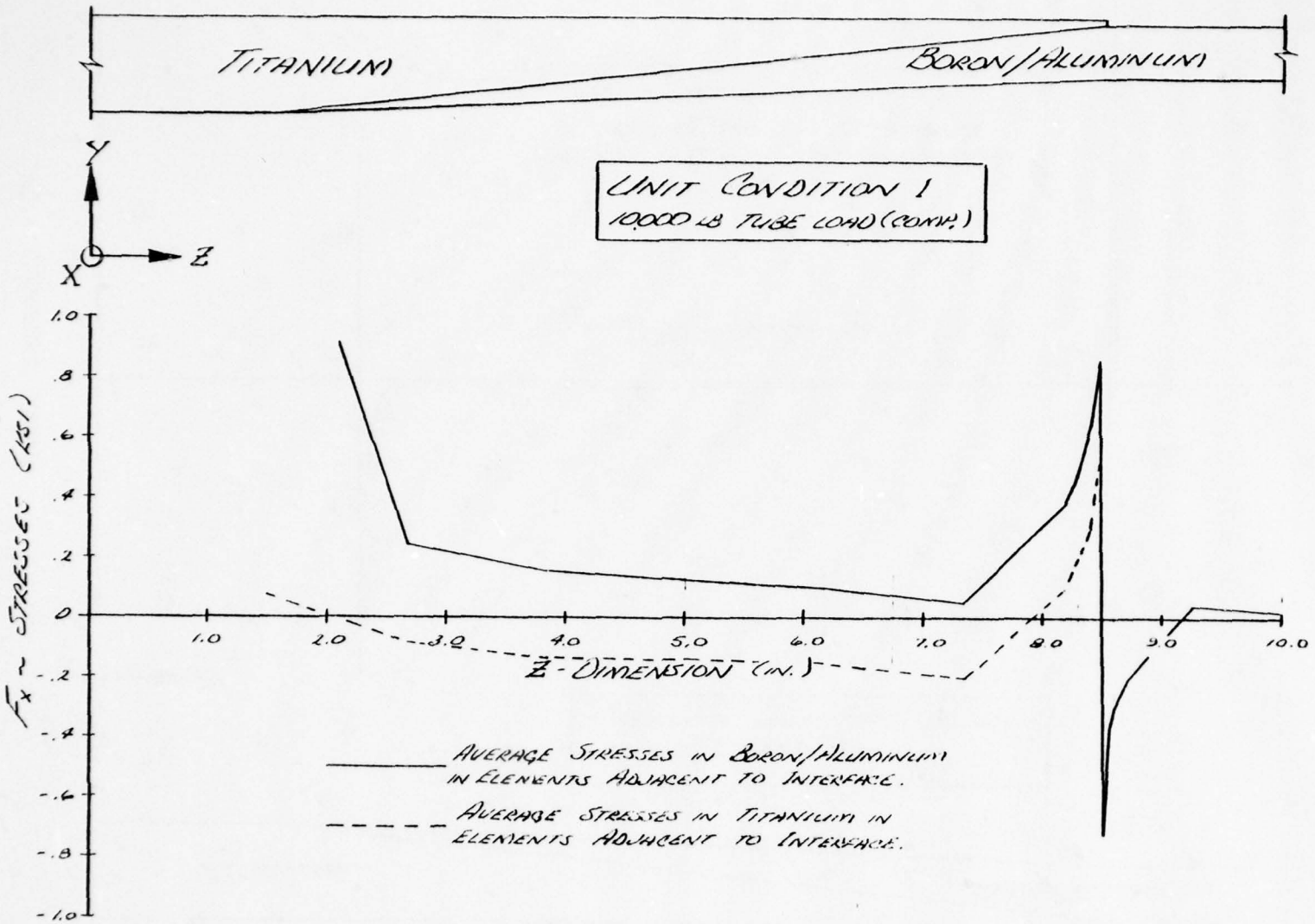

Figure A-8. Transverse Stresses Along the Joint Interface

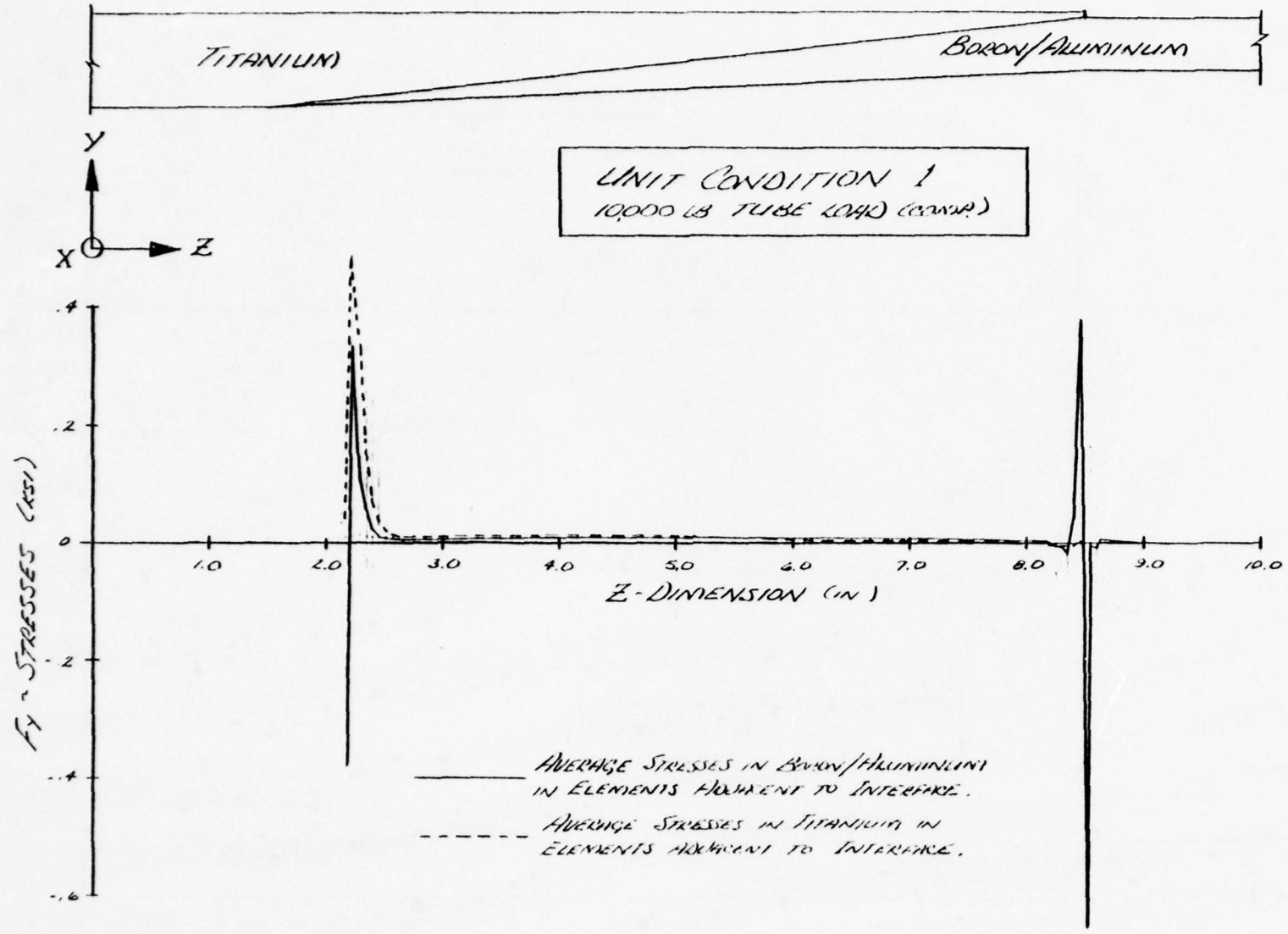

Figure A-9. Normal Stresses Along the Joint Interface

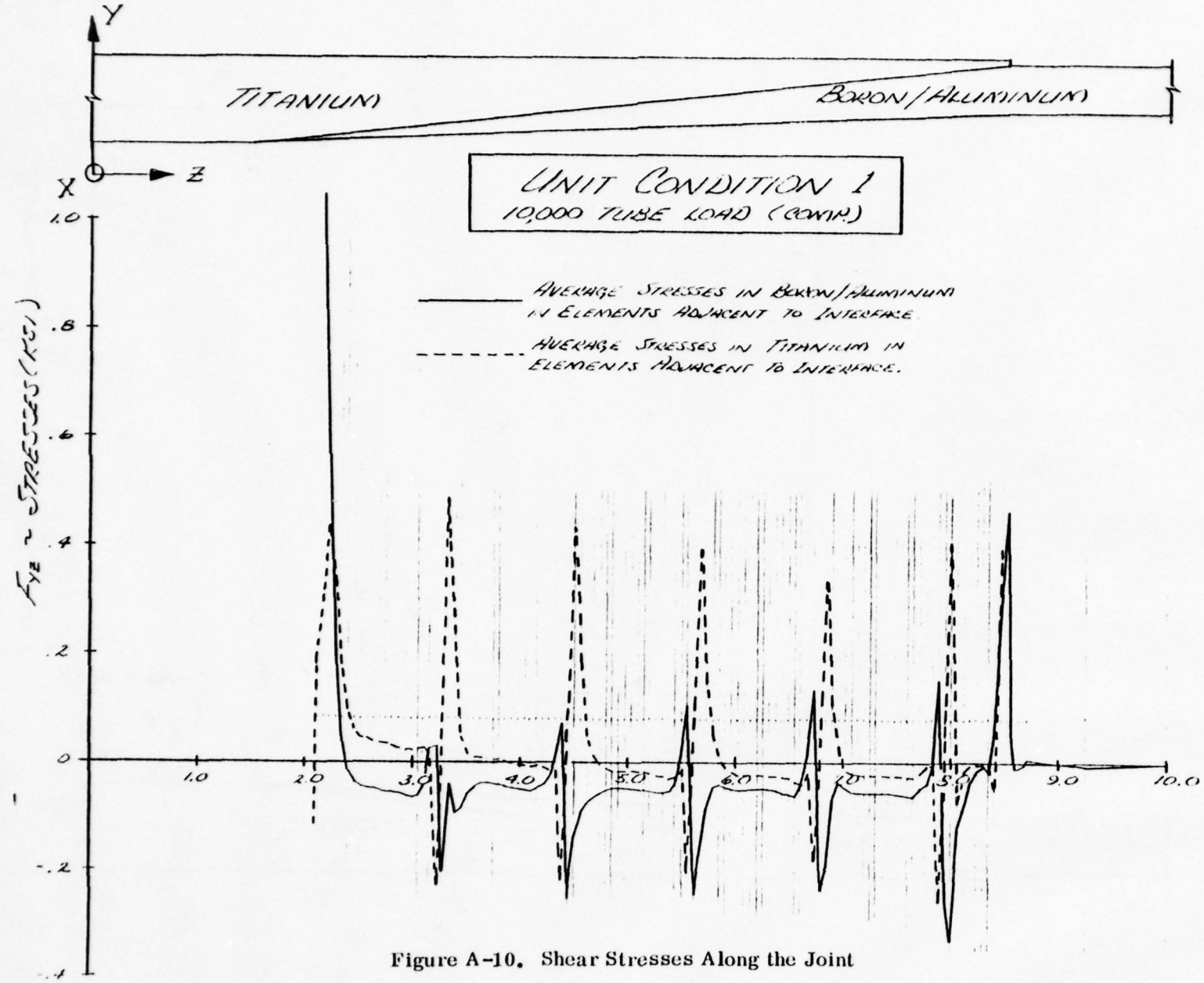

Figure A-10. Shear Stresses Along the Joint

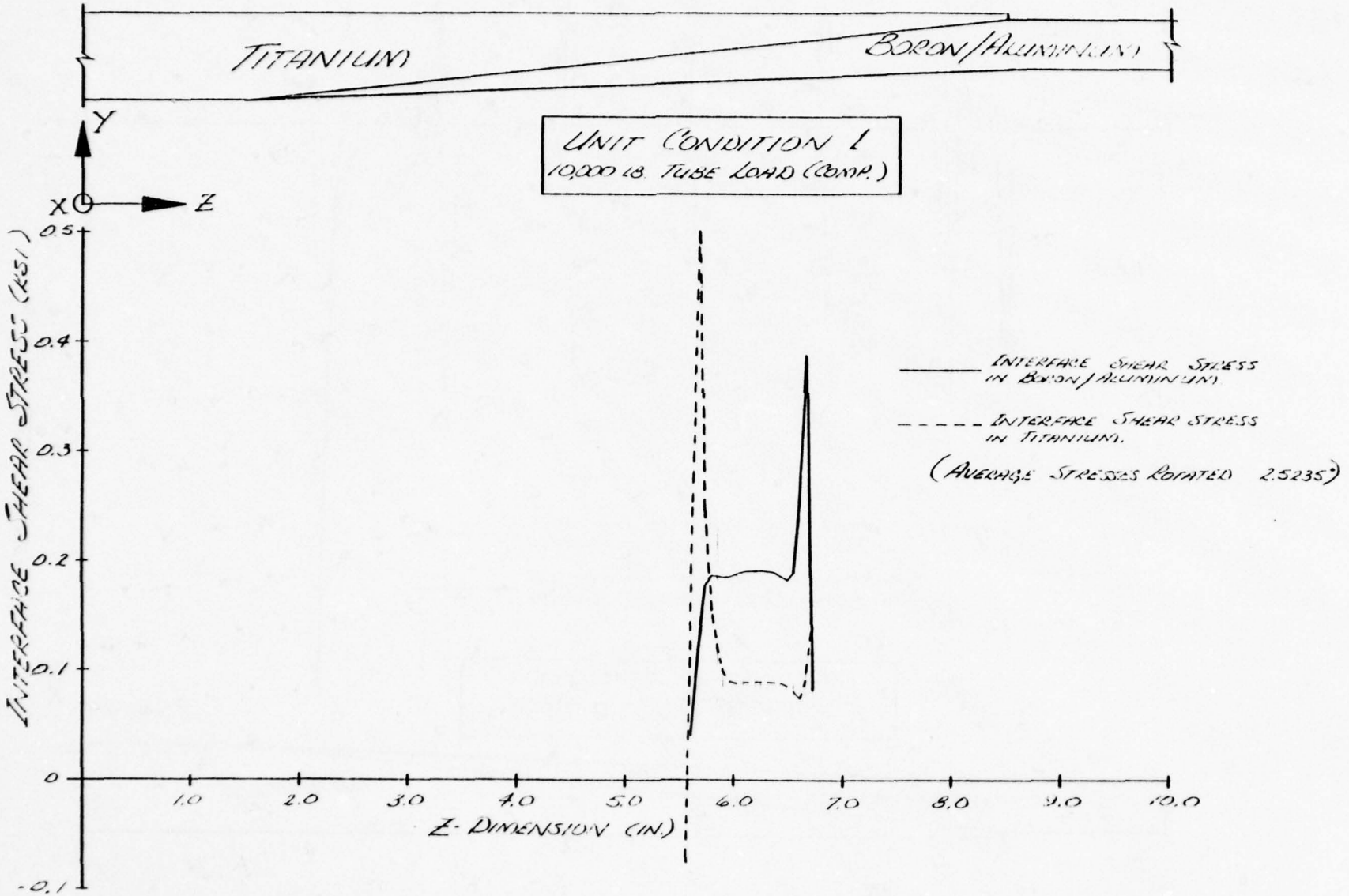

Figure A-11. Shear Stresses in the Plane of the Interface

Stress Checks of Boron/Aluminum ~ Titanium Interface

Boron/Aluminum

$$f_t = \frac{5.80\ (236,000)}{10,000} = 136.88 \text{ ksi (Ref. Figure A-7)}$$

F_{tu} = 167 ksi (Ref. Table A)

$$\text{M. S.} = \frac{167}{1.15\ (136.88)} - 1.0 = +0.061$$

$$f_c = \frac{5.80\ (141,000)}{10,000} = 81.78 \text{ ksi (Ref. Figure A-7)}$$

F_{cu} = 250 ksi (Ref. Table A)

$$\text{M. S.} = \frac{250}{1.15\ (81.78)} - 1.0 = +1.658$$

$$f_{s_{ult}} = \frac{1.10\ (236,000)}{10,000} = 25.96 \text{ ksi (Ref. Figure A-8)}$$

$$f_{s_{limit}} = 25.96 \times \frac{1}{1.5} = 17.31 \text{ ksi}$$

F_{su} = 19,000 psi (Ref. Table A)

The peak calculated shear stress exceeds the allowable. However, Convair testing to date indicates that shear peaks do not initiate shear strength failures. Local yielding can occur. Reference to the typical torsional stress vs strain curve in Figure A-10 show that 0.2% offset is not exceeded by the limit peak shear stress.

Titanium

$$f_t = \frac{3.32\ (236,000)}{10,000} = 78.352 \text{ ksi (Ref. Figure A-7)}$$

F_{tu} = 130.00 ksi (Ref. No. 3)

$$\text{M. S.} = \frac{130.0}{1.15\ (78.352)} - 1.0 = +0.443$$

Titanium (continued)

$$f_c = \frac{3.32\,(236,000)}{10,000} = 78.352 \text{ ksi (Ref. Figure A-7)}$$

$$F_{cy} = 126.0 \text{ ksi (Ref. No. 3)}$$

$$\text{M. S.} = \frac{126.0}{1.15\,(46.812)} - 1.0 + 1.341$$

$$f_s = \frac{.49\,(236,000)}{10,000} = 11.564 \text{ ksi (Ref. Figure A-8)}$$

$$F_{su} = 80.0 \text{ ksi}$$

$$\text{M. S.} = \frac{80}{1.15(11.564)} - 1.0 = + \text{High}$$

Thermally induced stresses due to a temperature change of 100° F are shown in Figures A-12 through A-15. The diffusion bonding process involves heating the B/Al tube and titanium collar assembly to 975° F. Creep and yielding of the aluminum matrix material will strongly influence the residual stresses remaining as the assembly cools. Convair has insufficient data and experience to quantify the final residual stresses to be superimposed on the mechanically induced stresses. NDT techniques are available to measure residual stresses and one of these would have to be used along with structural tests to accumulate data before a purely analytical approach could be used with confidence.

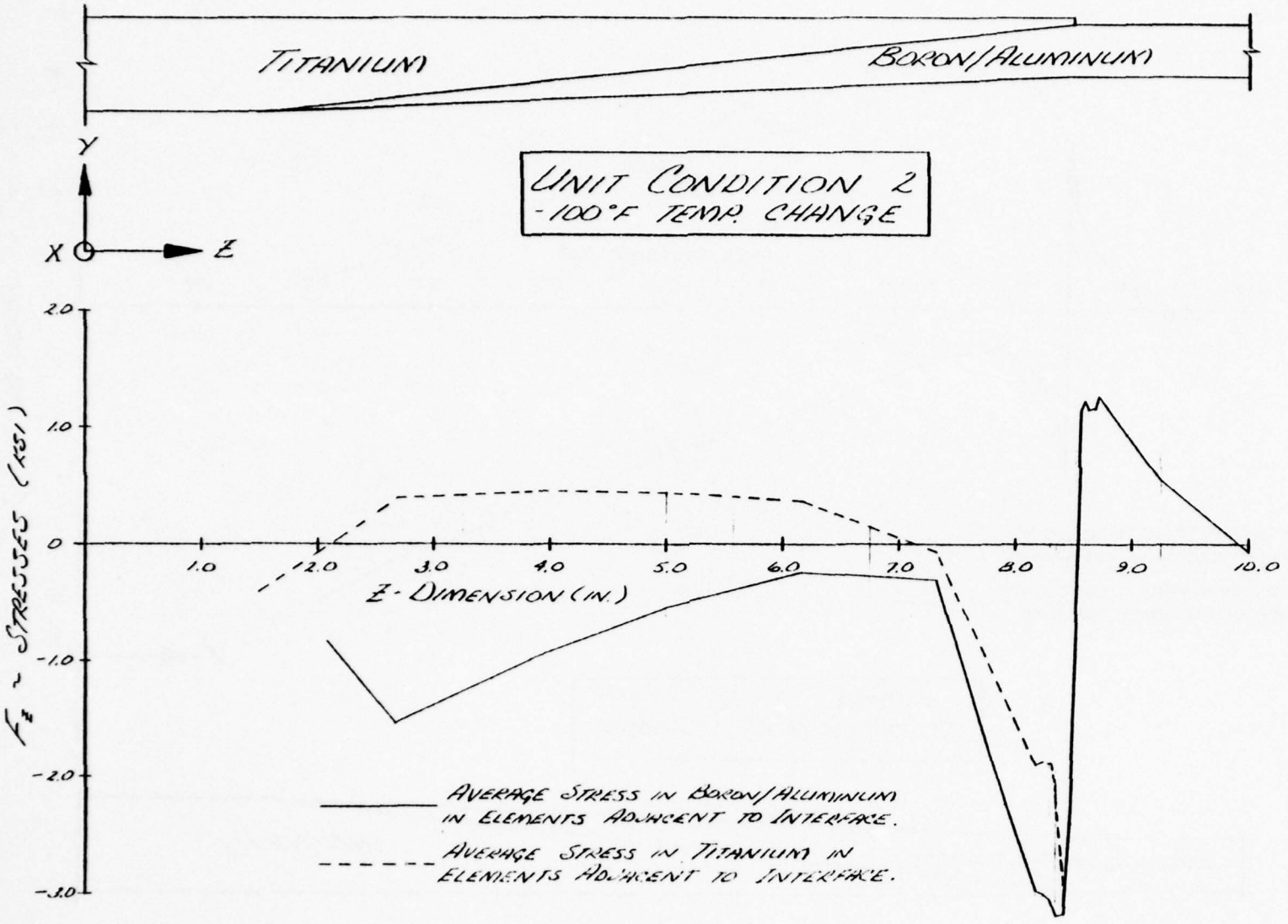

Figure A-12. Axial Stresses Along Joint Due to Temperature Change

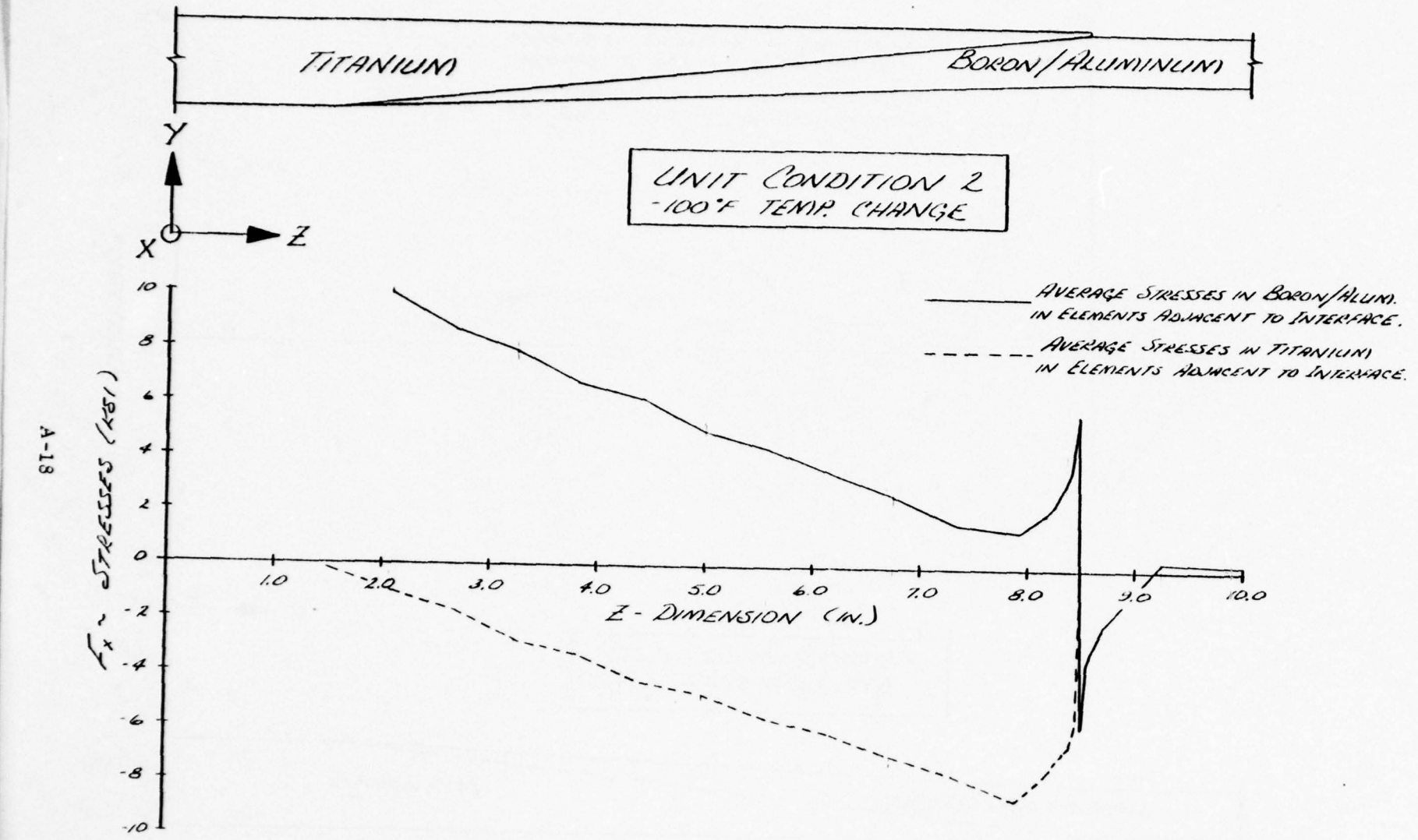

Figure A-13. Transverse Stresses Along Joint Due to Temperature Change

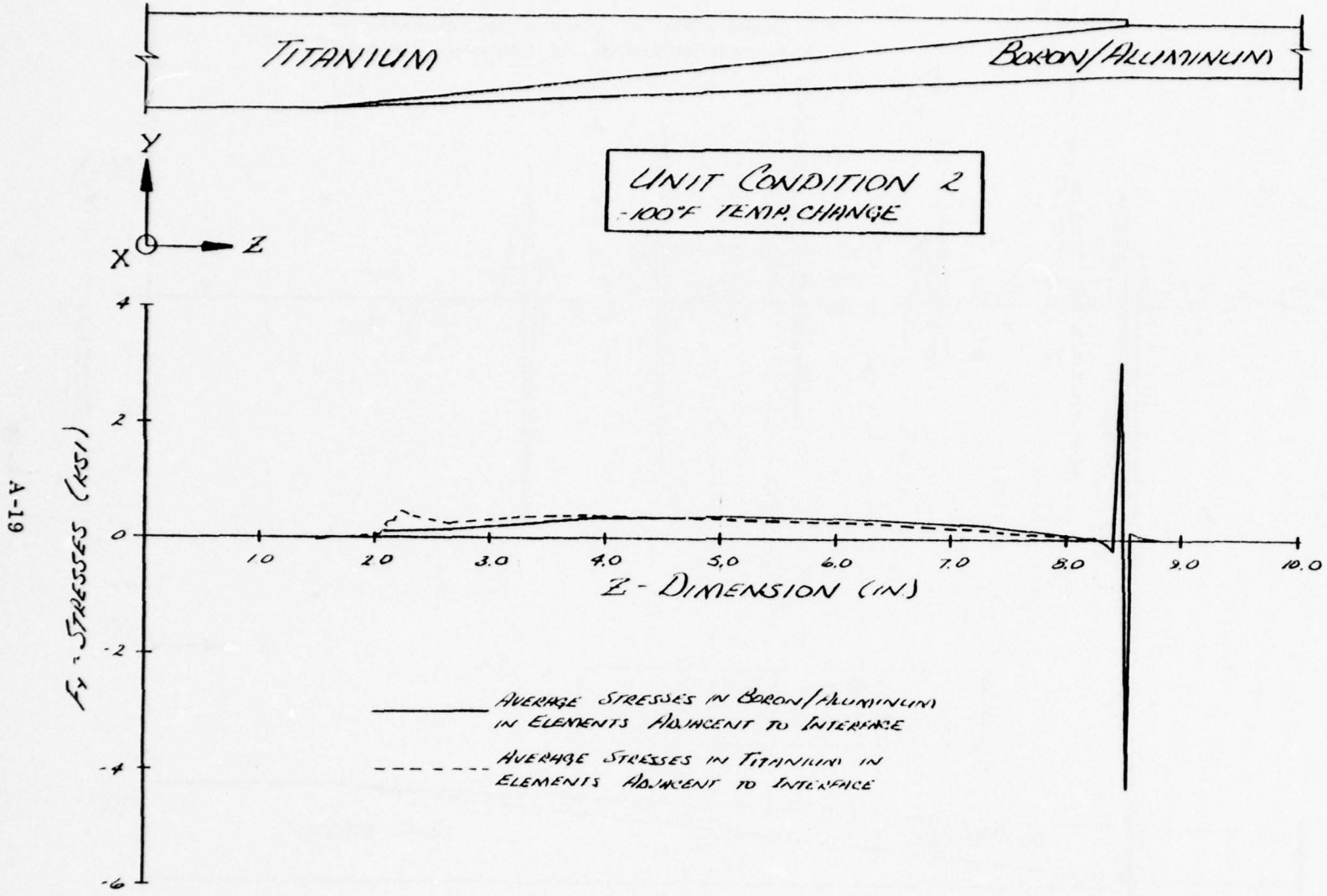

Figure A-14. Normal Stresses Along Joint Due to Temperature Change

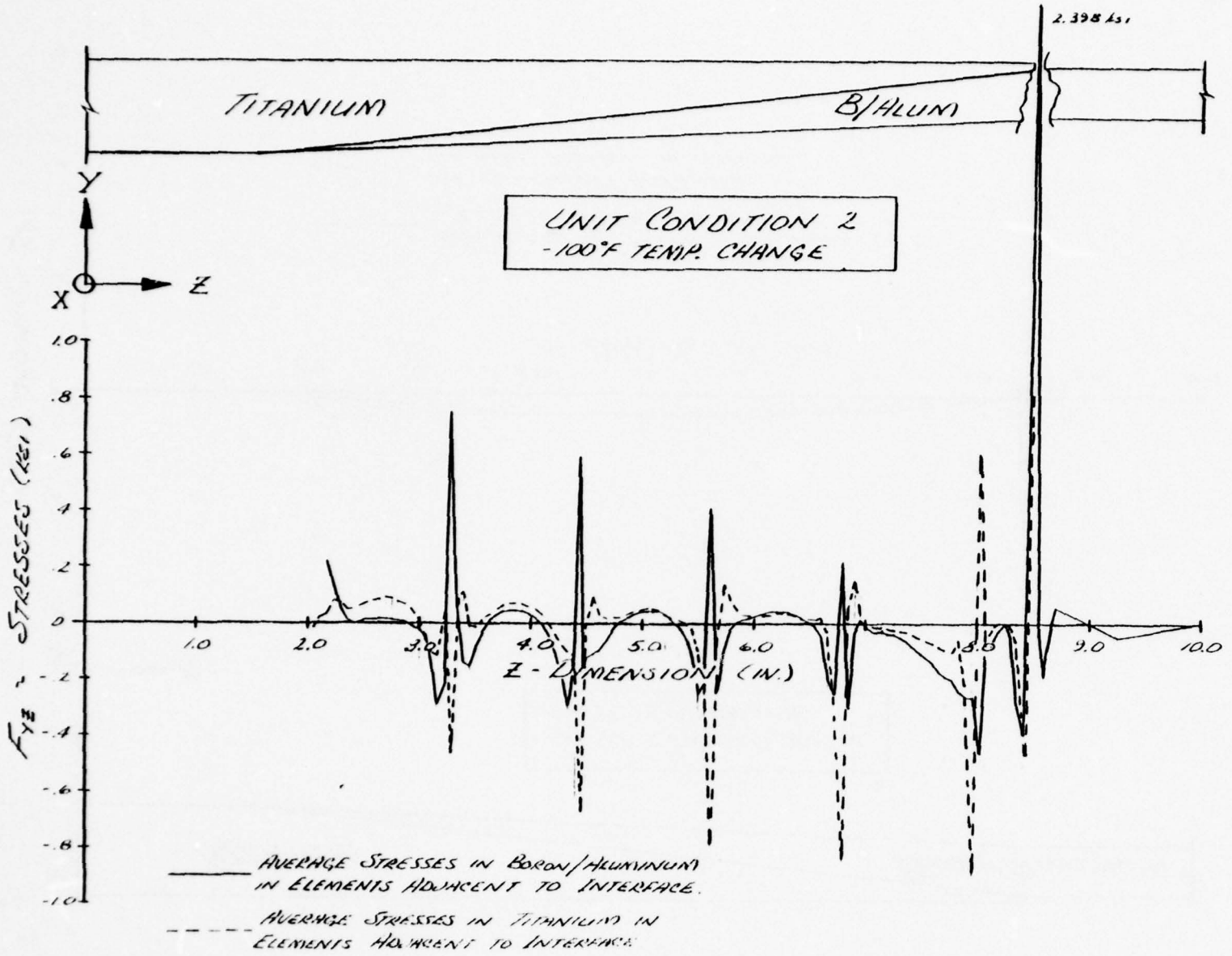

Figure A-15. Shear Stresses Along the Joint Due to Temperature Change

72 CO 432
COMPOSITE DRAG LINK

A.4 FITTING - FORWARD

LUG STATIC STRENGTH ANALYSIS
REF. 5, SECT 10.6

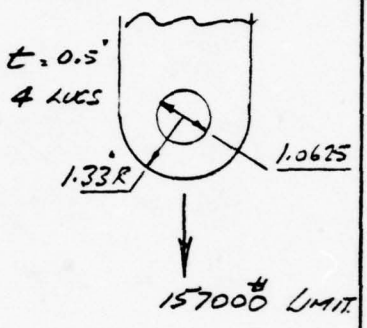

TENSION ON NET SECTION

$$P_{TU} = K_T F_{TU} A_t$$

$$A_T = (W-D)t = (2.66 - 1.0625)\,4 \times .5 = 3.195 \text{ in}^2.$$

FOR Ti-6AL-4V ANNEALED FITTING.
$F_{TU} = 130{,}000$ psi, $G = 0.921$, $H = 0.0748$

$$\lambda = \frac{D}{W} = \frac{1.0625}{2.66} = 0.399 \quad \therefore K_T = 0.94$$

$$P_{TU} = 0.94 \times 130000 \times 3.195 = 390\,429 \text{ lb.}$$

ASSUMING MAXIMUM LOAD/LUG = 1.2 PANLOADS.

$$M.S.\ (\text{ULT. TENSION}) = \frac{P_{TU}}{1.2\, P_{ULT} \times K_F} - 1.$$

$$= \frac{390429}{1.2 \times 157000 \times 1.5 \times 1.15} - 1.$$

$$= +0.20$$

WHERE K_F = FITTING FACTOR = 1.15.

PREPARED BY	DATE	CHECKED BY	DATE	REVISED BY	DATE
A. S. WILSON	10/23/74	C. J. Tammer	11-4-77		

T2 CO 432
COMPOSITE DRAG LINK

FITTING - FORWARD

SHEAR TEAROUT - BEARING

$P_{BRU} = K_{BR} F_{TU} A_{BR}$

$e/D = 1.33/1.0625 = 1.252$

$D/t = 1.0625/.5 = 2.125 \quad \therefore K_{BR} = 1.20$

$A_{BR} = Dt = 1.0625 \times .5 \times 4 = 2.125$

$\therefore P_{BRU} = 1.2 \times 130000 \times 2.125 = 331500$ lb

$$M.S\ (\text{SHEAROUT - BEARING}) = \frac{P_{BRU}}{1.2\ P_{ULT} \times K_n} - 1$$

$$= \frac{331500}{1.2 \times 157000 \times 1.5 \times 1.15} - 1$$

$$= +0.02$$

LUG YIELDING

$P_y = K_{BRY} A_{BR} F_{TY}$

For $e/D = 1.25 \quad K_{BRY} = 1.25$

$\therefore P_y = 1.25 \times 2.125 \times 120000 = 312750$ lb.

$$M.S.\ (\text{YIELDING}) = \frac{318750}{1.2 \times 157000 \times 1.15} - 1 = +0.47$$

PREPARED BY	DATE	CHECKED BY	DATE	REVISED BY	DATE
R.S. Wilson	10/23/74	C.J. Tammer	11-4-77		

72 CO 432

COMPOSITE DRAG LINK

FITTING FORWARD

LUG FATIGUE STRENGTH

STRESS CONCENTRATION FACTOR (REF 6, FIG. 83)

$$\frac{a}{W} = \frac{1.0625}{2.66} = 0.399 \quad \therefore K_{TB} = 1.89$$

$$\sigma_{max} = \frac{P.K_{TB}}{Dt} = \frac{157000 \times 1.89}{1.0625 \times .5 \times 4} = \underline{139638 \text{ psi}}$$

EQUIVALENT NET SECTION K_T

$$\frac{P.K_T}{(W-D)t} = 139638$$

$$\therefore K_T \text{ (NET SECTION)} = \frac{139638(W-D)t}{P}$$

$$= \frac{139638(2.66-1.0625).5 \times 4}{157000}$$

$$= 2.842$$

$\therefore$ S-N DATA FROM REF 3 FOR $K_T = 3.3$ IS APPLICABLE.

$$\text{MAXIMUM FATIGUE STRESS} = \frac{157000 \times 1.2}{(2.66-1.0625).5 \times 4} = \underline{58967 \text{ psi}}$$

FOR A REQUIRED LIFE OF $2000 \times 2 = 4000$ CYCLES THE ALLOWABLE MAXIMUM STRESS $F_{MAX} \approx 75000$ psi REFERENCE FIGURE A-16 ..

$$\therefore \text{M.S. (LUG FATIGUE)} = \frac{75000}{58967} - 1 = +0.27$$

PREPARED BY	DATE	CHECKED BY	DATE	REVISED BY	DATE
R. S. WILSON	10/13/77	C. J. Tammer	11-4-77		

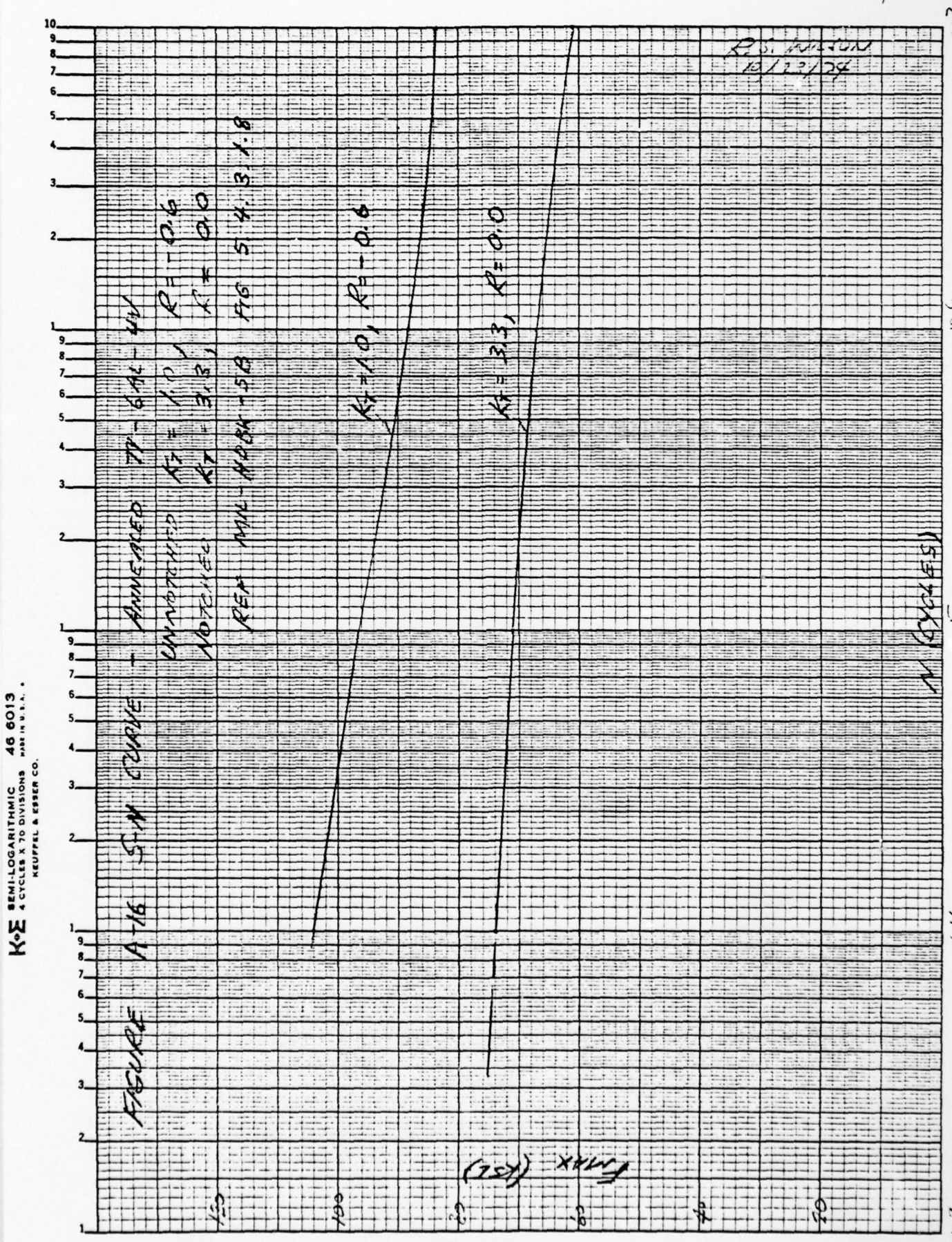
FIGURE A-16 S-N CURVE - ANNEALED Ti-6Al-4V
UNNOTCHED $K_T = 1.0$, $R = -0.6$
NOTCHED $K_T = 3.3$, $K = 0.0$
REF. MIL-HDBK-5B FIG 5.4.3.1.8
$K_T = 1.0$, $R = -0.6$
$K_T = 3.3$, $R = 0.0$
f_{MAX} (KSI)
N (CYCLES)
K&E SEMI-LOGARITHMIC 46 6013
4 CYCLES X 70 DIVISIONS
KEUFFEL & ESSER CO.

72 CO 432

COMPOSITE DRAG LINK

FITTING - FORWARD

DETERMINATION OF MINIMUM LOAD PATH AREAS:

ONE QUDRANT OF THE DOUBLY SYMMETRICAL END FITTING IS SHOWN FULL SIZE ON PAGE A-25. FULL SIZE SECTIONS CUT 0.5 INCHES APART ARE SHOWN ON PAGES A-26. TO 2-28.

THE FOLLOWING ASSUMPTIONS ARE MADE IN ORDER TO SIMPLIFY THE ANALYSIS;

1. A FACTOR OF 1.20 WILL BE USED TO ACCOUNT FOR NON-UNIFORM LOAD DISTRIBUTION AMONG THE LUGS.

2. LOADS MAY SHEAR OUT AT 15° FROM ONE SECTION TO THE NEXT WITHOUT THE NECESSITY OF KICK LOAD ANALYSIS.

PREPARED BY	DATE	CHECKED BY	DATE	REVISED BY	DATE
E. L. Wilson	11-4-72	C. J. Tammer	11-4-72		

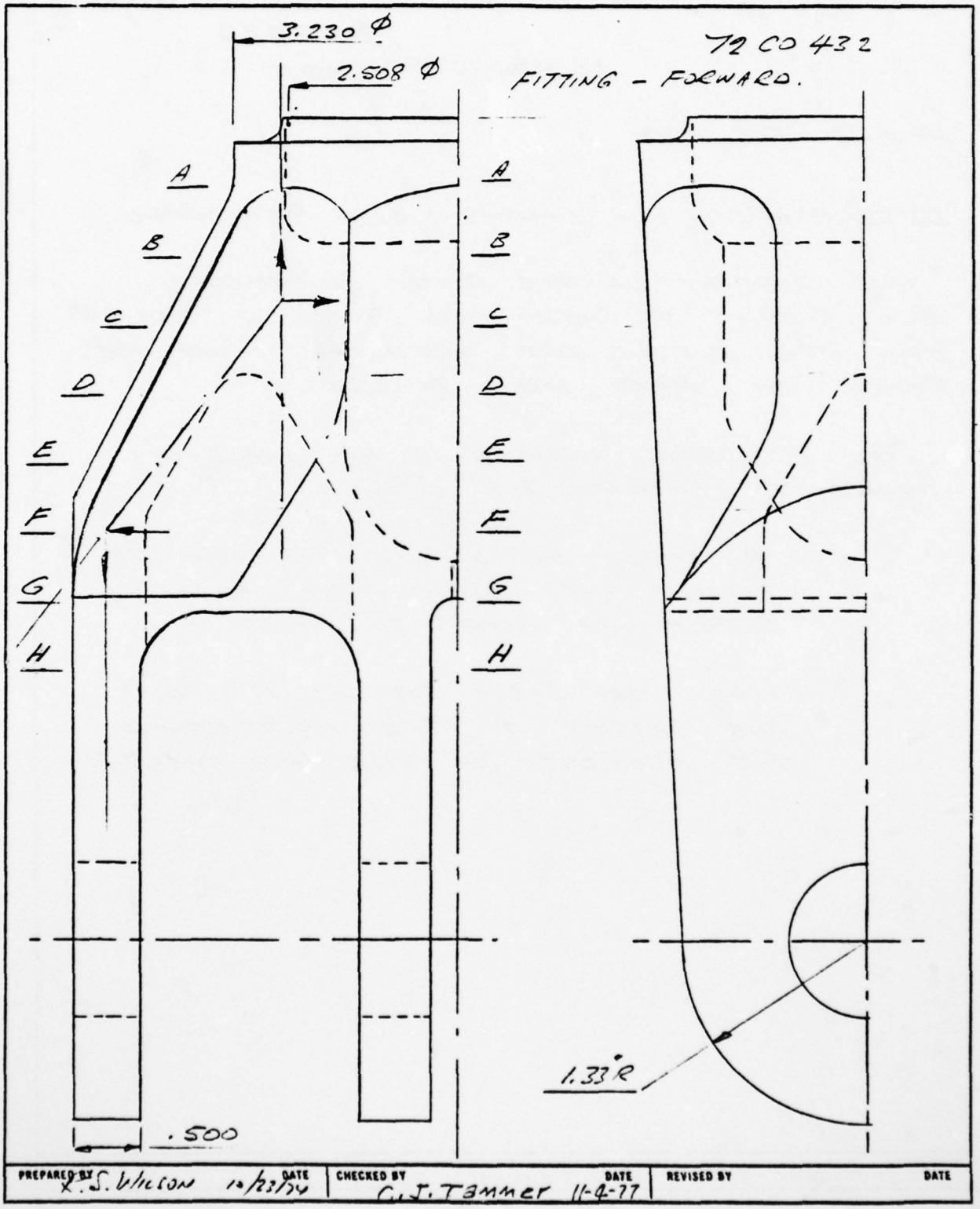

PREPARED BY	DATE	CHECKED BY	DATE	REVISED BY	DATE
K. S. Wilcox	10/23/74	C. J. Tammer	11-4-77		

72 CO 432

COMPOSITE DRAG LINK

FITTING - FORWARD

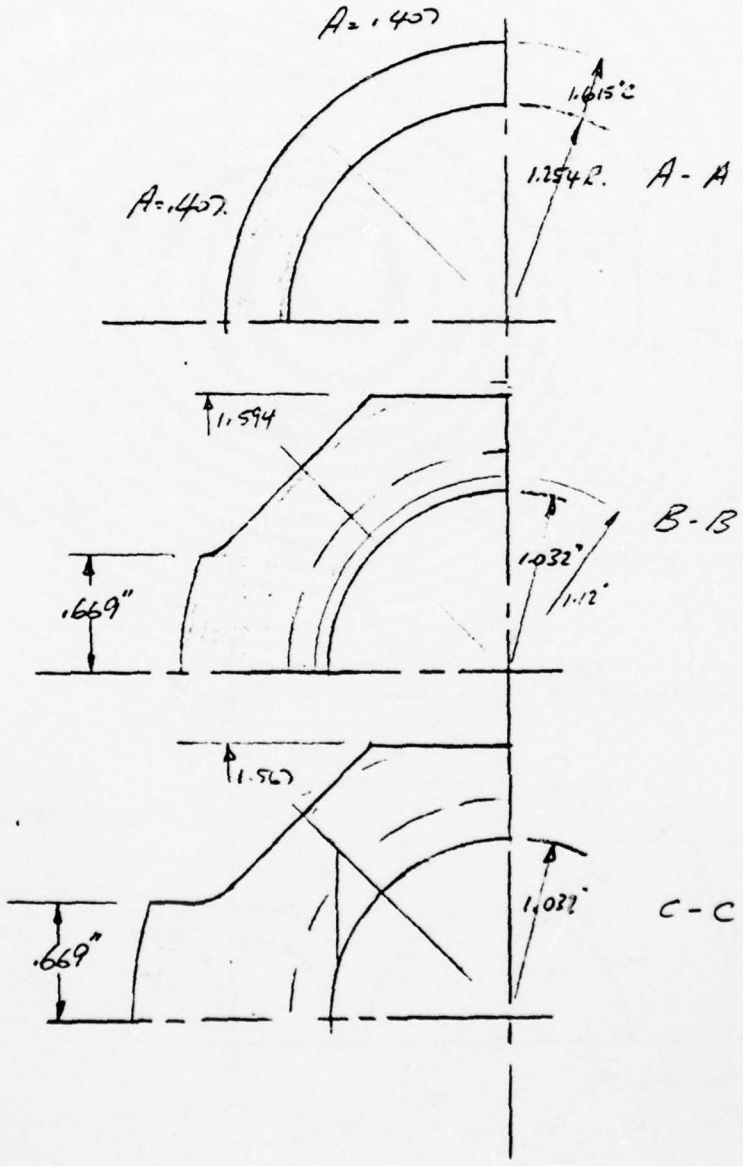

PREPARED BY	DATE	CHECKED BY	DATE	REVISED BY	DATE
R. S. WILSON	10/23/74	C. J. Tanner	11-4-77		

72 CO 432

COMPOSITE DRAG LINK

FITTING – FORWARD

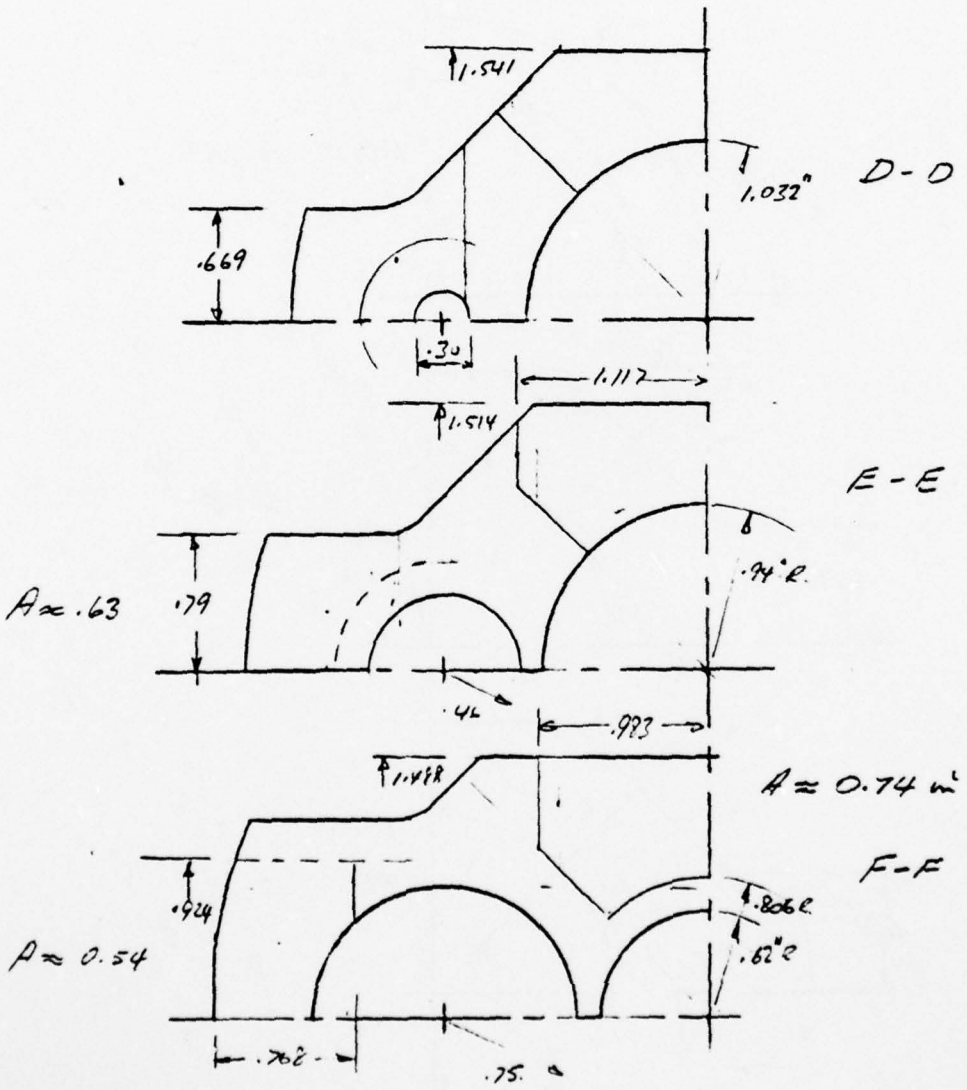

PREPARED BY	DATE	CHECKED BY	DATE	REVISED BY	DATE
L. S. Wilcox	10/12/77	C. J. Tanner	11-4-77		

72 CO 432

COMPOSITE DRAG LINK.

FITTING - FORWARD

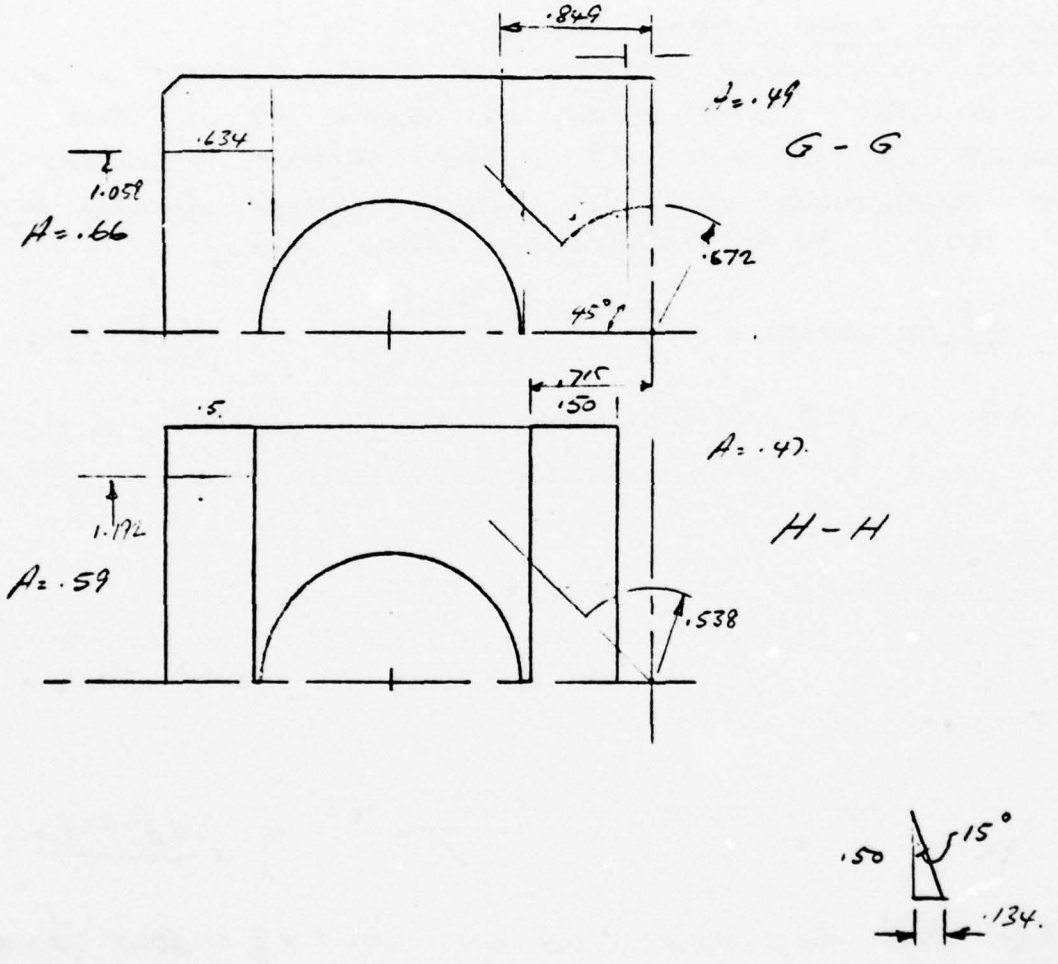

PREPARED BY	DATE	CHECKED BY	DATE	REVISED BY	DATE
L. S. Wilson	10/23/74	C. J. Tammer	11-4-77		

72 CO 432

COMPOSITE DRAG LINK

FITTING - FORWARD.

MINIMUM LOAD PATH CONTD.

THE MINIMUM SECTION IN THE FITTING IS AT SECTION AA. THE AREA IN EACH 1/8 OF THE COLLAR IS 0.407 IN.^{2} THE OCTANT NEAREST THE OUTERMOST LUGS IS MOST HIGHLY LOADED DUE TO THE 26½° INCLINED LOAD PATH.

$$f_t\ (\text{ULTIMATE}) = \frac{157000 \times 1.5 \times 1.2}{8 \times \cos(26.5) \times .407} = 96983 \text{ psi.}$$

$$M.S.\ (\text{TENSION ULTIMATE}) = \frac{130000}{96983 \times 1.15} - 1 = +0.17$$

FATIGUE

REFERENCE 7, TABLE VIII, NO 8 INDICATES THAT AN ELASTIC STRESS CONCENTRATION FACTOR OF 1.22 IS APPLICABLE TO THE RADIUS ADJACENT TO SECTION AA.

$$\therefore f\ (\text{FATIGUE}) = \frac{96983 \times 1.22}{1.5} = 78879 \text{ psi}$$

FOR THE REQUIRED LIFE OF 2000 X 2 = 4000 CYCLES THE ALLOWABLE FATIGUE STRESS (F_{MIN}) = 106000 psi. (REF FIGURE A-16)

$$\therefore M.S.\ (\text{FATIGUE}) = \frac{106000}{78879} - 1 = +0.34$$

PREPARED BY	DATE	CHECKED BY	DATE	REVISED BY	DATE
L.S. WILSON	10/13/74	C.J. Tammer	11-2-77		

72 CO 432

FITTING FOGNARD

KICK LOADS AT OFFSET OUTER LUG.

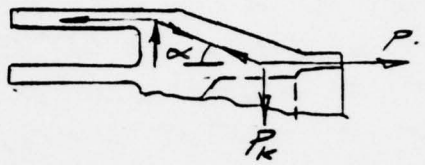

DESIGN LOAD/LUG = 1.2 $P_{AVE.}$

$$= \frac{157000}{4} \times 1.2 = \underline{47100^{\#} \text{ LIMIT.}}$$

$$P_K = P \tan(\alpha)$$
$$= 47100 \tan(37.0^\circ) = 35492^{\#}$$

CONSIDER CYLINDRICAL WALL AT END OF FITTING UNDER RADIAL KICK LOADS AS SHOWN.

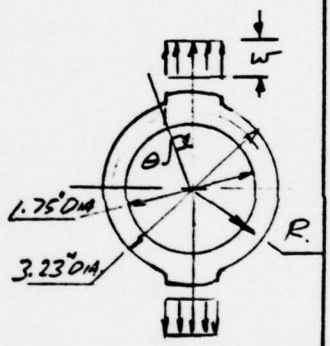

$$\text{LOAD/IN.} = W = \frac{P_K}{2R\theta} = \frac{35492}{2 \times 1.245 \times \left(\frac{22 \times 11}{180}\right)}$$

$$= \underline{37122 \ \#/\text{IN.} \ (\text{LIMIT.})}$$

FROM REF 7, TABLE VIII

$$M_1 = WR^2\left[.3183\left(\frac{\theta}{2} + \theta \sin^2\theta + \frac{3}{2}\sin\theta\cos\theta\right) - \frac{1}{2}\sin^2\theta\right]$$

$$= 37122 \times 1.245^2\left[.3183\left(\frac{.3840}{2} + .3840\sin^2(.3840) + \frac{3}{2}\sin(.3840)\cos(.3840)\right) - \frac{1}{2}\sin^2(.3840)\right]$$

$$= \underline{10006 \text{ IN LB (LIMIT.)}}$$
$$= \underline{15009 \text{ IN LB (ULTIMATE)}}$$

PREPARED BY	DATE	CHECKED BY	DATE	REVISED BY	DATE
R. S. WILSON	10/25/74	C. J. Tanner	11-2-77		

71 CO 432

COMPOSITE DRAG LINK

FITTING - FORWARD

FOR $0 < X < 22°$

$M = M_1 - .5 W R^2 \sin^2(X)$

$T = -W R \sin^2(X)$

$V = -W R \sin(X) \cos(X)$

FOR $22° < X < 90°$

$M = M_1 - W R^2 \left(\sin(\theta)\sin(X) - \frac{\sin^2(\theta)}{2}\right)$

$T = -W R \sin(\theta) \sin(X)$

$V = -W R \sin(\theta) \cos(X)$

X°	M	T	V
0	15009	0	0
10	13708	2090	11855
20	9961	8110	22281
30	4899	12984	22490
40	282	16693	19894
50	-3703	19894	16693
60	-6937	22490	12985
70	-9317	24403	8882
80	-10776	25575	4510
90	-11267	25970	0

THE ABOVE LOADS IN THE CYLINDRICAL WALL ARE PLOTTED ON FIGURE A-17.

PREPARED BY	DATE	CHECKED BY	DATE	REVISED BY	DATE
R.S. WILSON	10/30/74	C.J. Tammer	11-4-74		

FIGURE A-17 LOADS IN CYLINDRICAL WALL OF FITTING DUE TO KICK LOADS

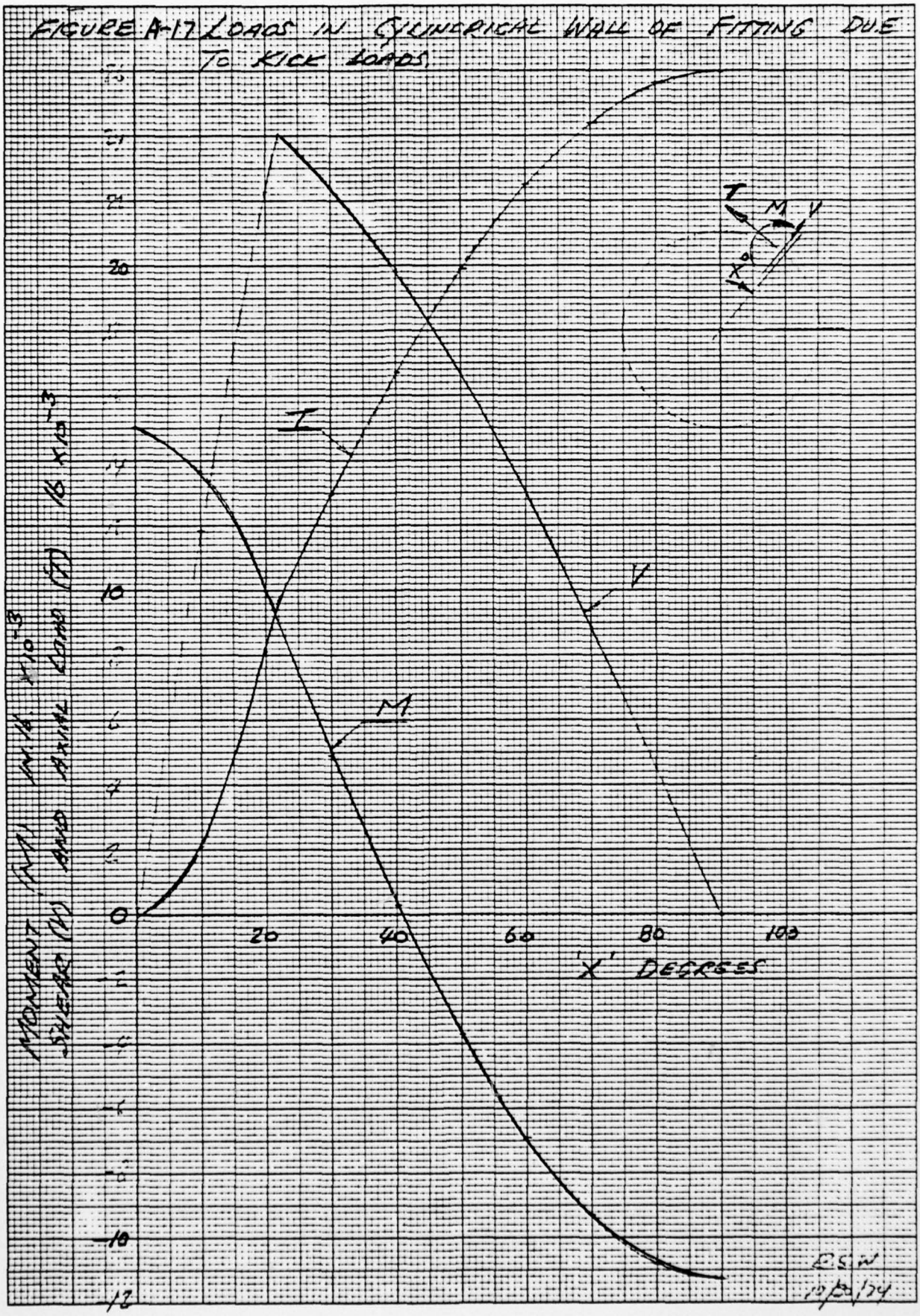

46 1323

K·E 10 X 10 TO ½ INCH 7 X 10 INCHES KEUFFEL & ESSER CO. MADE IN U.S.A.

72 C0432

COMPOSITE DRAG LINK

FITTING FORNARO

STRESSES IN FITTING SKIRT DUE TO KICK LOADS.

WALL BENDING AT $X = 0°$

$$f_b = \frac{6M}{bt^2} = \frac{6 \times 15009}{1.0 \times 0.74^2} = 164452 \text{ psi}$$

F_B. (Ti-6Al-4V ANNEALED) = 187000 psi. REF. 8

$$M.S.\text{ (WALL BENDING)} = \frac{187000}{164452} - 1 = +0.14$$

WALL BENDING AND HOOP TENSION AT $X = 90°$

$$f_b = \frac{6M}{bt^2} = \frac{6 \times 11267}{1.0 \times 0.74^2} = 123451 \text{ psi}$$

$$f_t = \frac{P}{bt} = \frac{25970}{1.0 \times .74} = 35094 \text{ psi}$$

$$R_B = \frac{f_b}{F_B} = \frac{123541}{187000} = 0.661 \qquad R_T = \frac{f_t}{F_{TU}} = \frac{35094}{130000} = 0.270$$

$$M.S.\text{ (COMBINED BENDING \& TENSION)} = \frac{1}{R_T + R_B} - 1$$

$$= \frac{1}{.27 + .661} - 1 = +0.075$$

PREPARED BY / DATE	CHECKED BY / DATE	REVISED BY / DATE
K. S. WILSON 10/30/74	C. J. Tammer 11-4-77	

72 C0433
COMPOSITE DRAG LINK

A.5 FITTING - AFT

LUG STATIC STRENGTH ANALYSIS

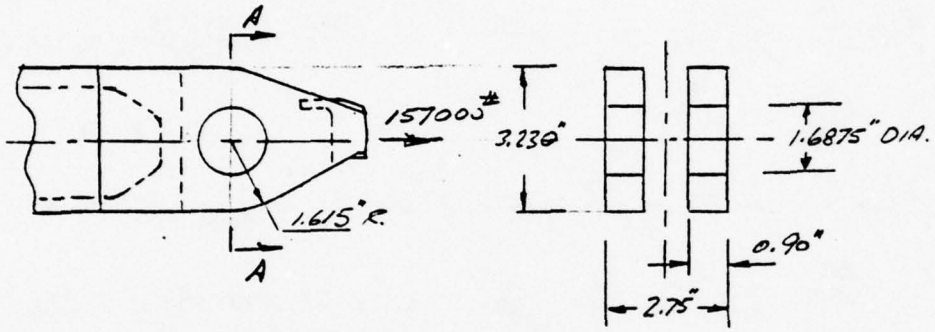

TENSION ON NET SECTION.

$$A_T = (W-D)t = (3.23 - 1.6875)2 \times .87 = \underline{2.684\ IN^2}$$

FOR Ti-6AL-4V ANNEALED (REF 5 SECTION 10.6)

F_{TU} = 130 KSI, G = 0.921, H = 0.0748

$$\lambda = \frac{D}{W} = \frac{1.6875}{3.23} = 0.52 \quad \therefore K_T = 0.955$$

$$P_{TU} = K_T \cdot F_{TU} \cdot A_T = 0.955 \times 130000 \times 2.684$$
$$= \underline{333218\#}$$

$$M.S.\ (NET\ TENSION) = \frac{333218}{157000 \times 1.5 \times 1.15} = \underline{+0.23}$$

PREPARED BY	DATE	CHECKED BY	DATE	REVISED BY	DATE
R.S. WILSON	10/20/74	C.J. Tammer	11-4-77		

72 CO 433

COMPOSITE DRAG LINK

FITTING - AFT

SHEAR TEAROUT - BEARING

$e/D = \frac{1.615}{1.6875} = 0.957$ $\quad D/t = \frac{1.6875}{.87} = 1.940$

$\therefore K_{BR} = 0.79$

$A_{BR} = Dt = 1.6875 \times .87 \times 2 = 2.936 \text{ in}^2$

$\therefore P_{BRU} = K_{BR} \cdot F_{tu} A_{BR} = 0.79 \times 130000 \times 2.936$

$= 301552$ lb.

$M.S.\,(\text{SHEAROUT - BEARING}) = \frac{301552}{157000 \times 1.5 \times 1.15} - 1 = +0.11$

LUG YIELDING

FOR $\frac{e}{D} = 0.957$ $\quad K_{BRY} = 0.90$

$P_y = K_{BRY} A_{BR} F_{ty} = 0.90 \times 2.936 \times 120000$

$= 317088$ lb.

$M.S.\,(\text{LUG YIELDING}) = \frac{317088}{157000 \times 1.15} - 1 = +0.75$

PREPARED BY	DATE	CHECKED BY	DATE	REVISED BY	DATE
R. S. Wilson	10/24/72	C. J. Tanner	11-9-72		

72 CO 433

COMPOSITE DRAG LINK

FITTING - AFT

LUG FATIGUE STRENGTH

STRESS ON NET SECTION = $\frac{P}{(W-D)t}$

= $\frac{157000}{(3.23-1.6875)2\times.87} = 58496$ psi

STRESS CONCENTRATION FACTOR FROM REF 6, FIG. 83.

$\frac{a}{W} = \frac{1.6875}{3.23} = 0.52 \quad \therefore K_T = 2.36.$

CONSERVATIVELY USING S-N CURVES FOR $K_T = 3.3$ FROM REF 3 FIG 5.4.3.1.8.

REQUIRED LIFE = 2000 × 2 = 4000 CYCLES.

$\therefore$ THE ALLOWABLE MAXIMUM STRESS $F_{MAX} \approx 75000$ psi REFERENCE FIGURE A-16.

M. S. (LUG FATIGUE) = $\frac{75000}{58496} - 1 = +0.28$

PREPARED BY	DATE	CHECKED BY	DATE	REVISED BY	DATE
L. S. WILSON	10/24/74	C. J. Tanner	11-4-77		

72CO432 & 72CO433

COMPOSITE DRAG LINK

A.6 FWD AND AFT FITTINGS

Ti-6AL-4V AS WELDED S-N DATA.

FATIGUE S-N DATA FOR THE UNMACHINED UN-STRESS RELIEVED END FITTING WELDED JOINTS IS BASED ON RECENT CONVAIR DATA (REF B) FOR THE SAME TYPE WELD IN 2.0 IN. O.D., 0.045 IN. WALL TITANIUM SPECIMENS. THE SPECIMENS WERE TESTED FOR FULLY REVERSED ($R = -1$) FATIGUE LOADING. THERE IS NO DATA FOR TUBE WALL THICKNESSES (0.36 IN) CORRESPONDING TO THE DRAG LINK FITTINGS CONSIDERED HERE, HOWEVER, STRESS CONCENTRATIONS AT THE UNMACHINED WELDS AND POSSIBLE JOINT MISALIGNMENT EFFECTS SHOULD BE REDUCED FOR THE THICKER WALL TUBE.

MEAN DATA FOR EACH TEST STRESS LEVEL IS PLOTTED ON A CONSTANT LIFE FATIGUE DIAGRAM IN FIGURE A-18. THIS FIGURE IS USED TO DERIVE DATA FOR $R = -0.6$ BY INTERPOLATION. THE DERIVED CURVE FOR $R = -0.6$ IS GIVEN IN FIGURE A-19.

PREPARED BY	DATE	CHECKED BY	DATE	REVISED BY	DATE
L. S. Hilson	10/31/77	C. J. Tanner	11-4-77		

AD-A058 888 GENERAL DYNAMICS SAN DIEGO CA CONVAIR DIV F/G 11/4
BORON/ALUMINUM LANDING GEAR FOR NAVY AIRCRAFT.(U)
SEP 78 N62269-74-C-0619
UNCLASSIFIED CASD-NADC-76-003 NL

2 OF 2
ADA
058888

END
DATE
FILMED
11-78
DDC

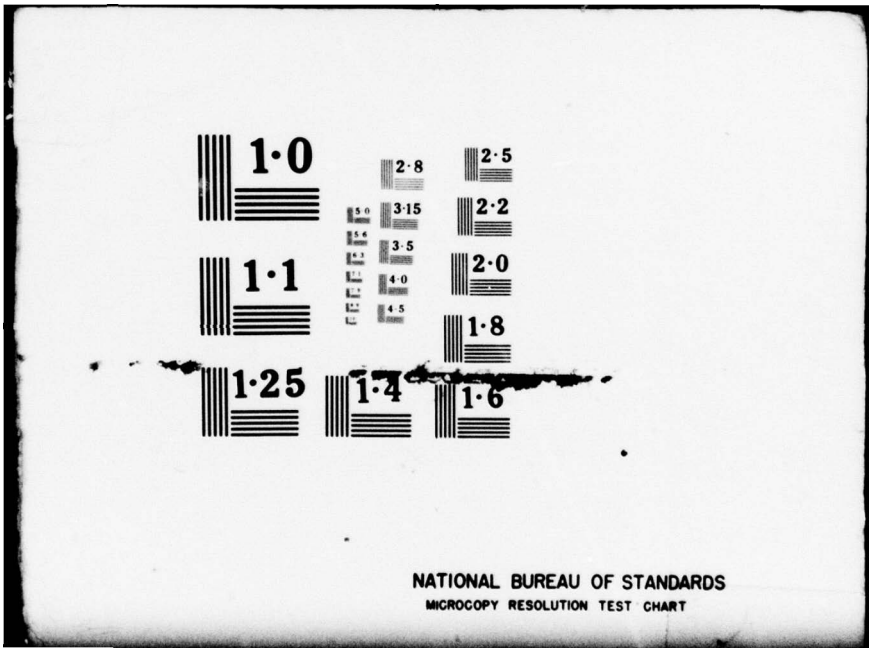
1·0
1·1
1·25
1·4
1·6
1·8
2·0
2·2
2·5
2·8
3·15
3·5
4·0
4·5
NATIONAL BUREAU OF STANDARDS
MICROCOPY RESOLUTION TEST CHART

FIGURE A-18 CONSTANT LIFE DIAGRAM FOR AS WELDED Ti - 6Al - 4V

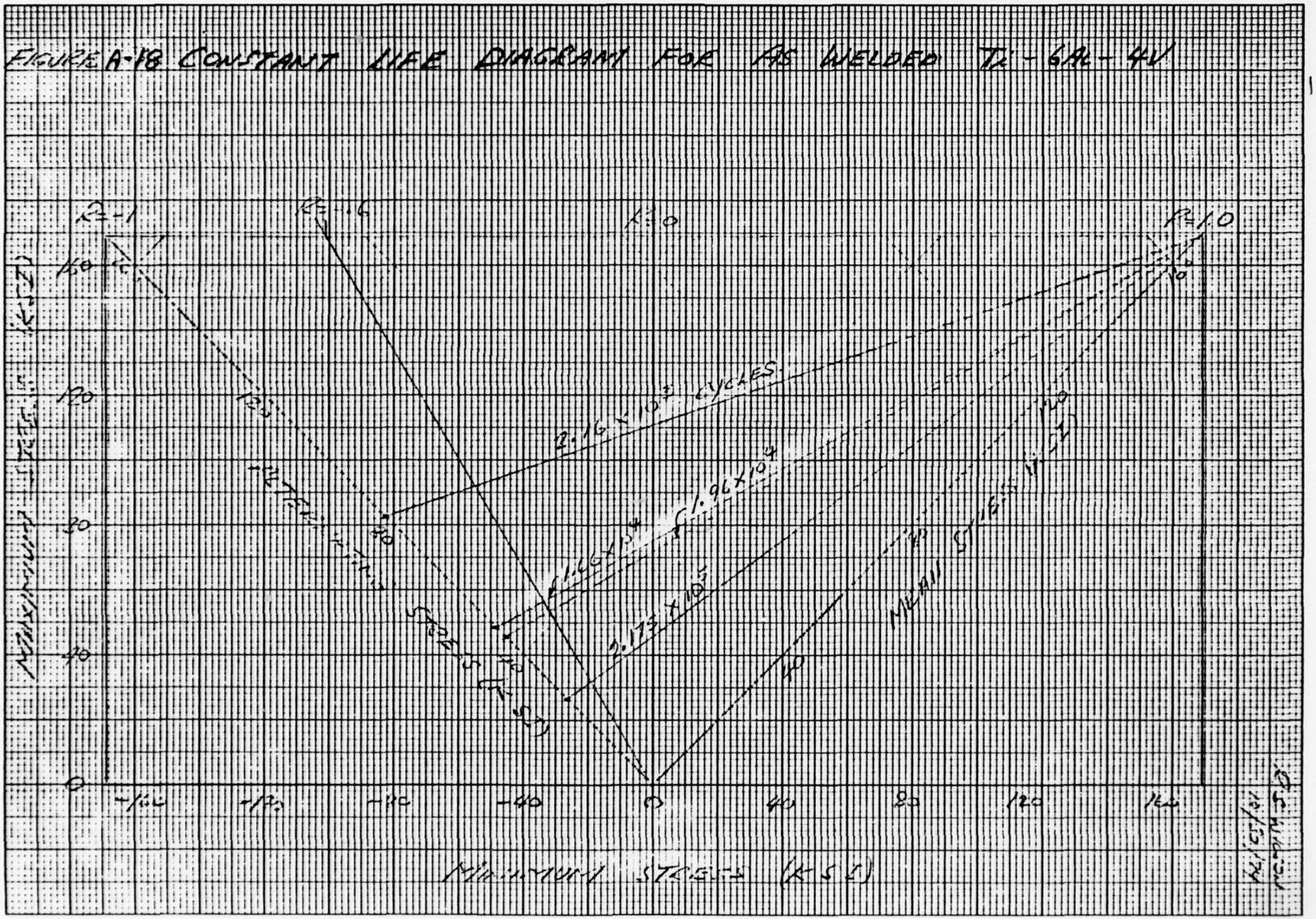

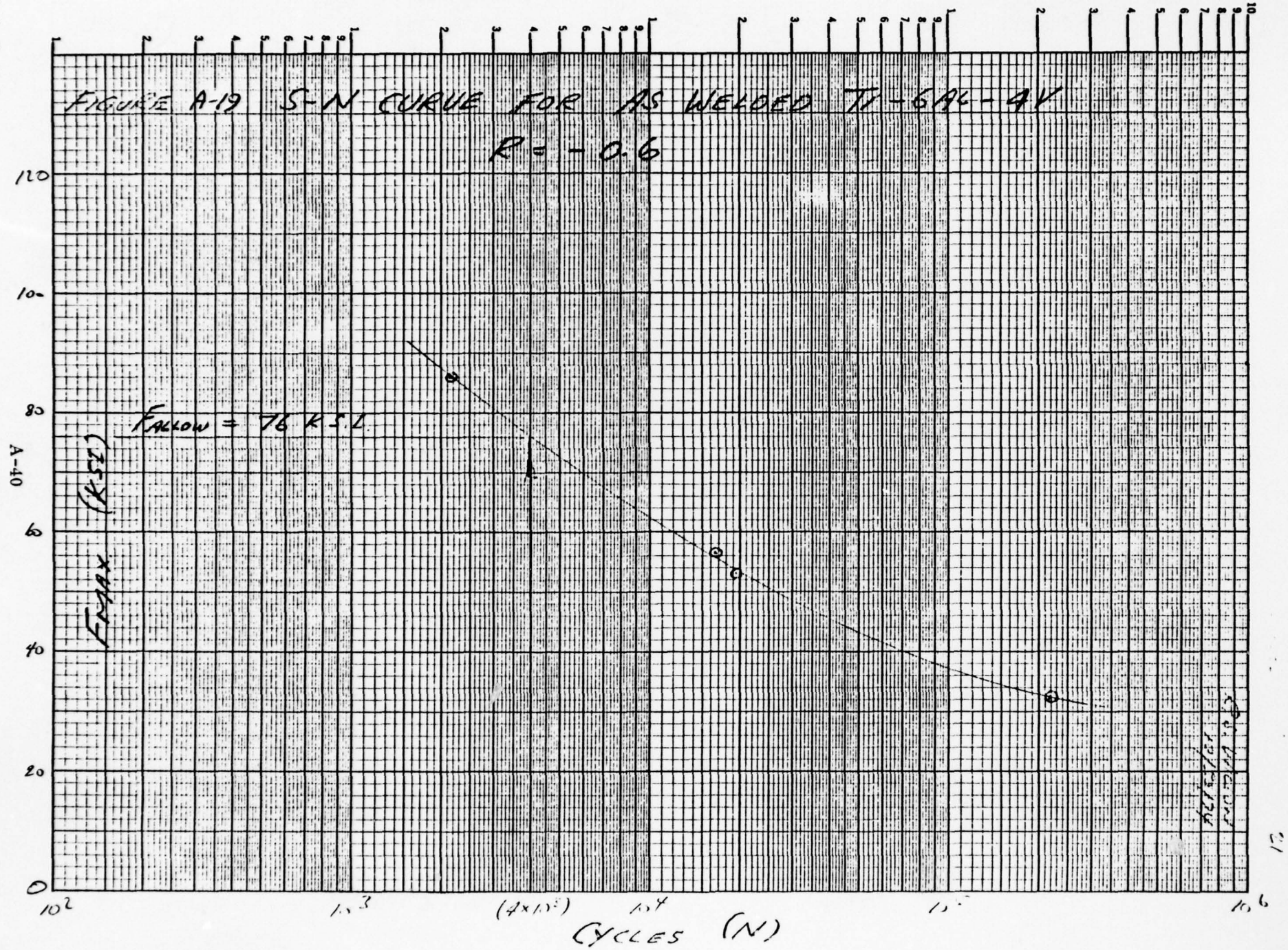

72 C0432 & 72 C0433
COMPOSITE DRAG LINK

FWD & AFT FITTINGS

WELD STATIC STRENGTH

ASSUMING A CIRCUMFERENTIAL PEAKING FACTOR OF 1.2 AT THE WELD

$$f_t = \frac{1.2\,P}{A} = \frac{1.2 \times 157000 \times 1.5}{\frac{\pi}{4}(3.23^2 - 2.508^2)} = 86853 \text{ psi}$$

ASSUME A 90% WELD EFFICIENCY

$$M.S. = \frac{.9\,F_{tu}}{f_t} - 1. = \frac{.9 \times 130000}{86853} - 1 = +0.35$$

WELD FATIGUE STRENGTH

$$\text{MAXIMUM FATIGUE STRESS} = \frac{f_{t\,ULT.}}{1.5} = \frac{86853}{1.5} = 57902 \text{ psi}$$

$$\text{STRESS RATIO} = R = \frac{P_{min}}{P_{max}} = \frac{-94000}{157000} = -0.60$$

REQUIRED FATIGUE LIFE = 2000 X 2 = 4000 CYCLES

FROM S-N CURVE FOR AS WELDED Ti-6Al-4V FIGURE A-12.

ALLOWABLE FATIGUE STRESS F_{max} = 76000 psi

$$\therefore M.S.\ (\text{WELD FATIGUE}) = \frac{76000}{57902} - 1 = +0.31$$

PREPARED BY	DATE	CHECKED BY	DATE	REVISED BY	DATE
R. S. Wilson	10/31/74	C. J. Tammer	11-4-77		

N62269-74C-0619

B/A1 LANDING GEAR LINK

A.7

FITTING - TEST SPECIMEN

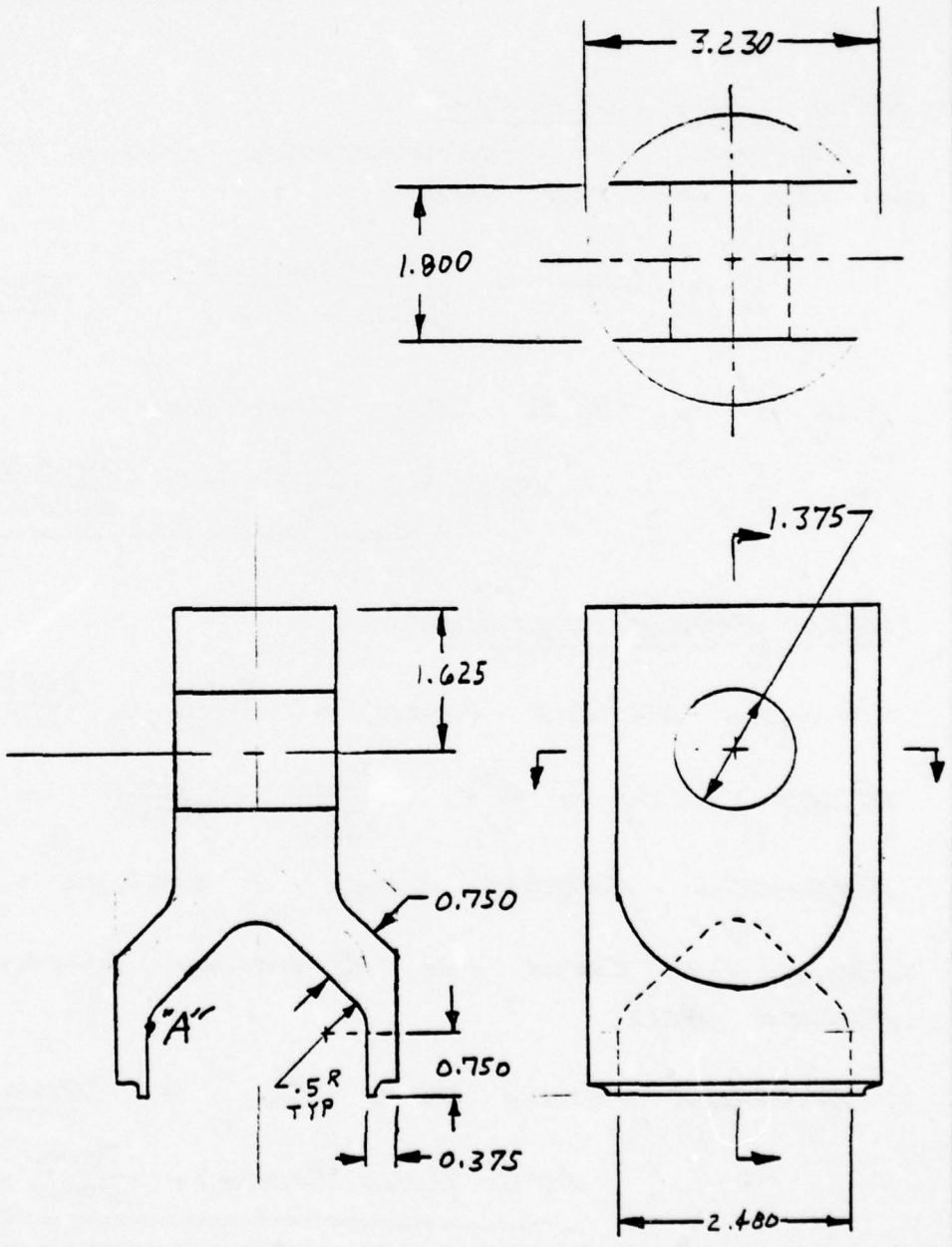

PREPARED BY	DATE	CHECKED BY	DATE	REVISED BY	DATE
MCCUTCHEN	9-13-74	C.J. Tammer	11-4-77		

NG2269-74-C-0619

B/AI LANDING GEAR LINK

FITTING - TEST SPECIMEN

Net Tension Area Lug:

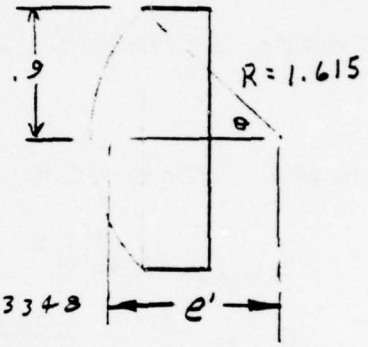

$\theta = \sin^{-1}\frac{.9}{1.615} = 0.5911$ radians

$A_{seg} = \frac{1}{2}R^2(2\theta - \sin 2\theta)$

$= \frac{1.615^2}{2}(2\times.5911 - \sin 2\times.5911) = 0.3348$

$A = 2\times\left[0.3348 + 1.8\times\left(1.615\cos.5911 - \frac{1.375}{2}\right)\right] = \underline{3.02221 \text{ in}^2}$

Calculate e': $\quad A = W\left(e' - \frac{D}{2}\right)$

$\frac{1}{2}\times 3.02221 = 1.80\left(e' - \frac{1.375}{2}\right) \Rightarrow \underline{e' = 1.527"}$

Ultimate strength Lug: Ref 2, section 10.6

For Ti-6Al-4V Annealed; $G = 0.921$, $H = 0.0748$

$\lambda = \frac{D}{W} = \frac{1.375}{2\times 1.527} = 0.450 \Rightarrow K_T = 0.953$

$P_{TU} = K_T F_{TU} A_T = 0.953\times 130{,}000\times 3.02221 = 374{,}422$ lbs

$M.S._{Tens} = \frac{374{,}422}{1.15\times 236000} - 1 = \underline{\underline{+0.380}}$

$e/D = \frac{1.625}{1.375} = 1.18 \Rightarrow K_{br} = 1.10$

$P_{BrU} = 1.10\times 130{,}000\times 1.375\times 1.8 = 353{,}925$ lbs

PREPARED BY	DATE	CHECKED BY	DATE	REVISED BY	DATE
MCCUTCHEN	9-13-74	C. J. Tammer	11-4-77		

N62269-74-C-0619

B/A1 LANDING GEAR LINK

FITTING - TEST SPECIMEN

Ultimate Strength Lug Cont:

$$MS_{Bru} = \frac{353925}{1.15 \times 236000} - 1 = \boxed{+0.304}$$

Ultimate Strength Pin:

$$A_{SHEAR} = 2\frac{\pi}{4} D^2 = \frac{\pi}{2} \times 1.375^2 = 2.9698 \text{ in}^2$$

$$f_s = \frac{P}{A} = \frac{236000}{2.9698} = 79467 \text{ psi}$$

$$MS_{shear} = \frac{156.000}{79467} - 1 = \boxed{+0.96}$$

$$r = \frac{e - \frac{D_h}{2}}{t} = \frac{1.625 - \frac{1.375}{2}}{1.80} = 0.52 \Rightarrow \gamma = 0.37$$

$$m = \frac{P_U}{A_{br} F_{TU}} = \frac{236,000}{1.8 \times 1.375 \times 130000} = 0.733$$

$$b_r = \frac{0.9}{2} + 0.37\,\frac{1.8}{4} + 0.010 = 0.627 \text{ in}$$

$$\sigma = \frac{236000 \times \frac{1}{2} \times 0.627 \times 32}{\pi \times 1.375^3} = 289,895 \text{ psi}$$

Using Ref. 8, pg 17.15.13;

$$F_{Bm} = 253 \times \frac{260}{200} = 328,900 \text{ psi}$$

$$MS_{Bending} = \frac{328,900}{289955} - 1 = \boxed{+0.13}$$

PREPARED BY	DATE	CHECKED BY	DATE	REVISED BY	DATE
MCCUTCHEN	9-10-74	C.J. Tammer	11-4-77		

N62269-74-C-0619
B/A1 LANDING GEAR LINK

FITTING - TEST SPECIMEN

Lug Fatigue Strength:

Concentration Factor, Ref. 6 Fig. 83

$a/w = \frac{1.375}{2 \times 1.527} = 0.450 \Rightarrow K_{T_{br}} = 2.14$

$\sigma_{max} = K_T \frac{P}{2h} = 2.14 \times 157000 / (1.375 \times 1.80) = 135{,}750$ psi

$F_{TY} = 120{,}000$ ∴ Assume yielding

$136 - 120 = 16 \Rightarrow R = -\frac{16}{120} = -0.13$ with $\sigma_{max} = 120$ ksi

Ref. 3, Fig. 5.4.3.1.8 gives a typical constant life of 10^4 cycles at $\sigma_{max} = 120$ ksi, $R = -0.13$.

If the max calculated stress were 145 ksi, the $R = -.21$ & $N \approx 4000$.

$$MS_{Lug\ Fatigue} = \frac{145}{136} - 1 = \underline{\underline{+0.066}}$$

Lug to Cylinder Transition, Fatigue Strength:

Based on previous analysis using an axisymmetric solid approximation, there is a stress concentration of approximately 2.0 at the inside radius (point "A", page). Also, assume a 15% circumfrential peaking.

PREPARED BY	DATE	CHECKED BY	DATE	REVISED BY	DATE
MCCUTCHEN	9-22-74	C.F. Tanner	11-4-77		

N62269-74-C-0619

B/A1 LANDING GEAR LINK

FITTING-TEST SPECIMEN

Lug To Cylinder Transition, Fatigue Strength: cont.

$$\sigma_{net} = 1.15\frac{P}{A} = \frac{1.15 \times 157{,}000}{\frac{\pi}{4}(3.230^2 - 2.480^2)} = 53{,}680 \text{ psi}$$

$$\sigma_{max} = k_T \sigma_{net} = 2 \times 53680 = 107{,}360 \text{ psi}$$

The +157 kip loads will be assumed to be paired with the -94 kip loads. The remaining loads are all compressive and will be ignored.

$R = \frac{-94}{+157} = -.60$ Ref 3, Fig 5.4.3.1.8 with $\sigma_{max} = 108$ ksi $\Rightarrow N_{TYP} \approx 4 \times 10^3$

$$MS_{Fatigue} = \frac{4 \times 10^4}{4 \times 10^4} - 1 = \boxed{+0.00}$$

Weld: Static strength

Assume the circumfrential peaking is 10% at the weld.

$$\sigma_{ult} = \frac{1.10P}{A} = \frac{1.10 \times 236000}{\frac{\pi}{4}(3.23^2 - 2.48^2)} = 77{,}182 \text{ psi}$$

3.3655

Assume a 90% weld efficicency.

$$MS_{weld\ static} = \frac{130{,}000 \times 0.9}{1.15 \times 77182} - 1 = \boxed{+0.32}$$

Weld: Fatigue Strength

$\sigma_{max} = \frac{77{,}182}{1.50} = 51455$ psi $\quad R = -0.60$

PREPARED BY	DATE	CHECKED BY	DATE	REVISED BY	DATE
MCCUTCHEN	9-22-74	C. J. Tanner	11-4-77		

NG2269-74-C-0619
B/A1 LANDING GEAR LINK

FITTING-TEST FITTING

Weld : Fatigue Strength: Cont.

There is no available data on the fatigue strength of an un-stress relieved, unmachined weld in this thick of section. Convair does have some recent data for the same type weld in 2.0" OD, 0.045 wall Titanium tested in R = -1.0 fatigue. This is described in reference 9. Ref. 9 lists the following tests:

σ	N
±44,231	20,722
±46,939	13,390
±45,017	9,143
±45,098	22,111
±46,748	24,861

The thicker walled link should have a lower stress concentration factor at the unmachined welds. The total stress excursion is less. Therefore, the weld is judged adequate in fatigue.

M.S. weld Fatigue = $\frac{1}{+}$

PREPARED BY	DATE	CHECKED BY	DATE	REVISED BY	DATE
MCCUTCHEN	9-22-74	C.J. Tanner	11-4-77		

N62269-74-C-0619
B/A1 LANDING GEAR LINK

A.8
LINK STABILITY

B/A1 : 28 ply @ .007 /ply ⇒ $t_{nom} = 0.196$

The material is tollerenced such that 1.05 $t_{min} > t_{nominal}$.

$OD_{B/A} = 3.125$ in $ID_{B/A1} = 2.733$ in

$I_{B/A1} = \frac{\pi}{64}\left(\overline{OD}^4 - \overline{ID}^4\right) = 1.942739\ in^4$

$EI_{B/A1} = 28.9 \times 10^6 \times 1.942739 = 5.614515 \times 10^7\ \#in^2$

Ti : The minimum Ti section is at the edge of the B/A1

$OD_{Ti} = 3.140$ in $ID_{Ti} = 2.530$ in

$I_{Ti} = \frac{\pi}{64}\left(\overline{3.14}^4 - \overline{2.53}^4\right) = 2.760684\ in^4$

$EI_{Ti} = 16.4 \times 10^6 \times 2.760684 = 4.527522\ \#in^2$

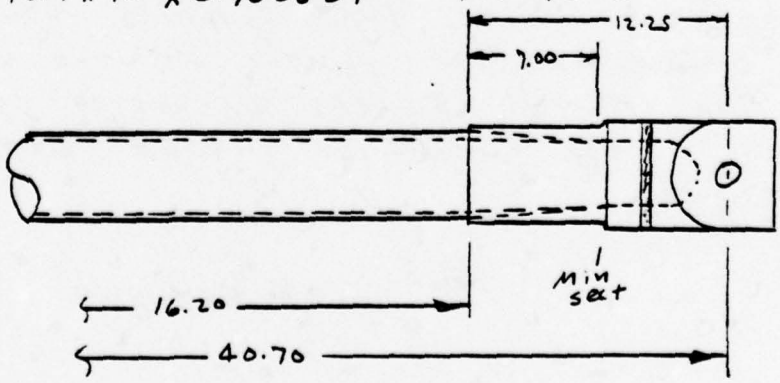

PREPARED BY	DATE	CHECKED BY	DATE	REVISED BY	DATE
MCCUTCHEN	9-23-74	C.J. Tanner	11-4-77		

N62269-74-C-0619

B/AI LANDING GEAR LINK

LINK STABILITY

Assume EI linearly tapers from edge of collar to pin and match EI at min section at 7.00 dimension

$$EI_{pin} = 5.6145\times10^7 - \left[\frac{5.6145 - 4.5275}{7.00}\times 12.25\times10^7\right] = 3.712277\times10^7 \#\,in^2$$

Using Ref. 5, Fig. 5.3.0.6:

$$EI_1/EI_2 = \frac{3.712277}{5.6145} = 0.661 \qquad a/L = \frac{16.20}{40.70} = 0.398$$

$$\Rightarrow m = 9.60$$

$$P_{euler} = \frac{9.60\times 5.614515\times10^7}{40.7^2} = 325,382\ lbs$$

Using Ref. 10, section 2.17:

$$P_{cr} = \frac{P_e}{1 + \frac{n\,P_e}{AG}}$$

Ref 11 gives $k = \frac{1}{n} = \dfrac{6E(1-m^4)(1+m^2)}{\nu G(2m^6+18m^4-18m^2-2) - E(7m^6+27m^4-27m^2-7)}$

where $m = \dfrac{R_{Inner}}{R_{Outer}} = \dfrac{2.733}{3.125} = .8746$

$$\frac{1}{n} = \frac{6\times28.9\left(1-\overline{.8746}^4\right)\left(1+\overline{.8746}^2\right)}{.27\times8.3\left(2\times\overline{.8746}^6+18\times\overline{.8746}^4-18\times\overline{.8746}^2-2\right)-28.9\left(7\times\overline{.8746}^6+27\times\overline{.8746}^4-27\times\overline{.8746}^2-7\right)}$$

$$\frac{1}{n} = 0.5239$$

$$A = \frac{\pi}{4}\left(D_O^2 - D_I^2\right) = \frac{\pi}{4}\left(\overline{3.125}^2 - \overline{2.733}^2\right) = 1.803538$$

PREPARED BY / DATE	CHECKED BY / DATE	REVISED BY / DATE
MCCUTCHEN 9-23-74	C.J. Tanner 11-4-77	

NG2269-74-C-0619

B/AI LANDING GEAR LINK

LINK STABILITY

$$P_{cr} = \frac{325382}{1 + \frac{325382}{.5239 \times 1.803538 \times 0.3 \times 10^6}} = 311{,}390 \text{ lbs}$$

Using Ref. 10, section 1.7 for maximum moment in a beam column:

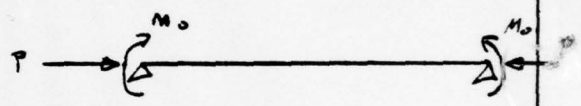

$$M_{max} = \frac{M_o}{\cos\left(\frac{\pi}{2}\sqrt{\frac{P}{P_{cr}}}\right)}$$

Also, assume a maximum manufacturing eccentricity of 0.030 in. in the same direction at each end.

$$M_{max} = \frac{141000 \times 0.030}{\cos\left(\frac{\pi}{2}\sqrt{\frac{141000}{311390}}\right)} = 8607 \text{ in lbs}$$

$$\sigma_{c\,max} = \frac{P}{A} + \frac{Mc}{I} = \frac{141000}{1.803538} + \frac{8607 \times 3.125}{2 \times 1.942738} = 78180 + 6922$$

$$\sigma_{c\,max} = -85102 \text{ psi}$$

Ref 2, Fig 5.2 gives compressive allowable stresses as a function of D/t.

$$\frac{D}{t} = \frac{3.125 - .196}{.196} = 14.94 \Rightarrow F_c > 225 \text{ ksi}$$

$$MS_{c\,B/A} > \frac{225}{85.1} - 1 = \underline{\text{+Large}}$$

PREPARED BY	DATE	CHECKED BY	DATE	REVISED BY	DATE
MCCUTCHEN	9-24-74	C.T. Tammer	11-4-77		

A.9 DAMAGE TOLERANCE

In order to determine initial flaw sizes for the damage tolerance testing described in Section 4, a series of fracture analyses were performed and they are presented here. The applicability of linear elastic fracture mechanics to composite materials is not established; nevertheless, it provided a rational basis for selecting initial flaw sizes and predicting failure loads for the required test program.

A.9.1 Predict failure stress for the B/Al tube with a part through crack (PTC) penetrating 3 plies of B/Al at the end of the titanium collar. Assume the crack extends 180° around the circumference.

The following analysis is based on Reference 12, page 256:

$$K_{IC} + 1.1\,\sigma\,\sqrt{\pi a_{cr}/Q_{cr}}\;\;M_k$$

where $Q = [\phi^2 - (.212)\,(\sigma/\sigma_{ys})^2]$

$\phi^2 = 1 + 4.5934\,(a/2C)^{1.6499}$

Q can also be read directly from Fig. 10 (ASTMSTP 381), given (a/2C) and (σ/σ_{ys}).

K_{IC} = Plane strain fracture toughness.

σ = Gross failure stress

a = crack depth

M_k = back face correction factor

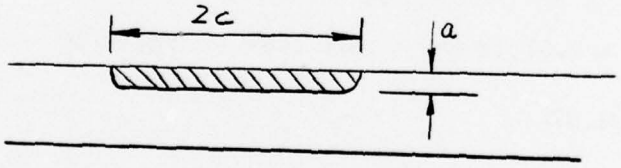

From fracture tests conducted at Convair of 10 ply and 40 ply UD STCA B/Al three point bend and center notch specimens:

$$K_Q = (3 \times 83.8 + 3 \times 85.1 + 2 \times 88.3)\,8 = 85.4 \text{ psi } \sqrt{\text{in}}$$

This represents our candidate plane stress fracture toughness. While two of the data points are for 40 ply through cracks, those two data points were suspect due to excessive crack widths. We really should use a value which represents K_{IC}, the plane strain fracture toughness for this assumed part through notch.

Data for one test for a part through notch in UD Condition F B/Al is:

depth = 0.026"

2C = length = 0.276"

$\frac{a}{2C} = \frac{.026}{.276} = .094$

t = 0.067"

depth/t = $\frac{.026}{.067}$ = 39%

W = 0.9614"

Net A = 0.05723 in^2

σ_{net} = 134.6 psi

P = 7700#

$\sigma / \sigma_{ys} \simeq 0.5$

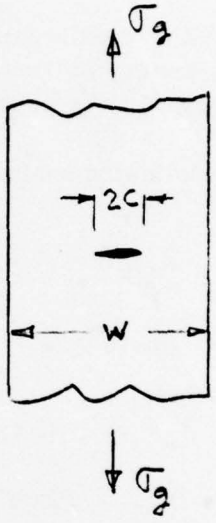

$\sigma_{gross} = \frac{7700}{(.9614)(.067)} = 119.5$ ksi

$\phi^2 = 1 + 4.5934\,(.094)^{1.6499} = 1.093$

$Q = 1.093 - (.212)(.5)^2 = 1.04$

$K_{IC} + (1.1)(119.5)\sqrt{3.14159 \times .026/1.04}\ (1.07)$

Assuming $M_k \simeq 1.07$ for a/t = .026/.067 = 39%, A/2C = .094

$K_{IC} = 36.8$ ksi $\sqrt{in}$ (1.07)

$\underline{K_{IC} = 39.4 \text{ ksi } \sqrt{in}}$

Assume K_{IC} (UD-STCA-B/Al) = 39.4 ksi $\sqrt{in}$ for this STCA tube (Derived for Condition F B/Al)

$a = .020"$ (3 plies x .0068"/ply)

$2C = 1/2\ \pi D = 1/2\ \pi\ 3.125 = 4.9"$

$\frac{a}{2C} = \frac{.020}{4.9} = .004$ Assume a/2C 0 $M_k \simeq 1.014$

$\phi^2 \simeq 1.0$

$Q = 1.0 - .212\ (.5)^2 = 0.947$

$K_{IC} = 1.1\ \sigma\ \sqrt{\pi a_{cr}/Q_{cr}}\ M_k$

$$\sigma = \frac{K_{IC}}{1.1\ \sqrt{\pi a_{cr}/Q_{cr}}\ M_k} = \frac{39.4}{1.1\ \sqrt{3.14159 \times .020/.947}\ (1.014)}$$

$$= \frac{39.4}{(.28334)(1.014)}$$

$\sigma = 137.1$ ksi $\div$ 1.045

Predicted
$\sigma_{Gross} = 131.2$ ksi Predicted failure stress at Ti collar.

1) This answer is based on 1 piece of fracture test data.
2) It assumes that linear elastic fracture mechanics applies to B/Al.
3) It assumes that the plane strain fracture toughness of 0° STCA B/Al is 39.4 ksi in may be significantly higher.

A.9.2 Select notch configuration for B/Al tubes and predict failure load of a tube which has been notched to a depth of 1/2 the wall thickness.

ANALYSIS

1) Two types of notches have been investigated to date at Convair: a machined notch of approximately 0.070 inches width and EDM notches of approximately 0.016 inches width. Some impact testing has been done on ND B/Al tubes which induced sharp cracks (a series of 10-15 adjacent fibers) in the B/Al. As a result, we either EDM sharp part through notches in these tubes or machine them in using another

method. Notch widths should be on the order of 0.015 - 0.020 inches. The fracture toughness data generated at Convair is for notch widths in this range.

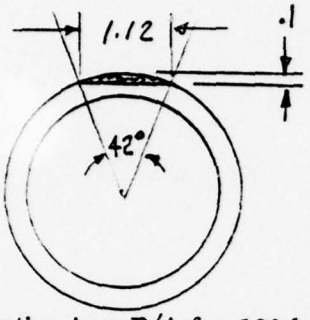

UD B/Al tube, STCA
28 ply t = 0.200"
OD = 3-1/8" = 3.125"
Pin-to-pin distance ~ 41"

R_o = 1.5625 R_i = 1.3625

The objective is a P/A for 130 ksi. This corresponds to an ultimate load of 236,000#.

$A = \pi(R_o^2 - R_i^2) = \pi(2.4414 - 1.8564) = 1.8378\ in^2$

P/A = 236,000/1.8377 = 128,421 psi

Check bending in this tube due to the local removal of the B/Al at the notch.

Overall bending should not be a problem. This is a localized effect.

Local wall bending may be significant depending on the depth of the notch. The back face connection factor, M_k, in the fracture equasion should account for this bending effect. Two problems with M_k are: (1) derived for isotropic materials, and (2) derived for flat coupons with part through cracks. The fact that our part through crack is in a UD B/Al tube instead of an isotropic flat coupon will certainly effect the back face connection factor. At this part, due to a lack of theoretrical data for B/Al, we will use the factors, M_k, developed for metals.

Reference 12, page 256

$$K_{IC} = 1.1\ \sigma\ \sqrt{\pi a_{cr}/Q_{cr}}\ \ M_k$$

where $Q = [\phi^2 - (1212)\ (\sigma/\sigma_{ys})^2]$

$$\phi^2 = 1 + 4.5934\ (a/2c)^{1.6499}$$

For the configuration selected (straight notch through 14 plies or .100")

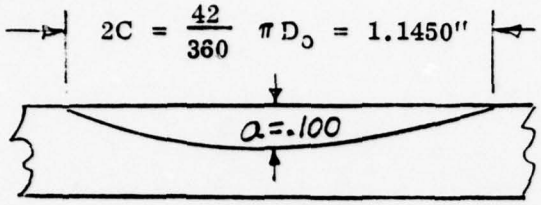

$$\frac{a}{2C} = \frac{0.100}{}$$

$$\sigma/\sigma_{ys} \simeq \frac{110 \rightarrow 130}{220} = .50 \rightarrow .59$$

Use 0.55

$$\phi^2 = 1 + 4.5934\,(.0373)^{1.6499}$$

$$\phi^2 = 1 + 4.5934 \times 0.0181$$

$$\phi^2 = 1.0831$$

$$Q = (1.0831)^2 - (.212)\,(.55)^2$$

$$= 1.1731 - .0641$$

$$Q = 1.1090$$

$$\sigma = \frac{K_{IC}}{1.1\sqrt{\pi a_{cr}/Q_{cr}}}\,M_k$$

Assume K_{IC} (UD STCA B/Al) = 39.4 ksi in. (Reference problem of 19 February 1975). This should be conservative. The single datapoint from which it is based was for bond F UD B/Al.

$$\sigma = \frac{39.4}{1.1\sqrt{\pi \times .1 \times 1.1090}\,M_k}$$

1.125

From Figure 16 (Deep Flaw Mag. Factor, M, used by NASA-MSC) B. Witzel

A/2B = .1/1.144 = .0374
A/T = .1/.2 = .5

$M_k = 1.125$

Part thru
$\sigma_{(a = .1)} = 53.9$ ksi

Much too small. Let's try a notch depth of 0.050".

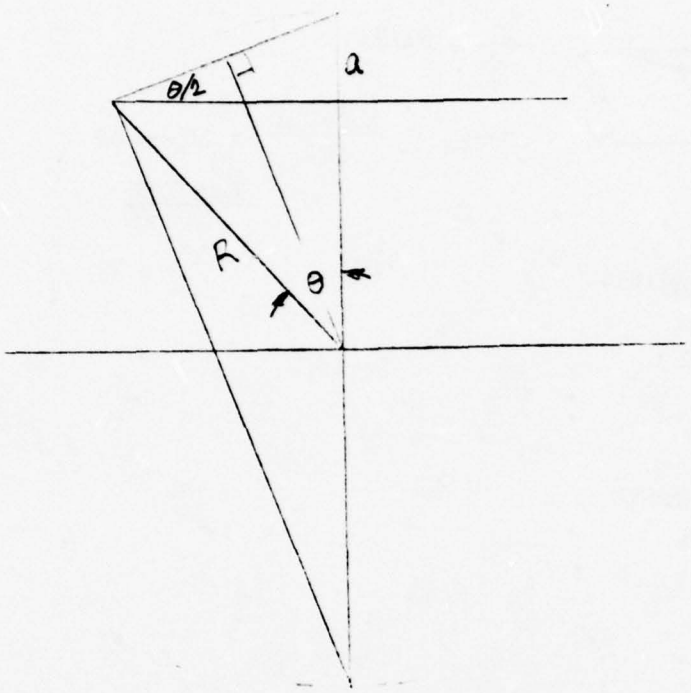

$$\text{Tan } \theta/2 = \frac{a}{b}$$

$$b = R/\text{Tan } \frac{\theta}{2}$$

$$\underline{2b = 2a/\text{Tan } \frac{\theta}{2}}$$

$$\text{Cos } \theta = \frac{R - a}{R}$$

$$\underline{\theta = \text{Cos}^{-1} \left(\frac{R - a}{R}\right)}$$

$$\text{arc} = \frac{2\theta}{360} \pi D_o$$

Check on $D_o = 3.125$ $\quad a = 0.1$

$R_o = 1.5625$

$$\theta = \text{Cos}^{-1} \frac{1.5625 - .1000}{1.5625} = \text{Cos}^{-1} .936 = .3597 \text{ rad} \quad \frac{360°}{2\pi \text{ rad}}$$

$\theta = 20.6°$

$\underline{2\theta = 41.2°}$

$2b = 2a/\text{Tan } \theta/2 = 2 \times .1/\text{Tan } 10.3° = .2/.1817$

$\underline{2b = 1.10"}$

$$\text{arc} = \frac{2\theta}{360} \pi D = \frac{41.2}{360} \pi \, 3.125 = 1.124"$$

$\underline{\text{arc} = 1.124"}$

Now let a = 0.05"

$D_o = 3.125 \qquad R_o = 1.5625$

$$\theta = \text{Cos}^{-1}\frac{1.5625 - .05}{1.5625} = \text{Cos}^{-1}\frac{1.5125}{1.5625} = .2537\ \frac{360}{2\pi}$$

(.968)

θ 14.53°

$\underline{2\theta = 29.06°}$

$$2b = 2a/\text{Tan}\frac{\theta}{2} = 2 \times .05/\text{Tan}\frac{14.53}{2}$$

(.1275)

$\underline{2b = .784"}$

$$\text{arc} = \frac{2\theta}{360}\ \pi D = \frac{29.06}{360}\ \pi 3.125$$

$\underline{\text{arc} = .793"}$

$$\frac{b}{2c} = \frac{.05"}{.784"} = .0638$$

$$\sigma/\sigma_{ys} = .55$$

$$Q^2 = 1 + 4.5934\ (.0638)^{1.6499}$$

(.0107)

$Q^2 = 1.049$

$$Q = 1.049 - (.212)^{.0641}(.55)^2$$

for $\frac{a}{2c} = .0638$ $\qquad \frac{a}{t} = \frac{.05}{.2} = .25$

$M_k = 1.03$

$Q = .985$

$$\sigma = \frac{39.4}{1.1\ \sqrt{\pi \times .05/9.85}\ \ 1.03}$$

Part thru

$\underline{\sigma(a = .05) = 87.1 \text{ ksi}}$

Note: Notation Changes here.

Assume now that both of these notches grow through the thickness and are arrested. Calculate failure load. Assume further that the sharp notch is the maximum length (2c).

Initial depth = 0.1"
2a = 1.124" a = 5.620
c = πD = 9.8175"

Initial depth = 0.05"
2a = 0.793" a = .3965
c = 9.8175"

$$K = (P_Q \; a^{1/2}/BW) \;\; 1.77 \left[1 - 0.1 \left(\frac{2a}{w}\right) + \left(\frac{2a}{w}\right)^2 \right] \quad \text{where } a = 1/2$$

$$K = \sigma_g \sqrt{\pi a} \left[1 - .1 \left(\frac{2a}{w}\right) + \left(\frac{2a}{w}\right)^2 \right]$$

$$\sigma_g = \frac{K}{\sqrt{\pi a} \left[1 - .1 \left(\frac{2a}{w}\right) + \left(\frac{2a}{w}\right)^2 \right]}$$

$$\sigma_g = \frac{84.0}{\sqrt{\pi \times .5620} \left[1 - .1 \; \frac{1.124}{9.8125} + \left(\frac{1.124}{9.8175}\right)^2 \right]}$$

$$\sigma_g = \frac{84.0}{\sqrt{\pi \times .3965} \left[1 - .1 \left(\frac{.793}{9.8175} + \left(\frac{.793}{9.8175}\right)^2 \right] \right.}$$

Thru
σ_g (a = 0.1") = 63.1 ksi

Thru
σ_g (a = 0.05") = 75.4 ksi

Summary

		To grow a thru crack		To fail through tube crack
2c = 1.124"	a = 0.1"	53.9 ksi	→ Theoretically Arrested	→ 63.1 ksi
2c = 0.793"	a = 0.05"	87.1 ksi	→ Complete Failure	

A.9.3 Two types of notches have been investigated to date at Convair: a machined notch of approximately 0.070 inches width (Reference 2) and Electrical Discharge Machine (EDM) notches of approximately 0.016 inches width (Reference 13). Impact testing performed to date on unidirectional boron/aluminum tubes has resulted in sharp cracks, in the form of a series of broken adjacent fibers, accompanied by a small permanent dent. The notch width (0.016 inches) utilized in Reference 13 for the fracture tests more closely models the observed impact damage, and as a result, it is proposed that EDM notches also be used here.

Failure Analysis

It must be emphasized that the calculations, for part through notches, are based on very few applicable experimental fracture data points. As more applicable fracture data becomes available, the predicted failure load will be revised.

The proposed EDM notch geometry as shown below:

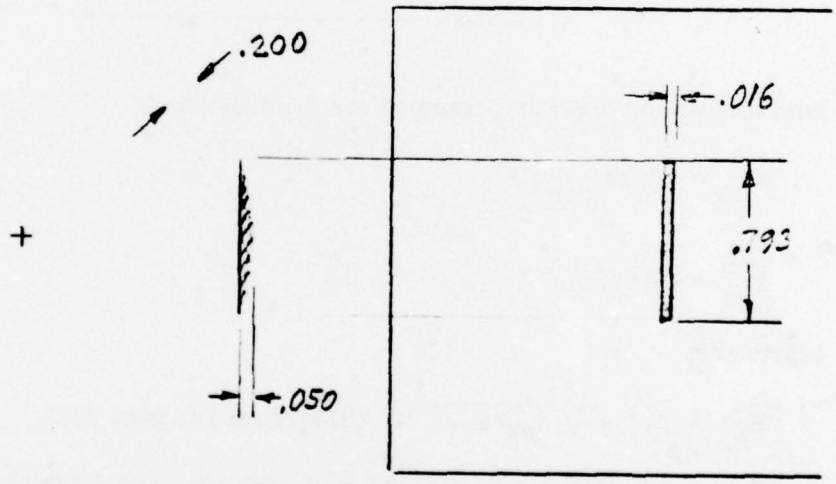

Our predicted gross failure stress for a 28 ply, 3-1/8" diameter UD STCA B/Al tube containing this part through crack is 87.1 ksi. This prediction is based on the fracture toughness data from Reference 14 and the isotropic part through fracture equation from ASTM STP 381 (Reference 12). While this notch geometry is much more severe than what would be expected from everyday service, the predicted gross failure stress is still slightly above design limit load - 85.4 ksi.

A.9.4 The objective here is to design a notch which will cause a static failure in the baseline 4340 steel landing gear strut at 160,000 pounds, since this was the predicted failure load of the damaged B/Al strut. An elliptical surface flaw will be machined in one flange as illustrated below.

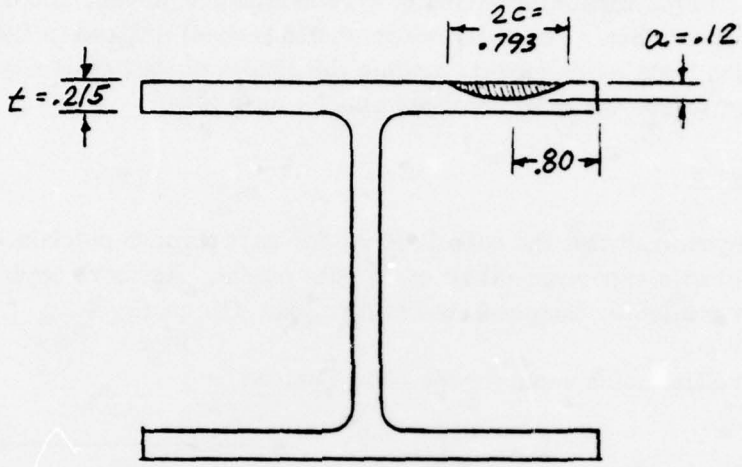

The following properties were assumed for the 4340 steel:

$$K_{IC} = 76 \text{ ksi } \sqrt{\text{in}}$$

$$\sigma_{ys} = 176 \text{ ksi}$$

The expression

$$K_{IC} + 1.1\,\sigma\,\sqrt{\pi a_{cr}/a_{cr}}\,M \quad \text{(Reference 14, page 256)}$$

was used to set the elliptical surface flaw's length, 2c, and depth, a, to satisfy the requirement of 160,000 pound ultimate strength. The term $Q = f(a/2c, \sigma/\sigma_{ys})$ and $M = f(a/2c, a/t)$, where M is a deep flaw back face magnification factor. The flaw length, 0.793", is the same as that machined into the B/Al. The required depth is 0.12", compared to a depth of 0.05" in the B/Al. In the B/Al, fatigue cycling seems to blunt the notch, which inhibits crack growth. In the steel, it is expected that the notch will tend to grow through the thickness and possibly grow to a critical size during the fatigue test.

APPENDIX B

C-SCAN RECORDINGS OF TUBE JOINTS

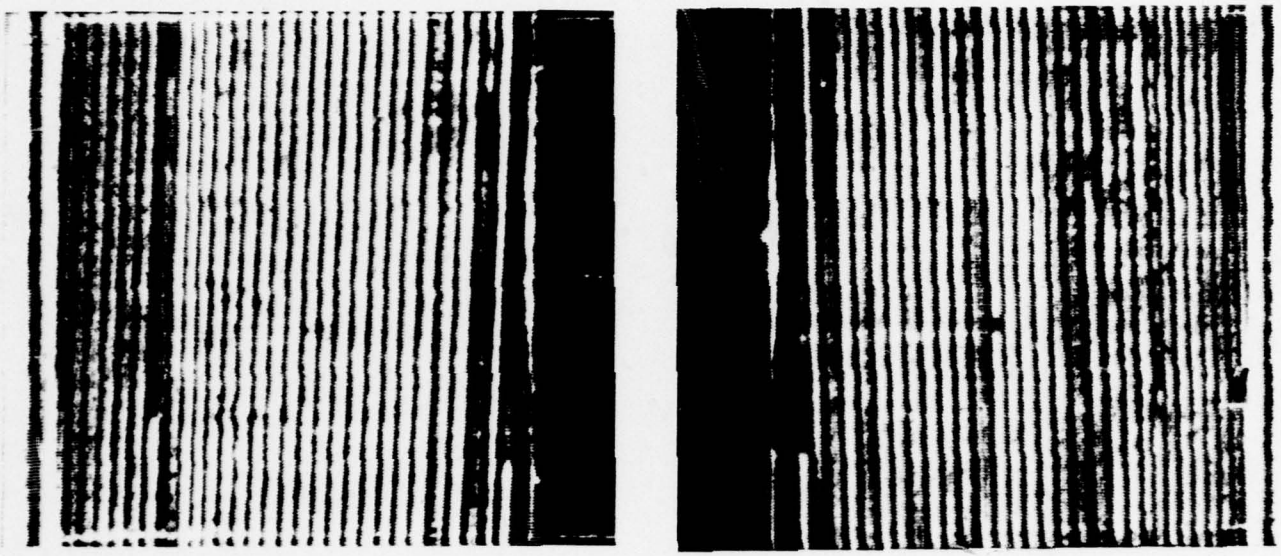

Figure B-1. C-Scan of Tube 001

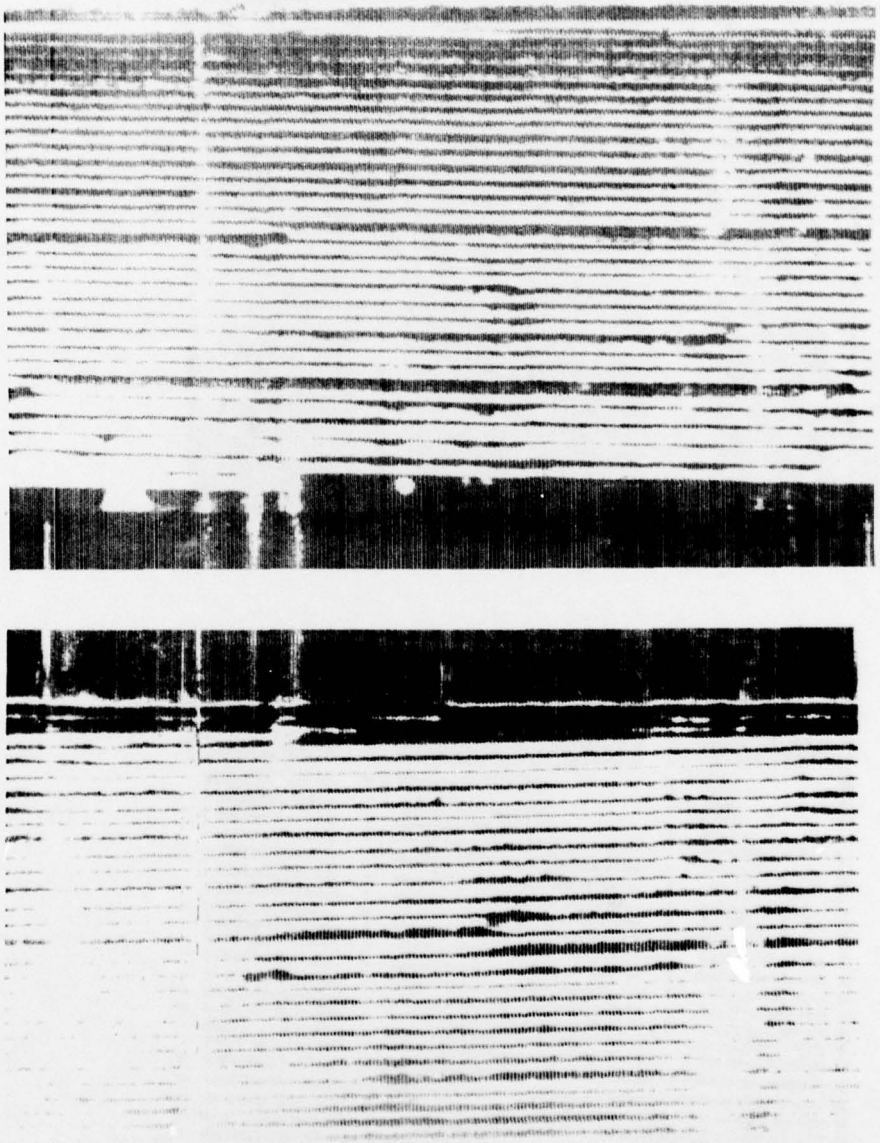

Figure B-2. C-Scan of Tube 002

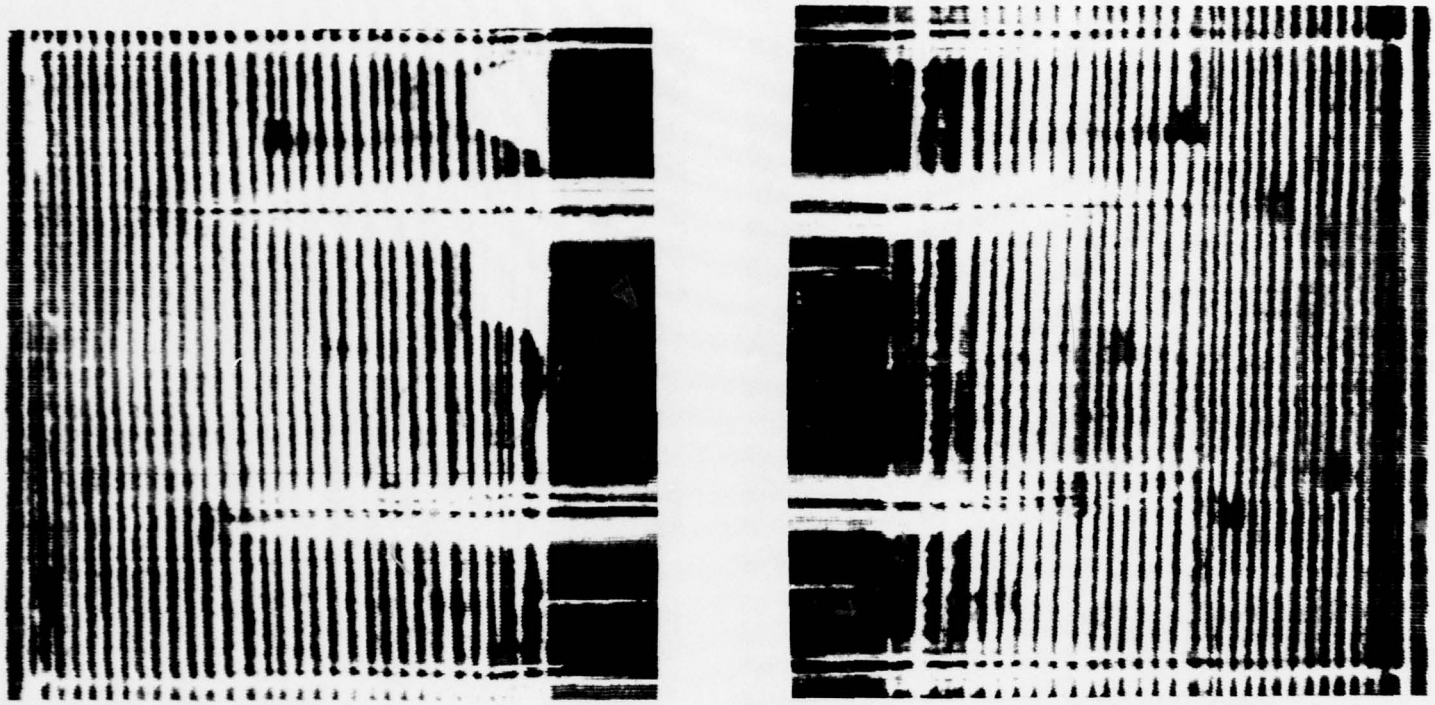

Figure B-3. C-Scan of Tube 003

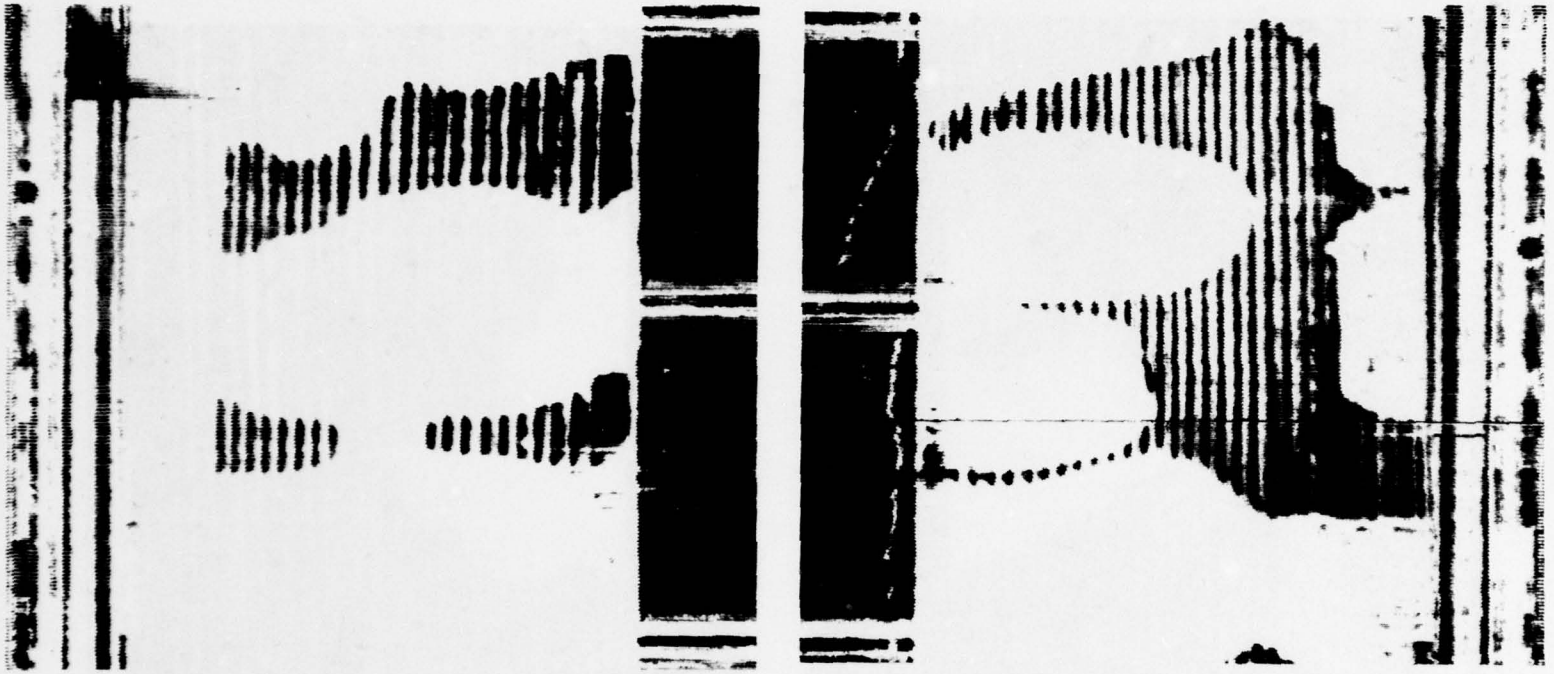

Figure B-4. C-Scan of Tube 004

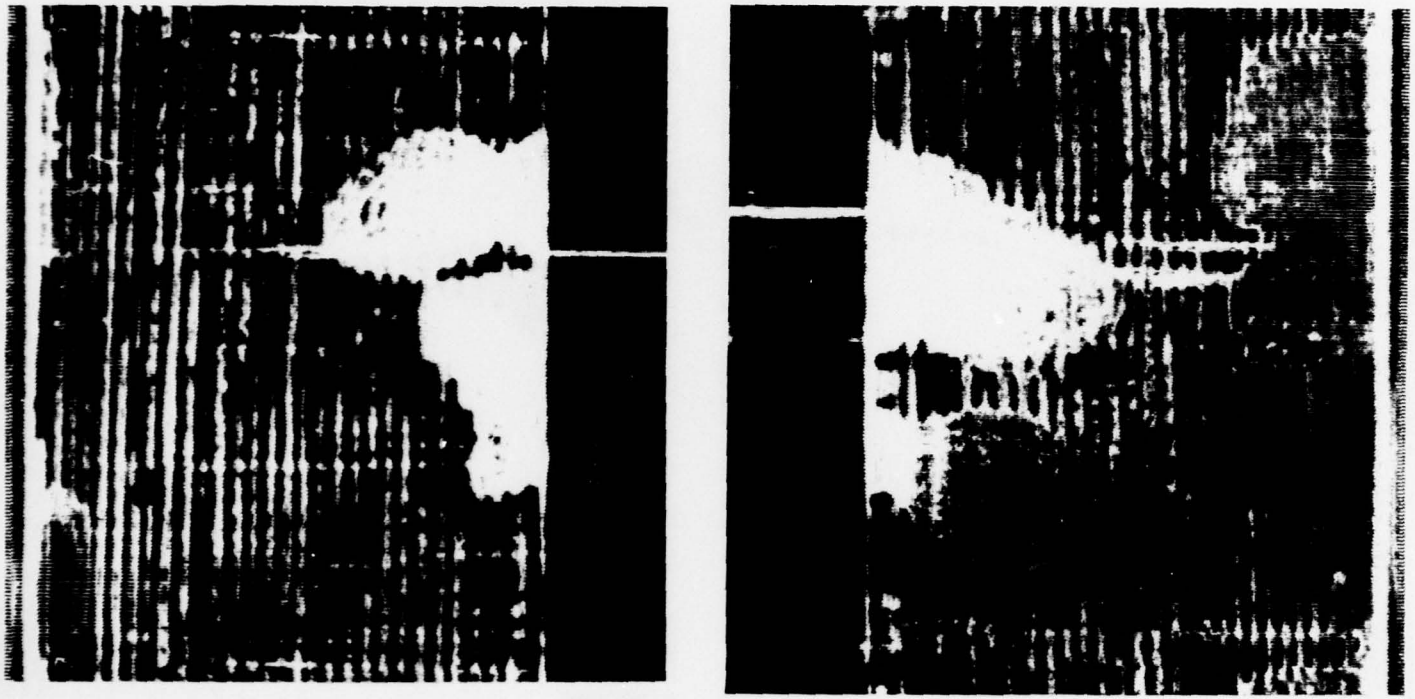

Figure B-5. C-Scan of Tube 005

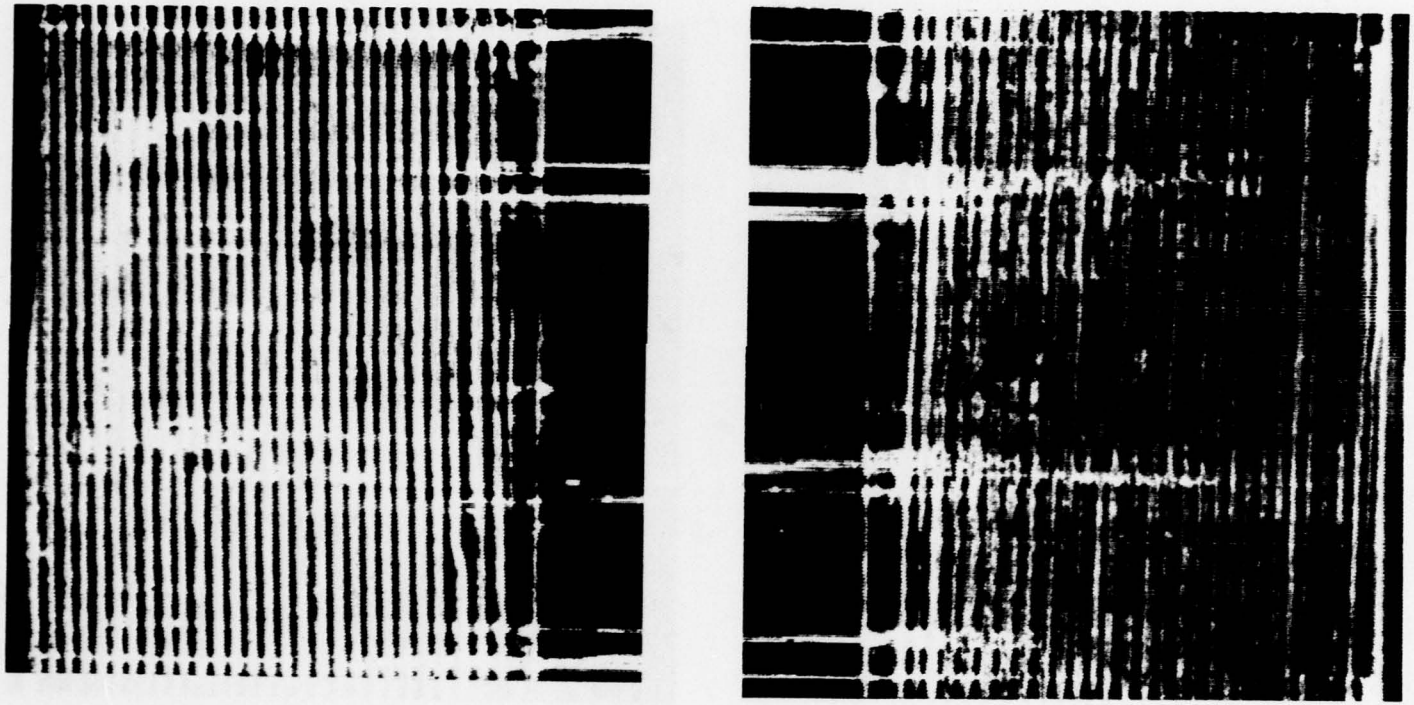

Figure B-6. C-Scan of Tube 006

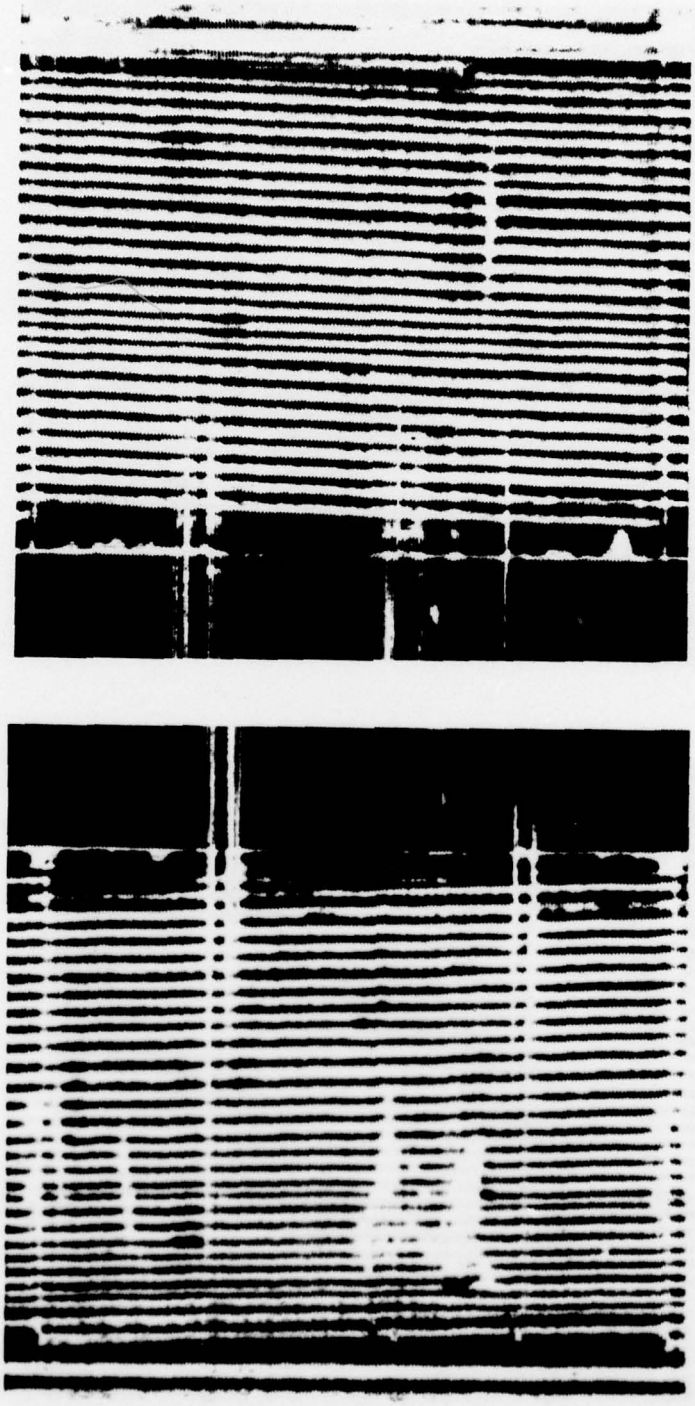

Figure B-7. C-Scan of Tube 007

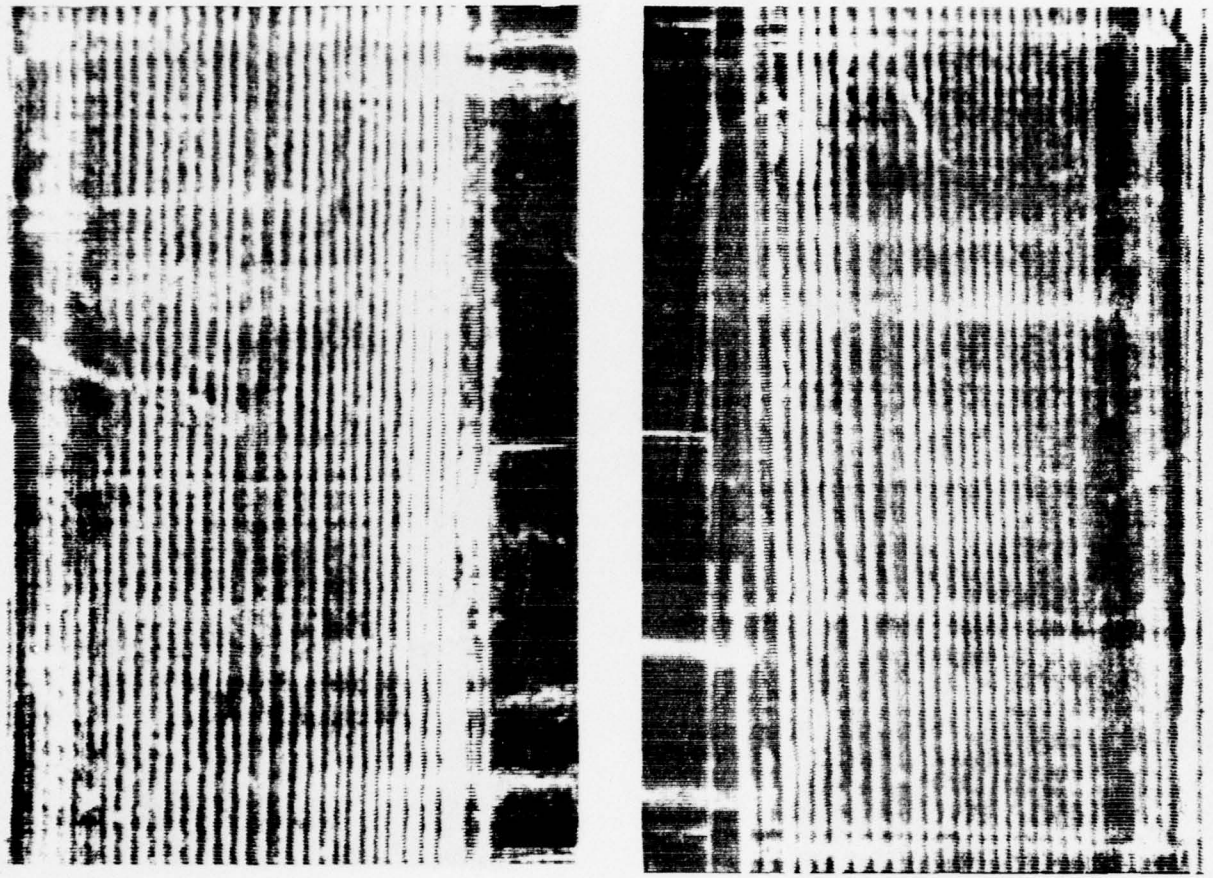

Figure B-8. C-Scan of Tube 009

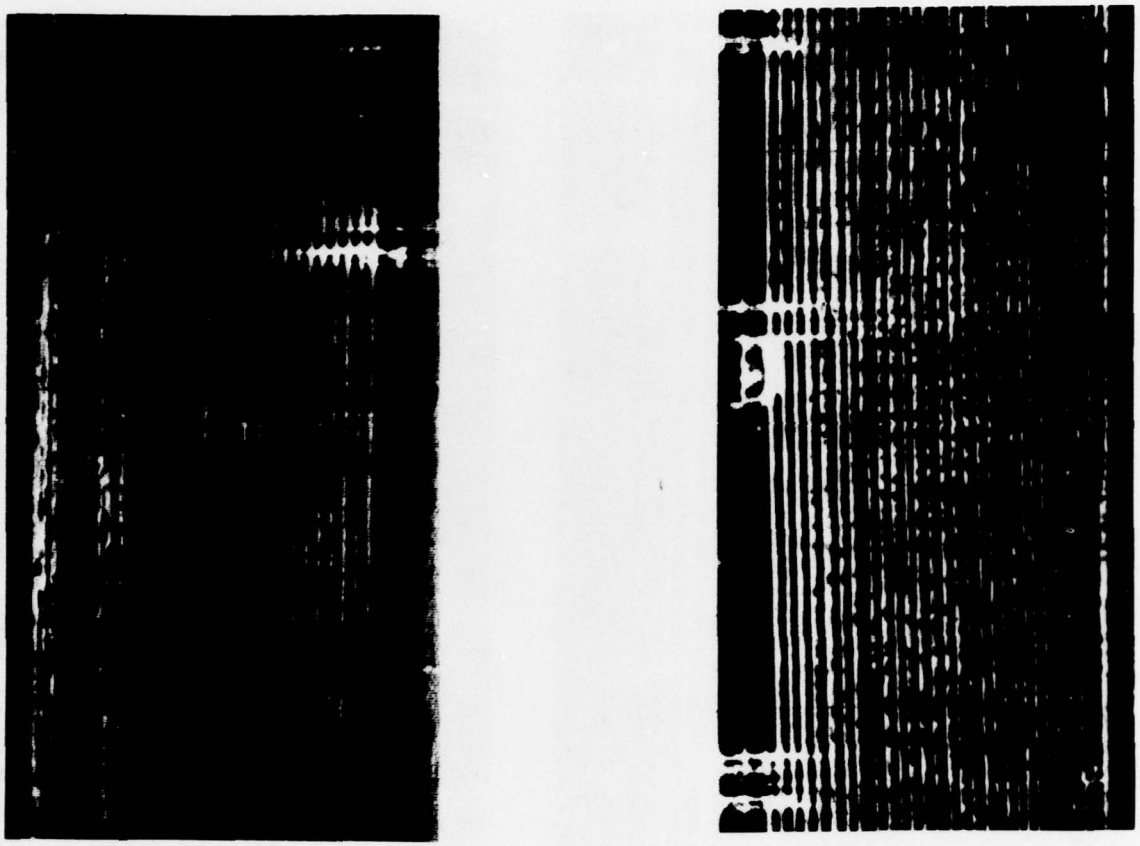

Figure B-9. C-Scan of Tube 012

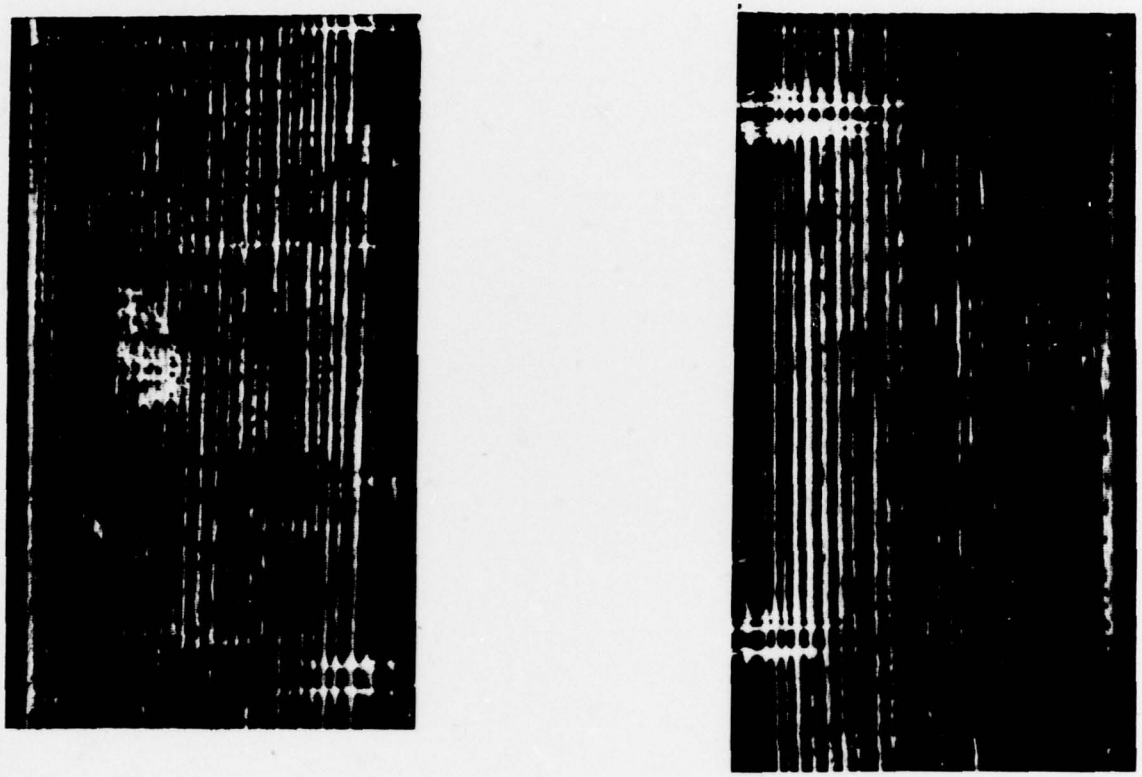

Figure B-10. C-Scan of Tube 013